The Pennsylvania State University

The Graduate School

College of Health and Human Development

COMPARISON OF CIRCULAR AND LEVER PEDALING: A MODELING APPROACH

A Thesis in

Kinesiology

by

Herman van Werkhoven

Submitted in Partial Fulfillment
of the Requirements
for the Degree of

Master of Science

August 2008

The thesis of Herman van Werkhoven was reviewed and approved* by the following:

Philip E. Martin
Professor of Kinesiology
Thesis Adviser

H. Joseph Sommer III
Professor of Mechanical Engineering

Stephen J. Piazza
Associate Professor of Kinesiology

John H. Challis
Associate Professor of Kinesiology
Graduate Program Chair of the Department of Kinesiology

*Signatures are on file in the Graduate School.

ABSTRACT

The circular bicycle drive system has remained relatively unchanged for a number of years despite many attempts at improved designs. One alternative to the traditional circular system is a design in which the rider produces force by pushing on levers, in an oscillating motion, instead of pushing on cranks following a circular path. The purpose of this study was to compare a traditional circular drive mechanism with a proposed lever pedaling design with respect to human effort required to achieve a power output of 250 W. By means of a computer modeling approach, simulations of circular and lever systems were performed using a dynamic optimization framework. A moment-based cost function was employed as the indicator of human effort needed to generate the 250 W power output. Results of the two systems were compared with respect to the magnitude of the cost function output; and net joint moments at the hip, knee, and ankle needed to produce the required power output. Although the joint ranges of motion for the two systems were similar, the predicted joint moments were higher for the lever system at all lower extremity joints. Consequently, the cost function for the lever system (531 $N^2 \cdot m^2$) was 29% higher than the value for the circular system (413 $N^2 \cdot m^2$). Because of the oscillating nature of the lever action, power transfer from the cyclist to the bicycle does not occur continuously for the lever system as it does with the circular system. Accelerations of the levers were higher than those of the chainring and crank in the circular system. The range of the instantaneous power generated about the crank or chainring axis of rotation was 2.2 times greater for the lever system (1055 W operating

range) than the circular system (480 W range). These results indicated the lever system transferred power from the cyclist to the bicycle less effectively than the circular system. It was concluded that a traditional circular propulsion system required less human effort than the lever system proposed in this study to sustain a 250 W power output.

TABLE OF CONTENTS

LIST OF FIGURES

LIST OF TABLES

NOMENCLATURE

I_{eff}	Effective rotational inertia of bicycle around crank/lever axis acting at the chainring
$L(x(t), u(t), t)$	Integral portion of cost function
M_h, M_k, M_a	Net joint moments at the hip, knee, and ankle, respectively, for the three DOF model
M_{h1}, M_{k1}, M_{a1}	Net joint moment at the hip, knee, and ankle, respectively, for the one DOF model
M_t, M_s, M_f	Net moments acting on the thigh, shank, and foot, respectively
r	Bicycle gear ratio
T_{eff}	Effective total resistance torque acting on bicycle-rider system around crank/lever axis
t	Time
t_f	Simulation final time
$u(t)$	Control function – continuous net joint moment input function for 1 DOF model
u_1	Right hip joint moment input for one DOF model
u_2	Right knee joint moment input for one DOF model
u_3	Left hip joint moment input for one DOF model
u_4	Left knee joint moment input for one DOF model
ω	Chainring angular velocity in revolutions per minute
$x(t)$	State variable function
x_1	Crank/lever angle
x_2	Angular velocity of crank/lever
x_3	Integral portion of cost function as appended to the state variable function

ACKNOWLEDGEMENTS

This work would not have been possible without the inspiration of Mort Silverberg, whose enthusiasm shaped this project and enabled me to do the research.

I want to acknowledge and thank Dr Philip E Martin, my thesis adviser, for his invaluable guidance and support throughout this thesis endeavor. You gave me this opportunity and I am truly grateful.

I also would like to thank Dr H Joseph Sommer III for his continuous help and encouragement, and Dr Stephen J Piazza and Dr John H Challis for their time and advice when I needed it.

A thank you goes out to all graduate students, faculty members and staff at the Department of Kinesiology. I have made many friends during my stay and everybody's contribution to making my Penn State experience worth while is greatly appreciated.

Finally, I want to thank Katie – your love and support carried me through to the finish line. I could not have done this without you.

INTRODUCTION

The bicycle drive mechanism has remained relatively unchanged for more than a century, with the current system being introduced in the 1880's (Minetti, Pinkerton, & Zamparo, 2001). The cyclist generates power with the legs by turning fixed length crank arms around a fixed axle in the bottom bracket, thereby restricting foot motion to a circular path. The crank arms are typically connected to circular chainrings, which transfer power to the back wheel through a chain assembly. Alternative drive mechanisms (e.g., non-circular chainrings, variable-length crank systems, linear drive systems) have been proposed by researchers and inventors, although to date none of these designs have shown real potential as a replacement or competitor for the current circular drive (Kyle, 2003). Some of these mechanisms have undergone careful investigation by researchers. These include non-circular chainrings (e.g., Henderson, Ellis, Klimovitch, & Brooks, 1977; Kautz & Hull, 1995; Miller & Ross, 1980; Ratel, Duche, Hautier, Williams, & Bedu, 2004), variable-length crank systems (e.g., Hue, Chamari, Damiani, Blonc, & Hertogh, 2007; Hue, Galy, Hertogh, Casties, & Prefaut, 2001; Zamparo, Minetti, & di Prampero, 2002), and a variable-phase crank system (e.g., Lucia et al., 2004; Santalla, Manzano, Perez, & Lucia, 2002). Using both modeling and experimental approaches, these studies have focused mainly on two mechanical properties that are affected by the design and thereby change the biomechanics of the cycling task: a) variations in angular velocity of the crank, and/or b) variations in the effective moment arm of the chainring or crank. Some of these designs have found their way into the commercial market, e.g., O.Symetric, Q-Rings, Biopace (non-circular chainrings), and ROTOR cranks (variable-phase crank system), although none seem to have gained

substantial popularity. To date, experimental research results for these alternative drive systems have shown very limited, if any, performance improvement relative to the traditional circular drive system (e.g., Hull, Williams, Williams, & Kautz, 1992; Lucia et al., 2004; Ratel et al., 2004).

The biomechanics of the cycling task and consequently performance is dependent not only on the velocity but also the path of the pedals (Hull, Kautz, & Beard, 1991). Changes in pedal path and/or velocity potentially influence the joint range of motion as well as muscle function of the lower extremities. Research that focuses on alternative propulsion designs incorporating pedal paths other than circular has been much more limited than designs using a circular path. Examples of such alternative designs are linear motion drives and arcuate motion or lever pedaling systems. In a linear motion drive the pedals follow a linear instead of a circular path, whereas for a lever pedaling system, the pedals follow an arc trajectory. Harrison (1970) is one of the only investigators to have experimentally studied various movement types created by alternative designs. Using a multipurpose ergometer, Harrison investigated cycling and various rowing movements (combinations of the seat and feet either fixed or allowed to move) and the ability to produce maximum power over intervals ranging from ten seconds to five minutes. He found that a combined arm and leg linear rowing motion produced more power than cycling alone for all intervals. Also illustrating the use of an alternative propulsion system, the first single-rider human powered vehicle to exceed 50 mph (1983) was a special tricycle designed by Steven Ball where the rider lay in a prone position and used a linear drive applying power with both hands and feet (Price, 1995). It is important to note, however, that both the preceding examples are of systems using both

arms and legs to generate power. Furthermore, the body postures when doing the rowing motion on Harrison's ergometer and the position when riding Steven Ball's special tricycle are considerably different from the conventional cycling position. Nevertheless, these examples do suggest that systems other than the traditional circular drive mechanism used in conventional cycling are capable of producing significant power. Research on lever pedaling systems for the lower extremities has been limited to a system used in rehabilitation settings, the Step 'n Go tricycle (Treadle Power Inc., Burlington, VT; Miller, Peach, & Keller, 2001). This device has a lever or treadle system situated below the handle bars at the level of the front wheel axle. The rider pushes on the pedals while standing or with weight supported while seated. Miller and colleagues did not contrast the Step 'n Go propulsion system with a conventional system, but rather examined differences in EMG characteristics between seated and standing riding trials, finding that muscular activity was lower during standing for the highest power output (125 W), but higher during standing for the lower power outputs of 75 W and 100 W. To our knowledge no other research has been done to look at potential benefits or disadvantages of lever pedaling systems in cycling.

There are several reasons why an optimized lever pedaling system might prove advantageous from a human power development and delivery perspective. During circular pedaling instantaneous power output about the crank axle varies substantially throughout the pedaling cycle. When cyclists are maintaining an average power output of 350 W, the actual instantaneous power can range between 110 W and 600 W (Broker, 2003). These power output variations occur primarily because torque produced about the crank axle fluctuates due to changes in both the force applied to the pedal and the

orientation of that force relative to the crank arm. Due to these variations, instantaneous power output peaks when the crank arms are oriented close to the horizontal and is near its minimum when the cranks are near top and bottom dead center, i.e., oriented nearly vertical (Ericson & Nisell, 1988; Sanderson, 1991). Maximum force production occurs roughly between the 90° and 180° position (bottom dead center) of the crank (Broker & Gregor, 1996). One way to increase the amount of torque produced in this optimal force production range would be to increase the moment arm, or length of the crank. In conventional cycling this would be impossible due to ground clearance restrictions as the crank moves through bottom dead center. However, using a lever pedaling system in which the levers move through a more limited range rather than a circular path, the lengths of the levers may be increased. Combined with a more restricted angular operating range, the orientation of rider-generated pedal forces can potentially remain closer to a perpendicular orientation to the lever arm during the downstroke, thereby increasing the moment arm and the torque about the crank axle. Another possible benefit of a lever pedaling system has to do with the use of more limited ranges of motion at the hip, knee and ankle joints. Miller et al. (2001) argued that the Step 'n Go lever pedaling system reduces the range of motion at the joints compared to circular cycling, and that this reduced range of motion more effectively accommodates people with various cognitive, orthopedic and neuromuscular conditions. A lever pedaling system, therefore, can be seen as an alternative means of transport for people without the capability of producing the typical motion and/or forces required during conventional cycling.

There are also potential disadvantages to a proposed lever system that need to be considered. Unlike the traditional circular system, the pedals in a lever system do not

complete full revolutions, which require the levers to reverse direction at the start and end of each stroke. Thus, the levers likely experience large phases of acceleration at the start and end of each motion cycle. Another concern is the mechanical lever system design itself. The system would most likely require a more complex coupling system between the two levers and the rest of the drive system than the relatively simple circular system drive design.

One of the challenges of examining alternative cycling propulsion systems experimentally is the need to have fully functional drive systems capable of tolerating typical pedal forces and torques. Computer modeling and simulation offers a different approach to investigate these alternative propulsion systems. Modeling and simulation techniques can provide valuable insight into the underlying mechanisms of movement. This approach allows researchers to understand the influence of various design factors before considerable effort and expense are invested on construction and testing of new designs. Kautz and Hull (1995), for example, used dynamic optimization principles, specifically optimal control theory, to design a new elliptical chainring and compare its influences on pedaling mechanics with those of the traditional circular chainring setup. As a modeling and simulation approach, optimal control theory provides a means to estimate the controls (e.g., joint torques or muscle activation) employed by the system (i.e., the human body) to achieve a specific goal while the system dynamic equations of motion are being satisfied (Kautz & Hull, 1995). This approach has become common place in modeling and simulation studies of locomotion (e.g., Davy & Audu, 1987; Pandy & Zajac, 1991; Neptune & van den Bogert, 1998, Neptune & Hull, 1999). In cycling specifically, the advantage of such an approach compared to an inverse dynamic

optimization lies in the fact that no assumptions need to be made in advance regarding the forces or moments applied at the pedal. Instead, these values are calculated as part of the optimization routine (Kautz & Hull, 1995). Different solutions are evaluated with respect to a specific cost or objective function that is minimized (or maximized) in the optimization procedure. This cost function usually specifies some physiologically appropriate objective, for example, minimizing moments at the joints (e.g., Kautz & Hull, 1995; Redfield & Hull, 1986b), reducing muscle stresses (e.g., Hull, Gonzalez, & Redfield, 1988), or minimizing energy expenditure and maximizing mechanical efficiency (e.g., Umberger, Gerritsen, & Martin, 2006). Complex models using individual or grouped muscle characteristics to compute muscle stresses are valuable in understanding human functioning, but are computationally more costly than the more simplistic joint moment-based models. Furthermore, complex models do not always ensure more valid simulation results. For example, Hull et al. (1988) compared a muscle stress-based cost function to a more simplistic joint moment-based cost function used previously to assess optimal cadence in steady state cycling. Optimal cadences predicted by the two models were similar. Studies that have employed modeling and simulation methods to investigate alternative bicycle drive designs, however, are very limited. To our knowledge only one of these studies (Kautz & Hull, 1995) has used a dynamic optimization approach to examine an alternative propulsion setup in cycling.

Therefore, the primary purpose of this study was to compare a traditional circular drive mechanism with a proposed lever pedaling design with respect to human effort required to achieve a power output of 250 W. Simulations of both circular and lever propulsion systems were performed using a dynamic optimization framework to calculate

a moment-based cost function as the indicator of human effort needed to generate the 250 W power output. The optimized drive systems were compared to each other with respect to the magnitude of the cost function output, joint moments needed to produce the required output, and the ranges of motion at the joints. A secondary purpose of this project was to examine the sensitivity of the cost function to changes in crank length and crank cadence for the circular system and to changes in lever length, lever cadence, lever ROM, and average chainring angular velocity for the lever system. The sensitivity analyses provided an indication of how variation in the optimal system parameters would affect the cost function, and thus ultimately the human effort required to maintain a given power. For example, large sensitivity would highlight the importance of proper selection of the specific parameter, whereas small sensitivity would indicate that parameter variations would not significantly impact the required human effort.

METHODS

Model Characteristics

The bicycle-rider system was modeled in the sagittal plane and consisted of two five-bar linkages, one for each leg, for both circular pedaling and lever pedaling. The linkage components were the thigh, shank, combined foot and pedal, crank arm or lever, and seattube.

To model the lower extremities of the cyclist, the hip joints were assumed fixed and coinciding with the seat. This meant that the hip joint centers were located at the same position as the top of the seattube. The length of the foot segment was estimated as the distance between the ankle joint and the head of the first metatarsal, which was assumed as the connecting point of the foot with the bicycle pedal. Anthropometric and inertia properties for the lower extremity of a 50th percentile male U.S. rider (Fregley et al., 2000) were estimated from data provided by Drillis and Contini (1966, segment lengths) and Dempster (1955, segment center of mass locations, masses, and moments of inertia). All anthropometric and inertia values are presented in Appendix A.

To model the bicycle, the dynamic equations of motion for a bicycle derived by Fregly, Zajac, and Dairaghi (2000) were adapted for the current system. The expressions give the effective rotational inertia (I_{eff}) and resistive torque (T_{eff}) about the crank axis for the cyclist described above as follows:

$$I_{eff} = 10.422r^2 \quad (1)$$

$$T_{eff} = 2.125r + 1.379 \times 10^{-4} r^3 \omega^2 \quad (2)$$

where *r* indicates the gear ratio (ratio of front sprocket diameter to rear sprocket diameter) and ω is the cycling cadence in revolutions per minute. The original value for T_{eff} was derived by Fregly and colleagues for a conventional circular pedaled bicycle and in the current study was assumed to be the same for the lever pedaled bicycle. T_{eff}, which relates to resistive forces that the cyclist has to overcome during cycling, depends heavily on air resistance and rolling resistance (Martin, Milliken, Cobb, McFadden, & Coggan, 1998) and should be similar for both systems. I_{eff} was adapted from the original equations to exclude the rotational inertia of the crank itself. This enabled equation 1 to be used for both the crank and lever propulsion systems. I_{eff} for the rest of the rider-bicycle system was assumed to be equivalent for circular and lever pedaling.

A schematic of the complete rider-bicycle model for circular and lever pedaling is shown in figure 1. The circular pedaling system consisted of two crank arms which were 180° out of phase and connected to a chainring on which the effective rotational inertia and resistive torque acted. An overrunning clutch mechanism was not modeled in the circular pedaling application as pilot simulation results indicated the mechanism does not disengage during steady state pedaling at the required power output. The lever pedaling system consisted of two levers mechanically connected to each other through a reverse direction gear. Thus, the levers did not move independently from each other. The system had a unidirectional overrunning clutch mechanism between the levers and the chainring. The unidirectionality ensured that the chainring could only move in the direction that caused the bicycle to go forward. The overrunning clutch mechanism controlled the connection and disconnection of the chainring. When the lever that is moving in the same direction as the chainring reached the same angular velocity as the chainring, the

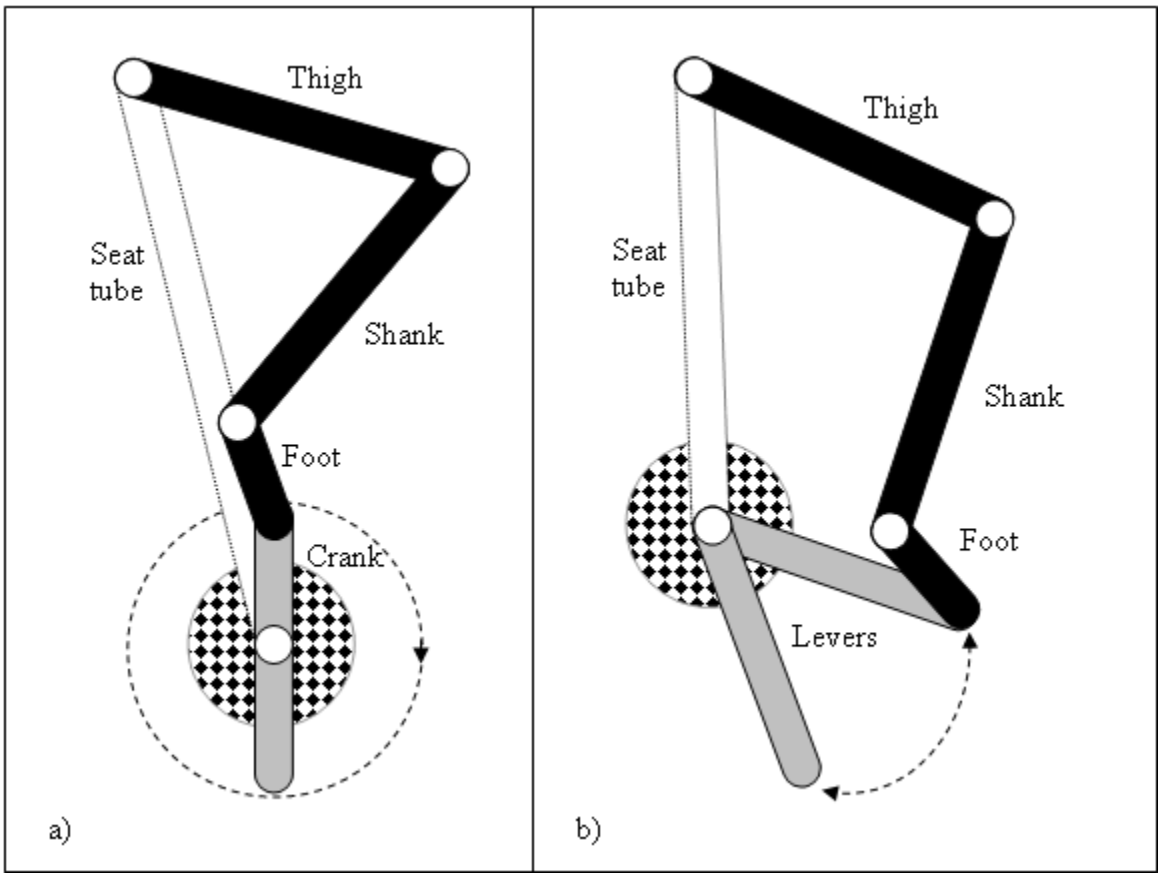

Figure 1. The components and motion path (dashed lines) of the a) circular and b) lever pedaling model (showing only one leg). The bicycle mechanical components were combined into one lumped model component with effective application at the chainring (checkered circle in figure).

lever and chainring engaged and moved together. The lever and chainring disengaged when the resultant lever torque becomes less than the resistive torque at the chainring.

Both of these systems constitute a three degree-of-freedom (DOF) model for seated pedaling using two legs. By knowing the kinematics of the crank and the kinematics of the two ankle joints, the system geometry would be completely specified. The three DOF system was reduced to a one DOF system by prescribing the ankle motion of both legs, as was done previously by Kautz and Hull (1995). This method reduces the

number of function inputs to be optimized and simplifies the simulation process. For the one DOF system the moment at the ankle is the moment necessary to constrain the motion. The moments, therefore, acting on the different leg segments for the three and one DOF models (Figure 2) can be considered as follows:

For the three DOF model

$$\sum M_t = M_h - M_k \tag{3}$$

$$\sum M_s = M_k - M_a \tag{4}$$

$$\sum M_f = M_a \tag{5}$$

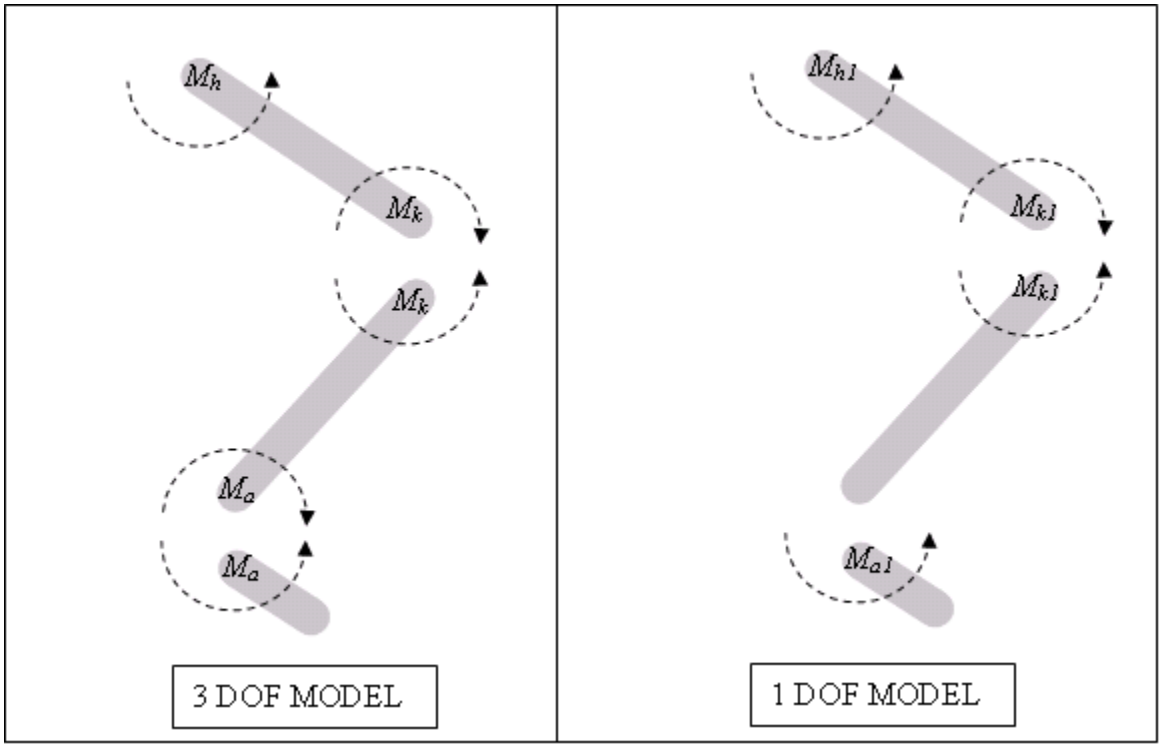

Figure 2. The three DOF model (left) and equivalent one DOF model (right) for a single leg. The one DOF model does not include a reaction torque at the ankle acting on the shank. Adapted from Kautz & Hull (1995).

For the one DOF model

$$\sum M_t = M_{h1} - M_{k1} \quad (6)$$

$$\sum M_s = M_{k1} \quad (7)$$

$$\sum M_f = M_{a1} \quad (8)$$

In this case M_{a1} is the moment required to constrain the movement of the foot segment and does not have an associated reaction moment acting on the shank segment.

The relationship between the one DOF model and the three DOF model are thus as follows:

$$M_a = M_{a1} \quad (9)$$

$$M_k = M_{k1} + M_{a1} \quad (10)$$

$$M_h = M_{h1} + M_{a1} \quad (11)$$

These relationships can be used to obtain net joint moments for a dynamically equivalent three DOF model. In order to apply the one DOF model simplification technique, the kinematics of the foot segment need to be known. For the purpose of this optimization study, experimental kinematic results related to the model optimized parameters for both circular and lever pedaling were not known a priori. An assumption therefore needed to be made regarding foot kinematics. To constrain foot motion, ankle angle, specified as the angle between the anterior shank and a line joining the lateral malleolus and head of the first metatarsal, was held constant. This fixed angle was set at 133° and was based on an average ankle angle calculated from experimental data measured during cycling (Hull

and Hawkins, 1990). The original range of motion of the ankle angle as measured by Hull and Hawkins was 25°.

Therefore, the one DOF model with associated one DOF hip and knee moments was used to solve the differential equations of motion with constrained relative foot motion. By integrating forward in time, movement kinematics as well as the dynamically equivalent three DOF joint moments were computed (Kautz & Hull, 1995).

Optimization Framework

Planar equations of motion for both the circular and lever mechanism were derived using the method of Haug (1989). Having the motion information, the next step was to develop the dynamic optimization framework for the specific task at hand. An average power output of 250 W was specified for both tasks, which represents an estimated average power output for experienced cyclists in endurance events (Vogt et al., 2007). The general optimization problem was formulated as follows (Kautz & Hull, 1995):

$$\min \frac{1}{t_f} \int_0^{t_f} L(x(t), u(t), t)dt \tag{12}$$

where L is the integral cost function, $x(t)$ is the state variable function, $u(t)$ is the control function, and t_f defines the simulation end time.

Many cycling simulations (e.g., Gonzalez & Hull, 1989; Kautz & Hull, 1995) have employed joint moment-based computer models. A common approach in simulations minimizes a cost function based on the sum of squares of hip, knee, and ankle moments (e.g., Kautz & Hull, 1995; Redfield & Hull, 1986b). In its simplest form absolute joint moments are used with equal weighting of concentric and eccentric contributions and equal

contributions of the three joints. Three potential refinements to the cost function were investigated in pilot analyses before the model was finalized, including: a) using net joint moments expressed relative to maximum flexion and extension moment capacities, b) representing eccentric effort as some fraction of concentric effort, and c) weighting contributions from the ankle, knee, and hip differently (e.g., Kautz (1992) doubled the relative cost of the knee in cycling simulations). These preliminary analyses were conducted to examine the effect of these three refinements on the accuracy of predicting experimentally-derived lower extremity joint moments. Appendix B contains the results of these analyses.

The cost function that was selected was based on minimization of relative moments generated about the hip, knee, and ankle joints. Relative moments were calculated by expressing the net joint moments as a percentage of maximum isometric moments at each of the joints. Moment generation capabilities differ not only between joints but also with the direction of movement, i.e., flexion and extension. For example, maximum isometric knee joint moment is roughly twice as high in extension as in flexion (Scudder, 1980). Maximum isometric moment values were obtained from experimental results for hip extension (Nemeth, Ekholm, Arborelius, Harms-Ringdahl, & Schuldt, 1983), hip flexion (Markhede & Grimby, 1980), knee extension and flexion (Scudder, 1980), ankle plantar flexion (Sale, Quinlan, Marsh, McComas, & Belanger, 1982), and ankle dorsiflexion (Marsh, Sale, McComas, & Quinlan, 1981). Appendix A contains maximum isometric flexion and extension moment values for the hip, knee, and ankle obtained from the published literature and used to normalize the joint moments in this study.

In addition, the weighting or contribution of the relative knee moment in the cost function was twice that of the ankle and hip joints (Kautz, 1992). McLean and LaFortune (1991) found that a cost function minimizing the sum of squared knee moments was a better predictor of the cadence at which oxygen consumption was minimized than cost functions including combinations of all joint moments or only the hip or ankle moments. Using a cost function that minimizes only the knee moments, however, is not feasible as preliminary modeling results using a dynamic optimization approach have shown that circular pedaling can be performed without any knee joint moment contribution. This has also been shown previously by Kautz (1992). It was therefore desirable to increase the relative contribution of the knee moment to the overall cost function without excluding the contribution of the other joints.

Finally, because eccentric muscle action has a lower associated metabolic cost than concentric muscle action, eccentric joint moments were weighted by a factor of 1/3 when computing the cost function. This decision was based on early research by Abbott, Bigland, and Ritchie (1952) who reported the cost of concentric muscle activity during cycling was 2.4 to 5.3 times more costly than eccentric muscle activity. Kautz and Hull (1992) also used a weighting factor value of 1/3 in a similar cycling simulation study.

Consequently, the final complete cost function evaluated in this study is reflected as follows:

$$\frac{1}{t_f}\int_0^{t_f} (\%M^*{}_{hr}{}^2 + 2\%M^*{}_{kr}{}^2 + \%M^*{}_{ar}{}^2 + \%M^*{}_{hl}{}^2 + 2\%M^*{}_{kl}{}^2 + \%M^*{}_{al}{}^2)dt \quad (13)$$

%M is the joint moment expressed relative to maximum isometric flexion and extension moments at the hip (h), knee (k), and ankle (a) joints (see Appendix A) for both right (r)

and left (l) legs. Furthermore, $\%M^{*} = \%M$ for concentric moments and $1/3 * \%M$ for eccentric moments. To avoid positive and negative joint moments canceling each other, all the terms were squared. This technique has been used in other cycling simulation studies (e.g., Hull & Gonzalez, 1988; Redfield & Hull, 1986b).

Equation 13 was subject to system differential equations:

$$\dot{x}(t) = f(x(t), u(t), t), \tag{14}$$

with

$$\dot{x}_1 = x_2, \tag{15}$$

$$\dot{x}_2 = f(x_1, x_2, u_1, u_2, u_3, u_4, t), \tag{16}$$

$$\dot{x}_3 = L(x(t), u(t), t), \tag{17}$$

$$u_1 = M_{hr1}, \tag{18}$$

$$u_2 = M_{kr1}, \tag{19}$$

$$u_3 = M_{hl1}, \tag{20}$$

$$u_4 = M_{kl1}, \tag{21}$$

M_{hr1}, M_{kr1}, M_{hl1}, and M_{kl1} are the respective right hip and knee, and left hip and knee moments associated with the one DOF model.

The conventional circular system was optimized for joint moments that minimized the cost function at the chosen power level. The system was also optimized for cadence and crank length. The effect of these two parameters on cycling performance has received considerable attention in research literature using both experimental and modeling approaches (cadence: e.g., MacIntosh, Neptune, & Horton, 2000; Marsh & Martin, 1993; Neptune & Hull, 1999; crank length: e.g., Inbar, Dotan, Trousil, & Dvir, 1983; Gonzalez & Hull, 1989; Too & Landwer, 2000). These parameters were included

as system parameters because of the importance afforded to them in previous research, which also allowed for the results from the current study to be readily compared to previous results. Apart from cadence and crank length, the bicycle geometrical configuration used during the optimization procedure was based on optimal experimental values reported in the research literature. Seat height was set at 100% trochanteric leg length (Nordeen-Snyder, 1977) and seat tube angle was set at 76° (Garside & Doran, 2000). To limit the possible search space of the optimization routine, the following ranges of values were used for cadence and crank length:

$$0.14m \leq Crank\ length \leq 0.20m \tag{22}$$

$$40rpm \leq Crank\ cadence \leq 160rpm \tag{23}$$

These ranges were selected to include ranges and optimal values previously used in other experimental and modeling studies (cadence: e.g., Coast & Welch, 1985; Marsh & Martin, 1993; Yoshihuku & Herzog, 1990; crank length: e.g., Inbar, Dotan, Trousil, & Dvir, 1983; Martin & Spirduso, 2001; Too & Landwer, 2000).

Initial and terminal constraints were introduced to specify conditions necessary to complete the task. For the circular system, the initial crank angle was set to 0 radians or top dead center:

$$x_1(0) = 0 \tag{24}$$

In addition, the final or terminal crank angle was specified as 2π radians or 360 degrees and the initial and final angular velocities of the crank were constrained so that they were equal:

$$x_1(t_f) = 2\pi \tag{25}$$

$$x_2(t_f) = x_2(0) \tag{26}$$

For the lever system, the geometrical configuration was selected based on the initial premise of the design: the ability to increase the length of the lever arms as well as the ability of the cyclist to produce high force in the working range or range of motion of the levers. When looking at cyclist force production during regular cycling, it is evident that force applied to the pedal increases rapidly just before the crank reaches the 90° position in the pedal cycle and then declines soon after the crank passes through bottom dead center (Figure 3). The midpoint in this range of high force production occurs at 135° (measured clockwise from top dead center). For the lever system the range of motion of the lever was also centered around this 135° position. To ensure that the legs were in similar positions during the lever system motion as the range of high force

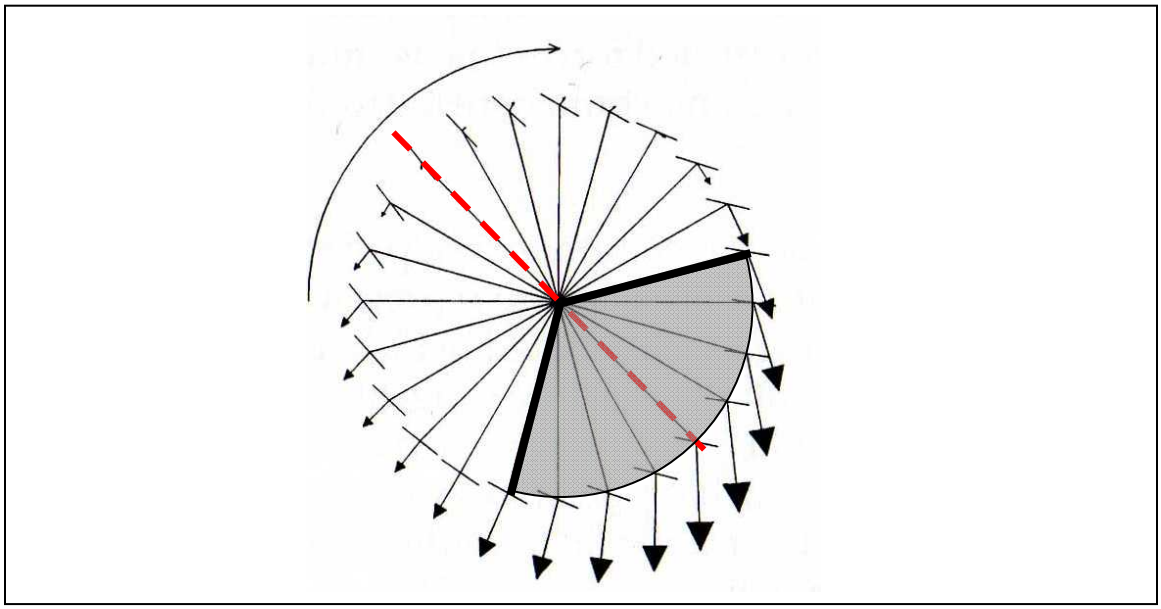

Figure 3. Variation in force production through one complete cycle during circular pedaling. Arrows indicate the magnitude and direction of force application. The area of high force production is depicted by grey shadow. The proposed lever range of motion was centered around the midpoint at 135° (dashed line). Adapted from Broker and Gregor (1996).

production for circular cycling, the lever endpoints were constrained to move through the same endpoint positions as a 0.17 m crank with a 120° range of motion centered around the 135° midpoint. To accomplish this, the position of the lever axis of rotation was shifted posteriorly and superiorly along the 135° line as the lever length increased (Figure 4). Seat tube height and seat tube angle, two other parameters that were fixed for the circular system for all possible crank lengths, were not fixed for the lever system. These parameters were both dependent on the lever axis position and the lever length and were

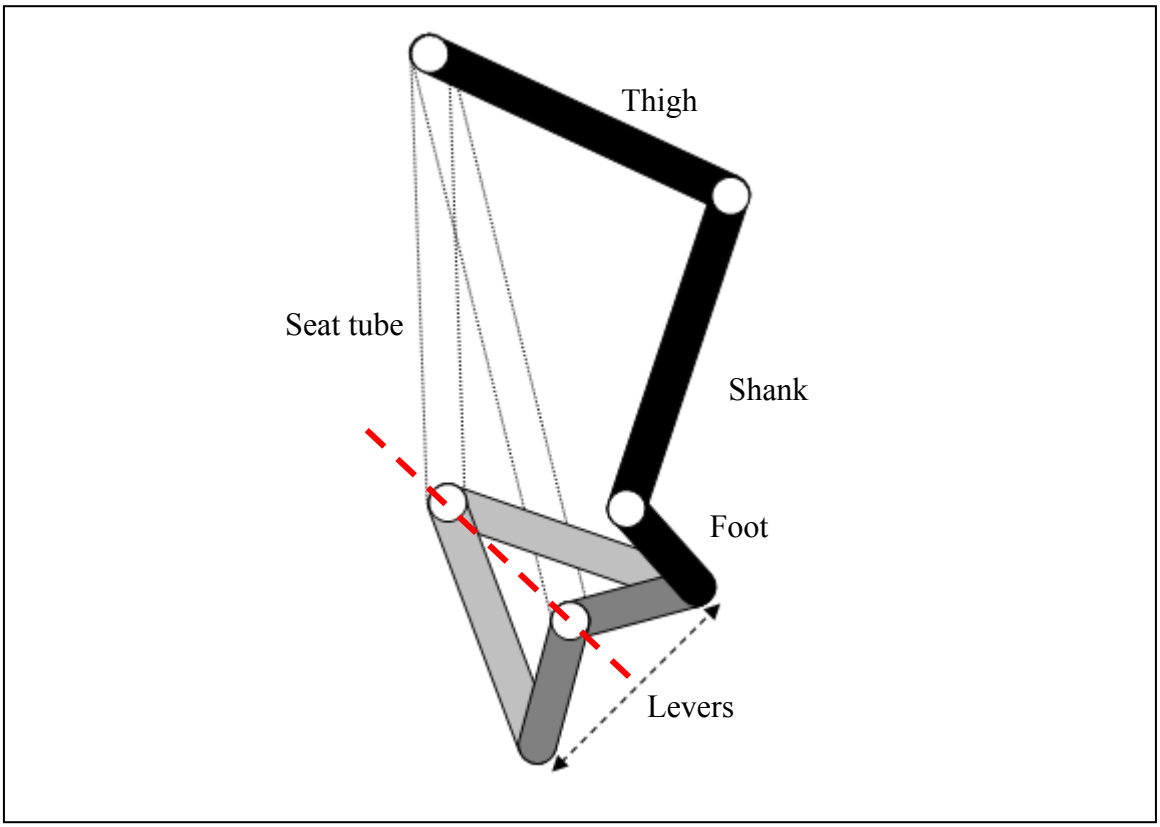

Figure 4. Two hypothetical lever system configurations with lever lengths equal to crank lengths (dark grey) and lever lengths equal to double the crank lengths (light grey). The range of motion of the levers was not constrained, but the lever endpoints had to move through the same endpoints as a crank of 0.17 m length and 120° ROM. The center of the angular range of motion for the crank was held constant at a crank angle of 135° (dashed line).

set based on the specific lever system configuration chosen by the optimization routine.

The lever system was optimized for joint moments that minimized the cost function at the specified power level as well as length of the levers, rate of lever oscillation or lever cadence, lever range of motion (ROM), and average chainring angular velocity. Lever cadence and lever length are equivalent parameters to crank cadence and crank length for the circular system. Average chainring angular velocity and lever ROM, the two other selected system parameters, are both unique to the lever system. When optimizing for crank cadence during circular pedaling the chainring angular velocity is known based on the direct linkage between these two components. This is not the case, however, for lever pedaling. For lever pedaling, both lever cadence and average chainring angular velocity need to be optimized. The lever cadence is calculated as the inverse of the time it takes for the levers to complete a full motion cycle, whereas the chainring angular velocity refers to the speed at which the chainring is rotating. Since the levers and chainring are not directly linked throughout the motion, lever cadence and chainring angular velocity are not equivalent. To limit the possible search space of the optimization routine, the following ranges of values were used:

$$0.17m \leq Lever\ length \leq 0.51m \tag{27}$$

$$40cpm \leq Lever\ cadence \leq 160cpm \tag{28}$$

$$40rpm \leq \omega_{chainring} \leq 160rpm \tag{29}$$

$$0^{\circ} \leq ROM \leq 360^{\circ} \tag{30}$$

Because a proposed advantage of the lever system is the potential to use longer levers, the minimum lever length allowed was the original 0.17 m crank length. The maximum

allowed length was set at 0.51 m, which was three times the original 0.17 m. Both lever cadence and average chainring angular velocity ranges were kept equal to the ranges used for circular pedaling. Note that lever cadence is measured in cpm, cycles per minute and not rpm, revolutions per minute, since the levers do not complete full revolutions during a cycle. Although the lever ROM limits were set at 0° to 360°, these limits were dependent on the length of the levers. The length of the levers and lever ROM were subject to constraints based on the ROM at the hip and knee joints as well as the possible ground clearance allowed. Since the current model did not include a trunk, hip joint angle was not used explicitly. Instead, thigh angle measured relative to a vertical reference was used to indicate motion at the proximal leg segment. Thigh and knee ROM's were limited to the maximum values found for the optimized circular system. Given that reduction in joint ROM was seen as one of the possible advantages of the proposed lever system, allowing the joint ROM constraints for the lever system to be larger than those for the circular system did not seem practical. This constrained the thigh angle to a lower limit of 93° (measured anteriorly with 180° being full extension). Similarly, the knee flexion angle was constrained to a lower limit of 55° (measured posteriorly with 180° being full extension). Pilot simulations revealed that upper limits for the joint angles were redundant. The system configurations and ground clearance constraint did not allow thigh and knee joint angles to range anywhere close to physiological upper limits. The ground clearance limit was set at the lowest possible ground clearance for the circular system with a crank length of 0.2 m.

For the lever system the initial lever angle was not a fixed constraint and was optimized through the ROM system parameter. The following terminal constraints were applied:

$$x_1(t_f) = x_1(0) \tag{31}$$

$$x_2(0) = x_2(t_f/2) = x_2(t_f) = 0 \tag{32}$$

Equation 31 constrained the model such that the beginning and end lever positions were the same. Equation 32 ensured the lever velocities at the top and bottom of the stroke were zero because of the reversal in direction of motion required at these positions.

Due to the symmetry of both systems after half a cycle, the number of optimization parameters was halved. Optimizing for joint moments of the right leg over the complete cycle meant that moments at the left leg joints were calculated using the following constraints for both systems:

$$u_3(t) = u_1(t + \frac{t_f}{2}) \tag{33}$$

$$u_4(t) = u_2(t + \frac{t_f}{2}) \tag{34}$$

Equations 33 and 34 ensured that the left hip and knee moments were half a motion cycle out of phase with those of the right hip and knee.

Simulation Properties

The optimal control problem was solved using a gradient-based non-linear constraint optimization algorithm in Matlab®. To validate optimal results, the simulations were also run using a particle swarm optimization (PSO) algorithm. Optimal results from the PSO algorithm did not differ from the optimal results gained by the

gradient-based optimization routine. The continuous controls, i.e., the joint moments, were parameterized using discrete nodes, where control values at intermediate points were determined using cubic spline interpolation. The number of nodes for each joint was selected based on the how well joint moment curves generated through interpolation matched actual circular pedaling data. The number of nodes was systematically increased from 1 to 50 and the root mean square error (RMSE) between experimental joint moment curves and joint moment curves generated using the cubic spline interpolation were calculated. The RMSE decreased sharply with increasing number of nodes up to 12 nodes, where a point of diminishing returns was reached. Using more than 12 nodes (13 to 50) resulted in small decreases in RMSE. Consequently, 12 discrete nodes were used for each joint during circular pedaling system simulations. The same number of nodes was used for lever pedaling system simulations.

Sensitivity Analyses

To investigate the sensitivity of the cost function output to changes in system parameters, the parameters were each individually varied and the system was optimized to determine changes in cost function output. For the circular system, the system parameters were crank length and crank cadence. For the lever system, the system parameters included lever length, lever cadence, lever ROM and average chainring angular velocity. The parameters for both systems were varied by ± 5% and ± 10 %. System parameter values as well as cost function output values were normalized in order to compare the sensitivity of the cost function output for various system parameters.

RESULTS

Model Validation

The validity of the model used in this study was evaluated by comparing joint moment results generated by the model to experimental results (Kautz & Hull, 1995) for cycling at 250 W with a cadence of 90 rpm and a crank length of 0.17 m (Figure 5). Joint moment profiles were similar for the model and experimental cases. More specifically, both model and experimental results at the hip showed a large extensor moment during the first half of the pedal cycle, corresponding to movement of the crank from top dead center to bottom dead center. Whereas model results for the hip indicated a switch from an extensor to a flexor moment near bottom dead center, experimental data indicated this transition occurred substantially later in the pedal cycle (approximately 75% of the pedal cycle). For both the model and experimental data, the net knee moment was initially extensor in nature before transitioning to a flexor moment at approximately 30% (experimental results) and 40% (model results) of the pedal cycle. Lastly, moments at the ankle were predominantly plantar flexor throughout the movement cycle for both the experimental and model case. Model results showed a small and brief dorsiflexor moment near top dead center that was not reflected by the experimental results. There were also some differences between the magnitudes of the joint moments of the model and experimental results. These differences, however, did not necessarily indicate that the model results were consistently lower or higher than experimental results. For example, at the hip the experimental peak extensor moment was larger than the model moment, but the peak flexor moment showed the opposite trend. At the knee, experimental results of flexor and extensor moments were larger than those for the model

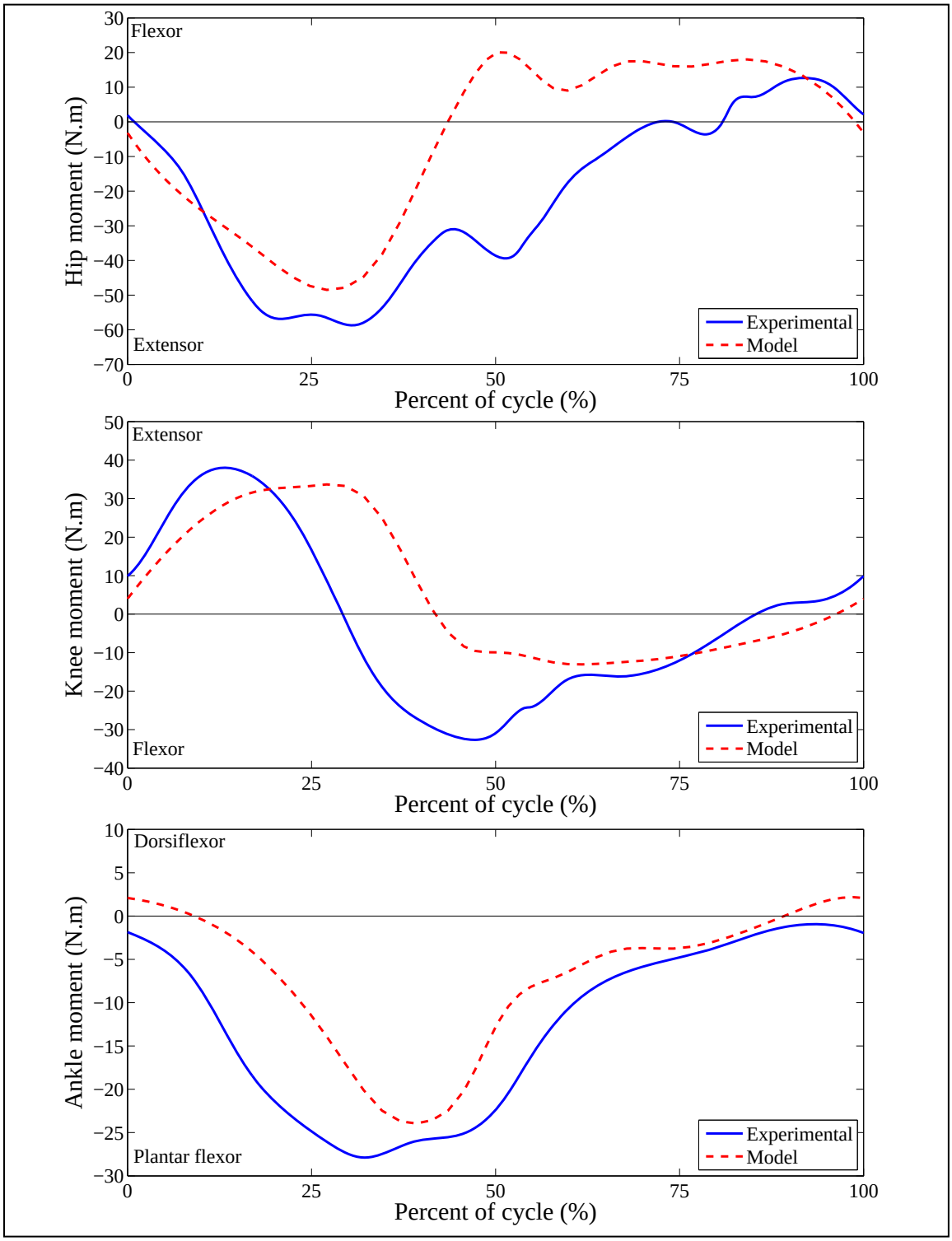

Figure 5. Joint moments for the hip (top), knee (middle), and ankle (bottom) comparing experimental (solid blue line) and model (dashed red line) results for a 250 W cycling task at 90 rpm, using a 0.17 m crank length. Experimental data were taken from Kautz and Hull (1995).

and at the ankle, experimental results showed a larger peak plantar flexor moment than the model results.

Although the model joint moment profiles were compared to one specific experimental study, many other experimental studies using different power output and cadences have shown comparable results (e.g., Gregor, Cavanagh, & LaFortune, 1985; Mornieux, Guenette, Sheel, & Sanderson, 2007; Redfield & Hull, 1986b; Van Ingen Schenau, Boots, De Groot, Snackers, & Van Woensel, 1992). All studies show the hip having an extensor moment throughout most of the pedal cycle before changing to a flexor moment as the crank approaches top dead center. The knee begins the pedal cycle with an extensor moment which changes to a flexor moment before the crank reaches bottom dead center. In all studies, the ankle experiences a plantar flexor moment throughout most of the cycle. Because of differences in power output and/or cadence, the magnitudes of the moments and timing of moment directional changes reflect inconsistencies across the various studies. In addition, Gregor et al. (1985) showed that large variability in magnitude and timing of moment profiles exists between individuals when cycling at the same power level and cadence. Differences in inertial properties between subjects or, in this case, model inertial properties, could also contribute to differences in the moment outcomes.

Other moment-based modeling studies (e.g., Kautz & Hull, 1995; Redfield and Hull, 1986b) show moment profiles similar to those for the current study. For example, Kautz and Hull (1995), who used a forward dynamic optimization framework, predicted similar flexor-extensor transition times as observed in this study. Both models predicted the transition from hip extensor to hip flexor moment occurs earlier than is suggested by

experimental results. The two models also predicted the transition from knee extensor moment to flexor moment occurs later in the cycle than experimental data show. In addition, both models showed a slight dorsiflexor moment around top dead center which were not indicated by experimental results. With respect to moment magnitudes, peak joint moments predicted by the current model were more consistent with experimental results than those by Kautz and Hull. In particular, the Kautz and Hull model underestimated the hip extensor and knee extensor moment to a greater extent than the current model. Results from Redfield and Hull (1986b) also underestimated the hip and knee joint moment peak values. Given the substantial variability in moment profiles reported by Gregor et al. (1985), the reasonable similarity between model results and published experimental data, and the close agreement between results of the current model and other published model results, it was concluded the current model reflected a sufficient level of validity to address effectively the research questions presented in this study.

For both circular and lever pedaling models, the hip joints were assumed fixed and coinciding with the seat. To further ensure the validity of the current model, the net vertical forces at the hips were quantified to determine if these forces exceeded the partial weight of the upper body (trunk, head, neck, arms). If the hip forces exceeded upper body weight, the rider would be lifted off of the seat and the assumption of a fixed hip joint position would become invalid. Results for the combined reaction forces at the hips did not exceed the partial body weight of the rider for either the circular or lever system. Consequently, these results confirmed that the assumption of fixed hip joints was appropriate.

System Cost Function, Kinetics, and Kinematics

The minimum cost function value for the lever system was 29% higher than the value for the circular system. The cost function for the circular system had a minimum value of 413 $N^2 \cdot m^2$. This minimum value was achieved at a crank cadence of 96 rpm and a crank length of 0.2 m, which was the maximum allowed crank length. In contrast, the minimum cost function value for the lever system was 531 $N^2 \cdot m^2$. The lever system minimum value was achieved at a lever cadence of 48 cpm with lever length of 0.2 m. The optimal lever range of motion (ROM) was 254° with the right lever starting 8° after top dead center and ending 82° beyond BDC. The optimal average chainring angular velocity was 113 rpm.

Peak moments for the hip, knee, and ankle for the lever system were substantially higher than those for the circular system (Table 1, Figures 6-11). For the lever system,

Table 1. Peak extensor and flexor moments (expressed in N·m) at the hip, knee, and ankle for circular and lever pedaling systems.

Joint moment	Circular system	Lever system
Hip		
Extensor	45	83
Flexor	20	34
Knee		
Extensor	29	53
Flexor	12	23
Ankle		
Plantar flexor	25	30
Dorsiflexor	3	9

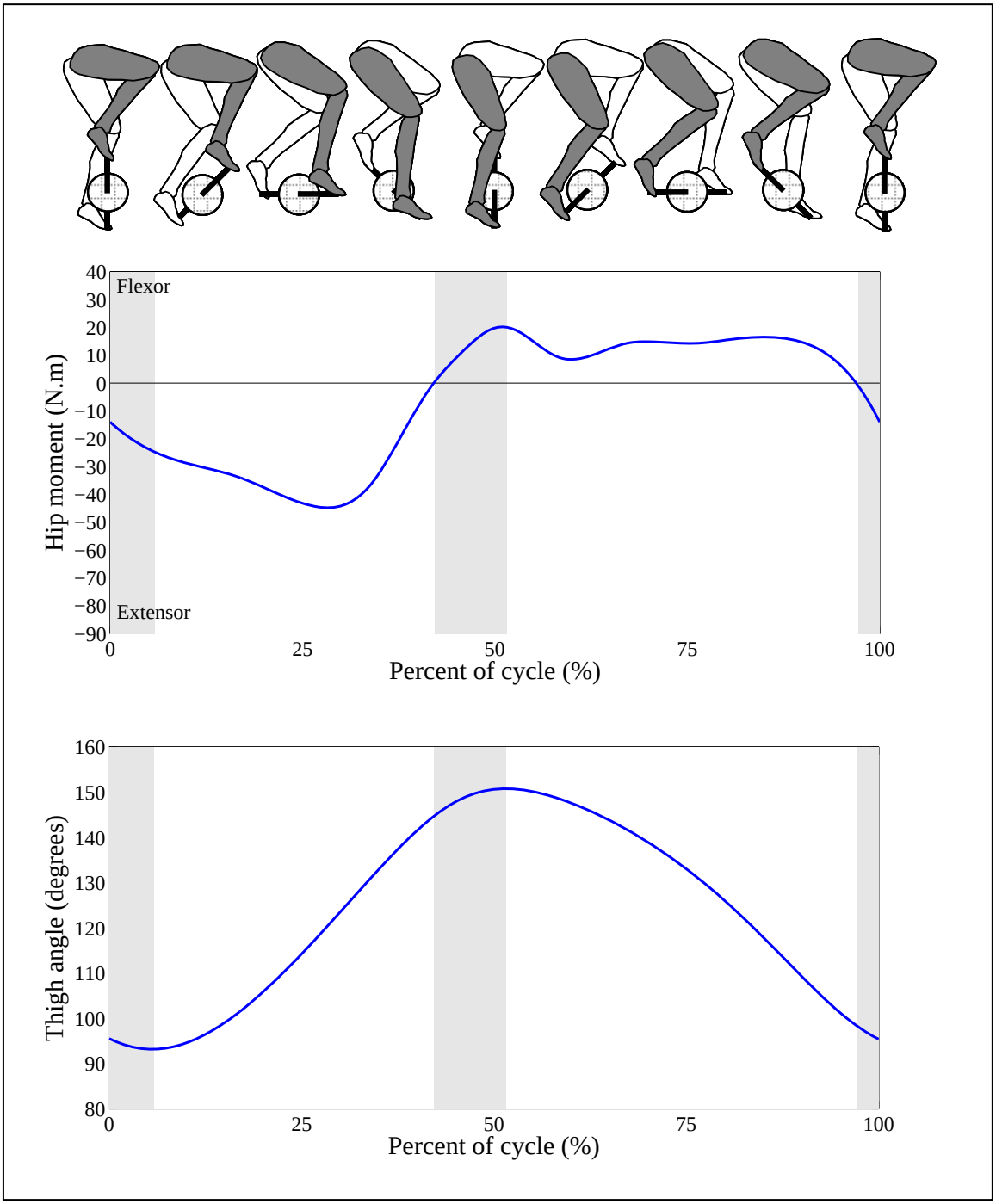

Figure 6. Right hip joint moment (top) and right thigh angle (bottom) for the optimized circular system at 250 W. The white and gray backgrounds indicate positive and negative work respectively. Thigh angle is measured anteriorly with 180° being fully extended. The hip experiences an extensor moment from just before top dead center until just before the crank reaches the bottom of the stroke. At this point the joint action changes to a flexor moment. Kinematically, the thigh has distinct intervals of extension and flexion, each lasting roughly 50% of the cycle.

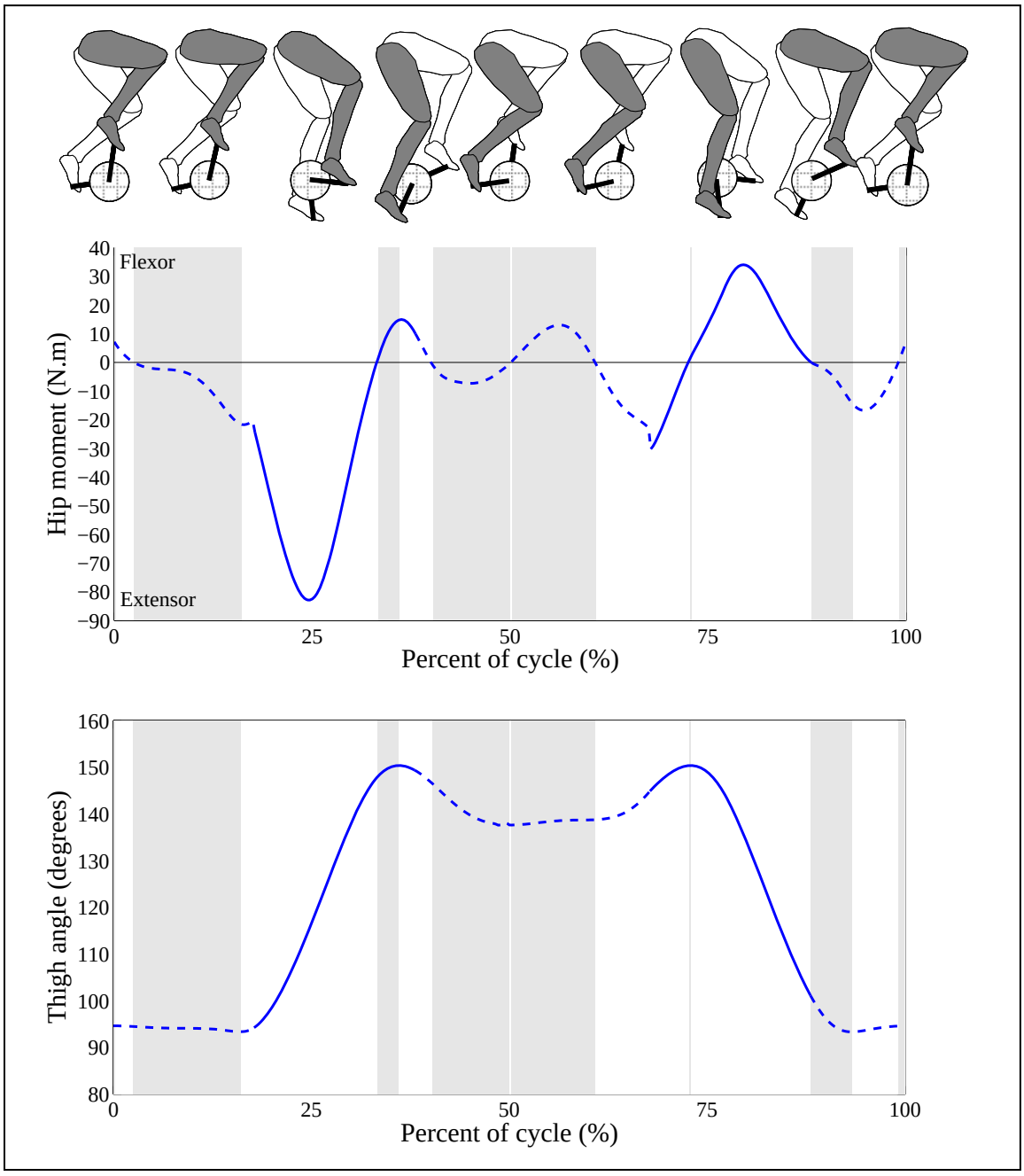

Figure 7. Right hip joint moment (top) and right thigh angle (bottom) for the optimized lever system at 250 W. The white and gray backgrounds indicate positive and negative work respectively. A solid line indicates that the lever and chainring are engaged. Thigh angle is measured anteriorly with 180° being fully extended. The joint experiences a very large extensor moment while the system is engaged and the lever is moving down. During the upward stroke the joint action reverses from extensor to flexor while the system is engaged. The thigh movement is characterized by fast extension as the lever is engaged during the downward movement and a fast flexion phase during the upward movement.

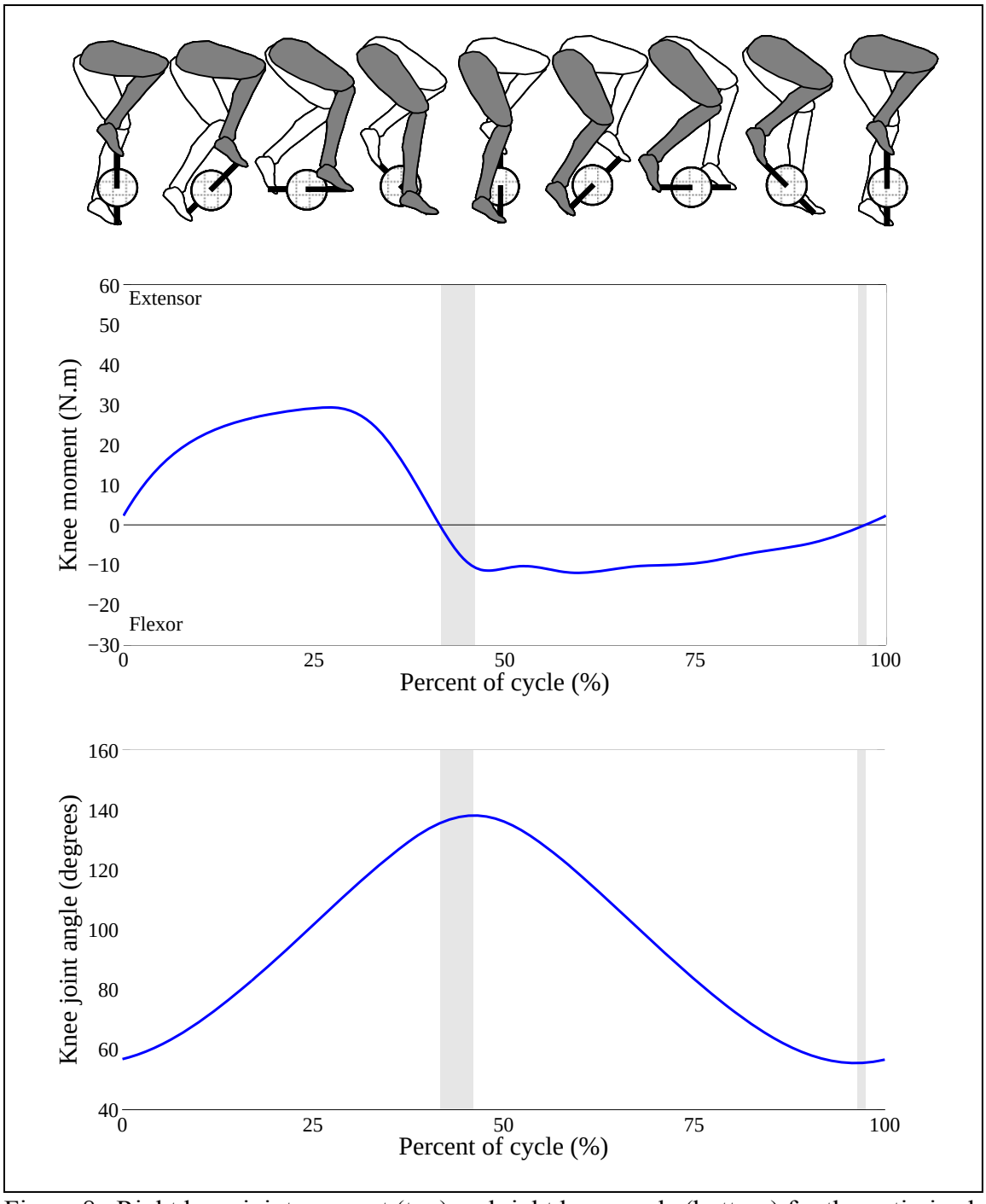

Figure 8. Right knee joint moment (top) and right knee angle (bottom) for the optimized circular system at 250 W. The white and gray backgrounds indicate positive and negative work respectively. Knee angle is measured posteriorly with 180° being fully extended. The knee joint experiences an extensor moment from starting around top dead center until just before bottom dead center. This is followed by a period of flexor action. Kinematically, the knee starts with a period of flexion which then changes to extension period, each lasting roughly 50% of the cycle.

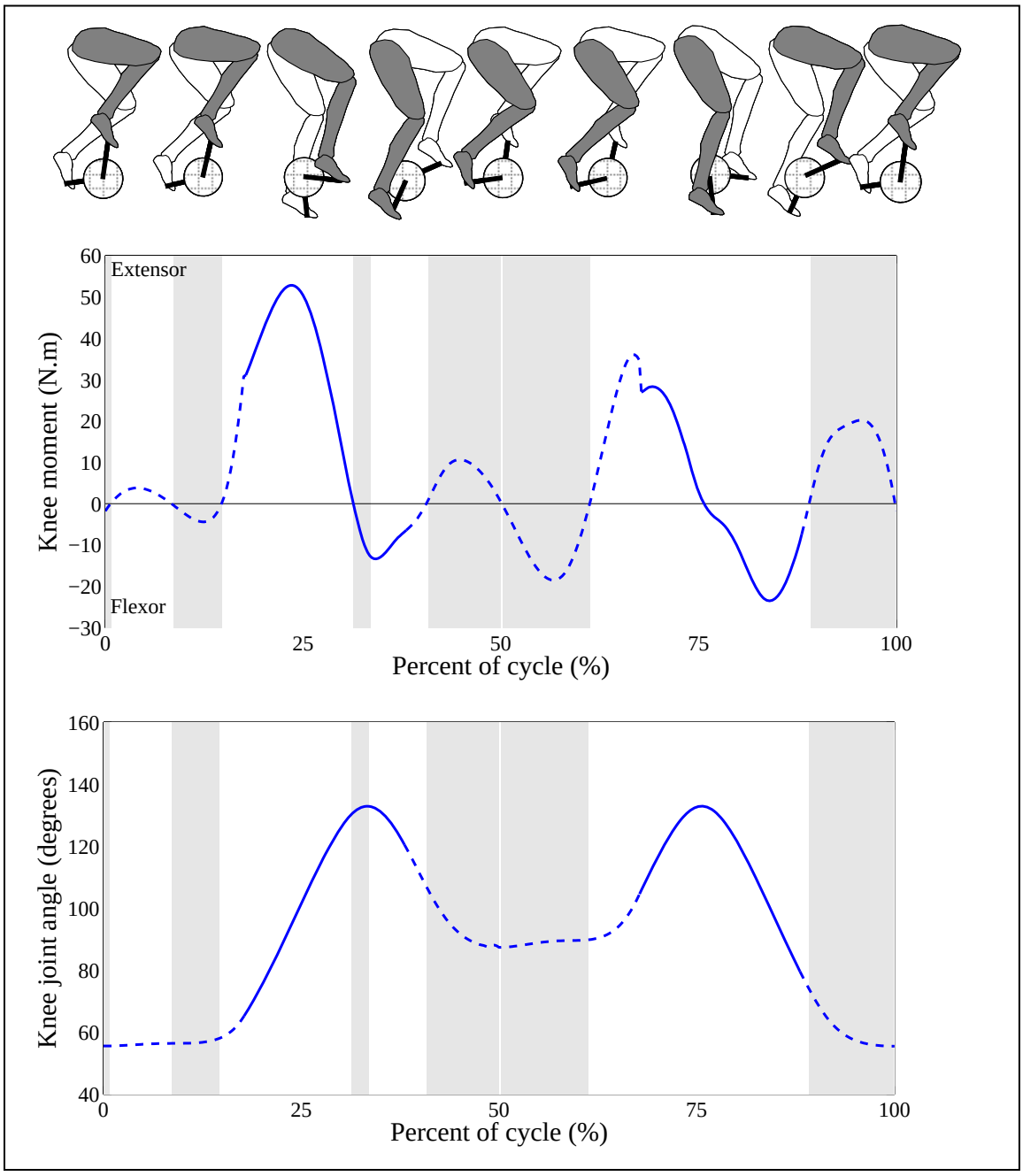

Figure 9. Right knee joint moment (top) and right knee angle (bottom) for the optimized lever system at 250 W. The white and gray backgrounds indicate positive and negative work respectively. A solid line indicates that the lever and chainring are engaged. Knee angle is measured posteriorly with 180° being fully extended. As with the hip, the moment at the knee shows a large extension peak early in the cycle starting just before the system engages. During the upward stroke the joint action reverses from extensor to flexor while the system is engaged. As with the kinematics of the thigh, the knee experiences rapid extension as the lever is engaged during the downward movement and a fast flexion phase during upward movement.

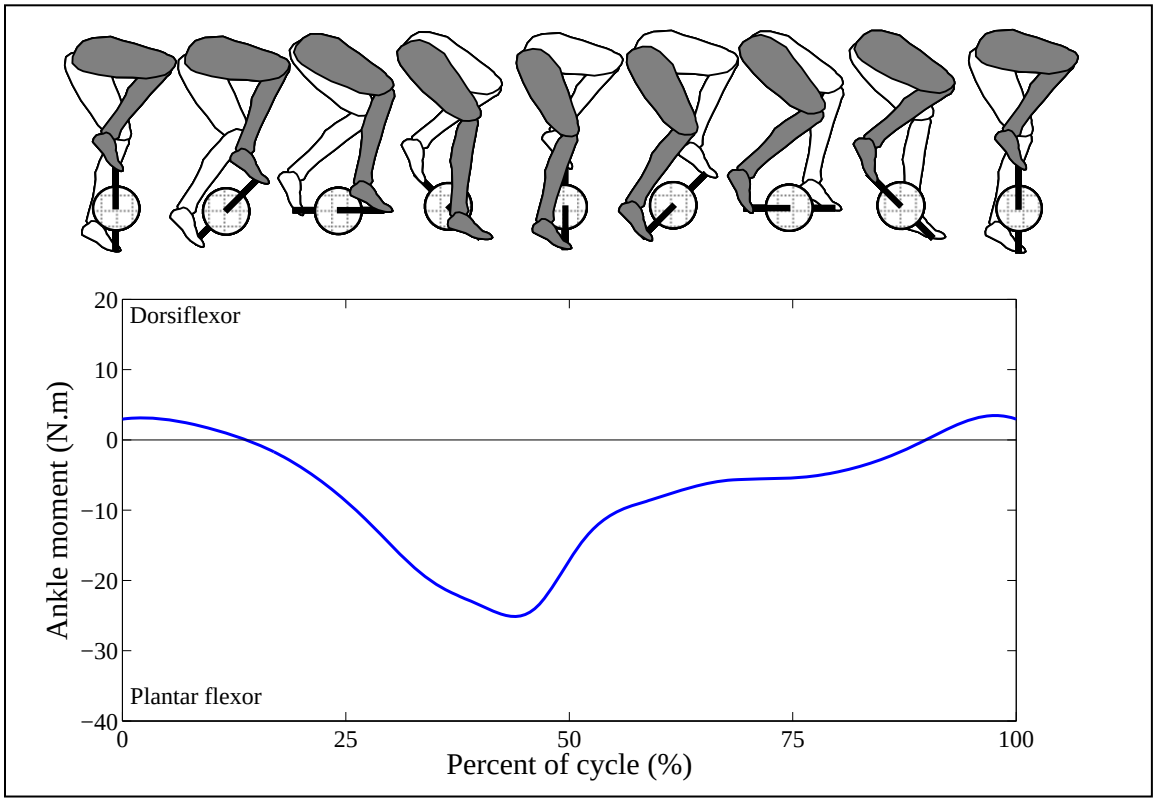

Figure 10. Right ankle joint moment for the optimized circular system at 250 W. During 76% of the cycle the ankle joint experiences a plantar flexor moment. For a short time interval just before and just after top dead center a small dorsiflexor moment occurrs.

the peak moments always occurred during phases when the lever and chainring were engaged (Figures 7, 9, 11).

Transitions between flexor and extensor moments were also different between the two systems. For the circular system, transitions occurred only twice during the motion cycle at each of the joints (Figures 6, 8, 10). The lever system joint moments showed larger fluctuations in amplitude during the cycle of movement, including more numerous transitions between net extensor and net flexor function (Figures 7, 9, 11).

The time of engagement between the lever/crank and chainring is another significant distinction between the lever and the circular results. The crank and chainring

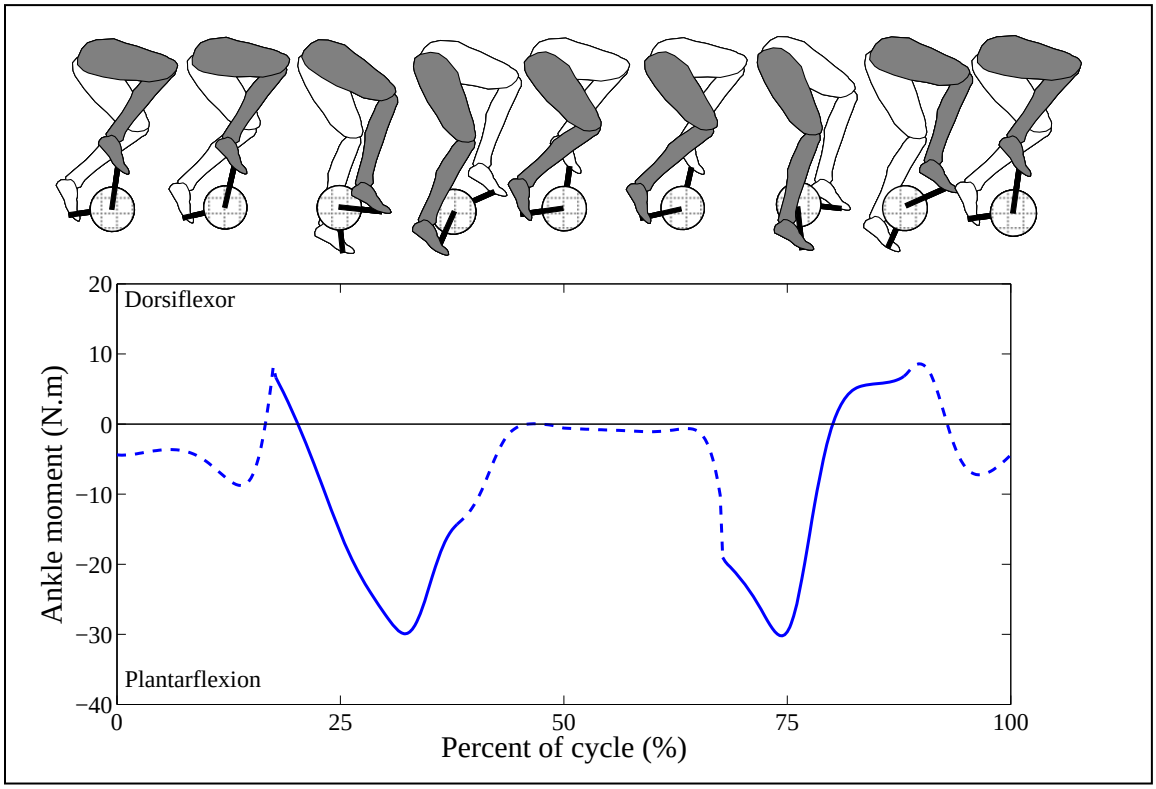

Figure 11. Right ankle joint moment for the optimized lever system at 250 W. A solid line indicates that the lever and chainring is engaged. During the intervals when the system is engaged the joint experiences large plantar flexor moments. This occurrs for both the downward and upward stroke.

were engaged throughout the motion cycle for the circular system indicating power was being input to the crank system by the legs continuously. The lever system was engaged less than half of the cycle time. When considering a half cycle of motion for the lever system from the initiation to the end of the downstroke, results indicated that the system spends the first 35% of the half cycle going from zero angular velocity to the same angular velocity as the chainring at which time the levers and chainring become engaged (Figures 7, 9, 11). The lever and chainring remain engaged for the next 41% of the half cycle of motion before disengaging for the final 24% of the half cycle as the lever angular velocity decreases as it approaches the end of the stroke.

Throughout the motion cycle of the circular and lever systems, phases of positive and negative work occurred at the joints, although phases of negative work were much smaller and occurred less frequently during circular pedaling (Figures 6-9). The ankle joint had no phases of positive or negative work since the ankle joint angle was fixed. During phases in which peak moments were produced for both systems, the hip and knee joints were mainly doing positive work. For the lever system, these phases also coincided with the intervals when the system was engaged.

Kinetic and kinematic measures associated with power transfer at the chainring (i.e., propulsive torque, chainring velocity, chainring acceleration, and power) also showed substantial differences between the circular and lever systems (Figures 12-15).

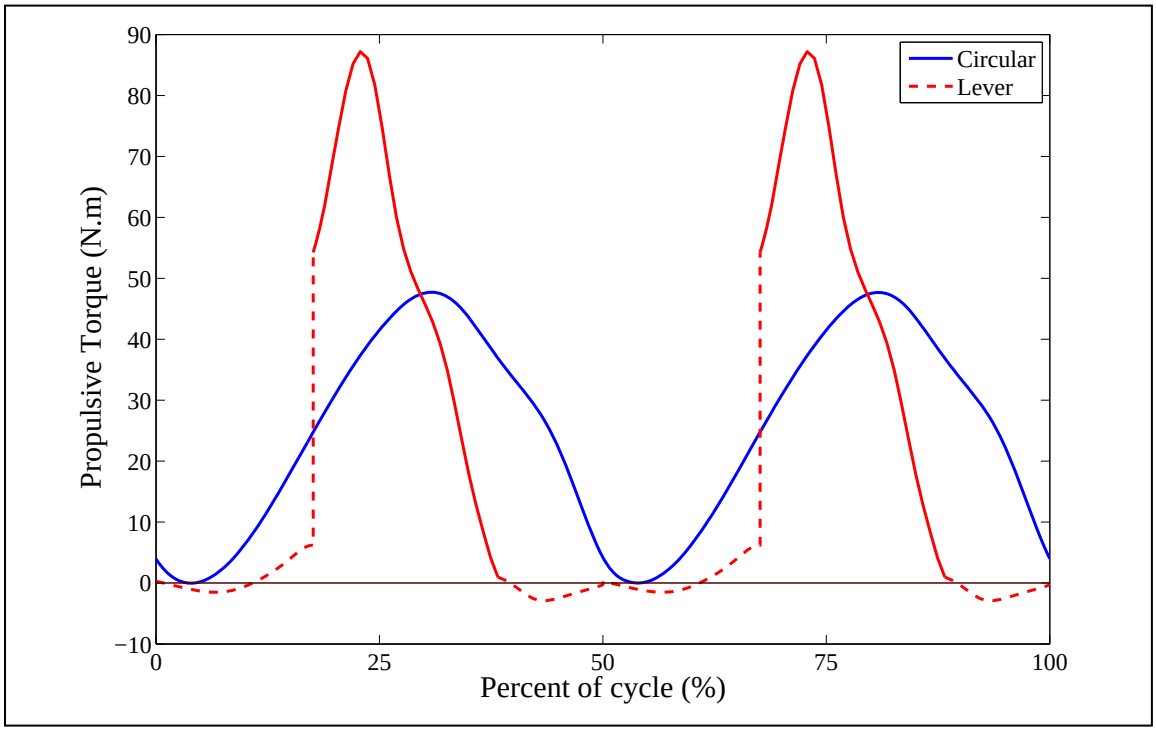

Figure 12. Propulsive torque for the circular system (blue solid line) and lever system (red dashed/solid line) respectively. A red solid line indicates that the lever and chainring are engaged. Maximum propulsive torque during the motion cycle for the lever system was much higher as compared to the circualr system. Propulsion torque for the lever system also showed substantially larger variability during the motion cycle.

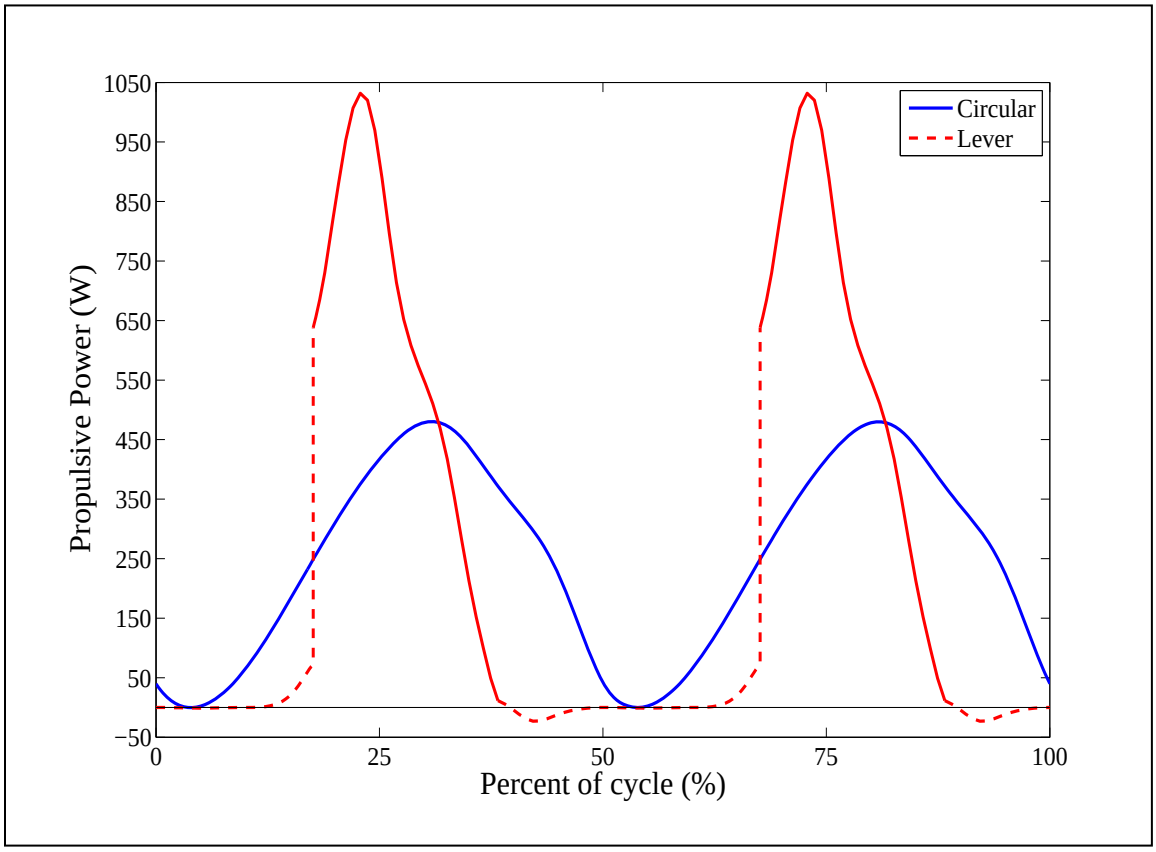

Figure 13. Propulsive power for the circular system (blue solid line) and lever system (red dashed/solid line) respectively. A red solid line indicates that the lever and chainring are engaged. As with propulsive torque, maximum propulsive power for the lever system showed larger peak values during the motion cycle as well as much larger variability throughout the motion cycle compared to the circular system. The lever system propulsive power dropped below zero for small intervals during which the system transferred power to the lower extremities. The circular system power remained positive.

Peak values and the operating ranges for all four of these variables were greater for the lever system. As an example, the instantaneous propulsive power for the lever system operated over a 1055 W range, whereas the instantaneous power for the circular system ranged from 0 to 480 W.

Thigh and knee angular ranges of motion (ROM) were similar for the two systems, with the lever system showing only slightly smaller ranges than the circular system (Table 2). Lever system peak angular velocities for thigh and knee extension

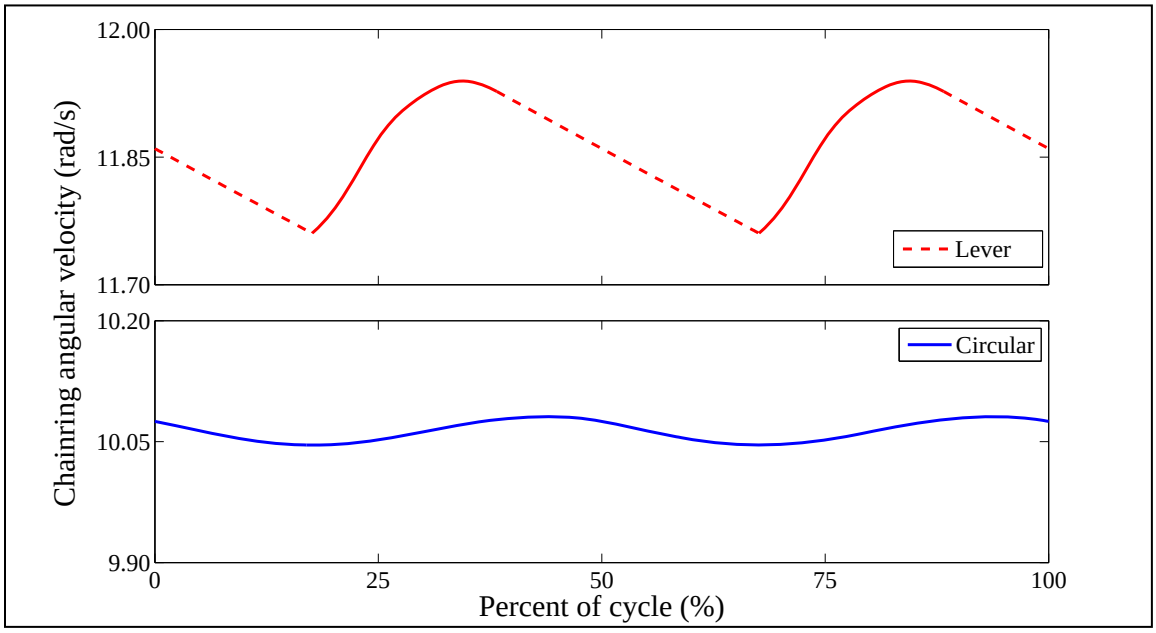

Figure 14. Chainring angular velocity (expressed in rad/s) for the circular system (blue soli d line) and lever system (red dashed/solid line) respectively. A red solid line indicates that the lever and chainring are engaged. The average chainring angular velocity for the lever system was higher than for the circular system. The lever system chainring angular velocity showed larger fluctuations during the motion cycle.

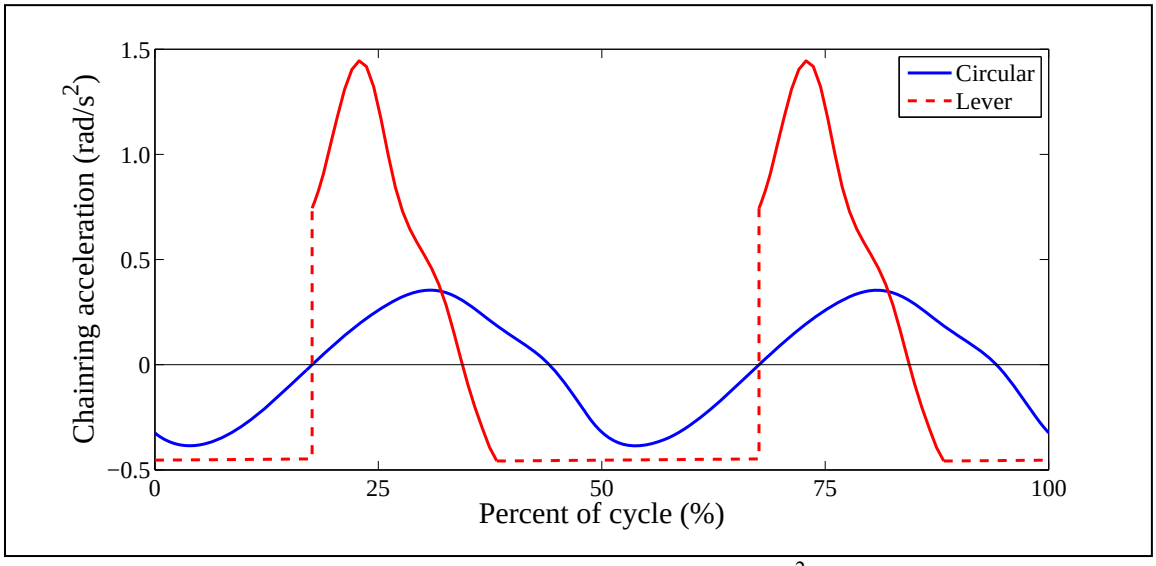

Figure 15. Chainring angular acceleration (expressed in rad/s^2) for the circular system (blue solid line) and lever system (red dashed/solid line) respectively. A red solid line indicates that the lever and chainring are engaged. The lever system experienced phases of much larger acceleration than the circular system. The circular system showed a much smoother profile as the system experienced very subtle acceleration during the motion cycle. During periods when the lever and chainring were disengaged, the chainring experienced nearly constant negative acceleration.

Table 2. Joint ranges of motion (expressed in degrees) at the hip and knee for circular and lever pedaling systems.

Joint	Circular system	Lever system
Hip	58	57
Knee	83	77

Table 3. Peak joint angular velocities (expressed in degrees/s) at the hip and knee for circular and lever pedaling systems.

Joint	Circular system	Lever system
Hip		
Extension	279	351
Flexion	303	352
Knee		
Extension	380	435
Flexion	380	438

and flexion were greater than those for the circular system (Table 3). For the lever system, the angular velocity peaks always occurred when the lever and chainring were (Figures 7, 9).

Sensitivity Analysis

The sensitivity analysis evaluated the impact of model system parameters (i.e., crank length and crank cadence for the circular system and lever length, lever cadence, lever ROM, and average chainring angular velocity for the lever system) on the cost functions for the two systems. For the circular system, sensitivity analysis results indicated that the moment-based cost function was nearly twice as sensitive to changes in

crank length than changes in crank cadence at system parameter values below optimal (Figure 16). However, the optimized cost function increased by less than 5% with 10% changes to crank length and crank cadence. Only the effect of reducing the crank length on the cost function was evaluated since the optimum crank length occurred at the maximum allowed value (and thus increasing the crank length was not feasible). Cost function sensitivity with respect to crank cadence was not symmetrical around the optimal value, as increasing crank cadence had a larger affect than cadence reduction.

The lever system showed larger sensitivity to all system parameters when compared to the circular system (Figure 17). For all the system parameters, the cost function minimum value increased by more than 5% when a 10% change in the system

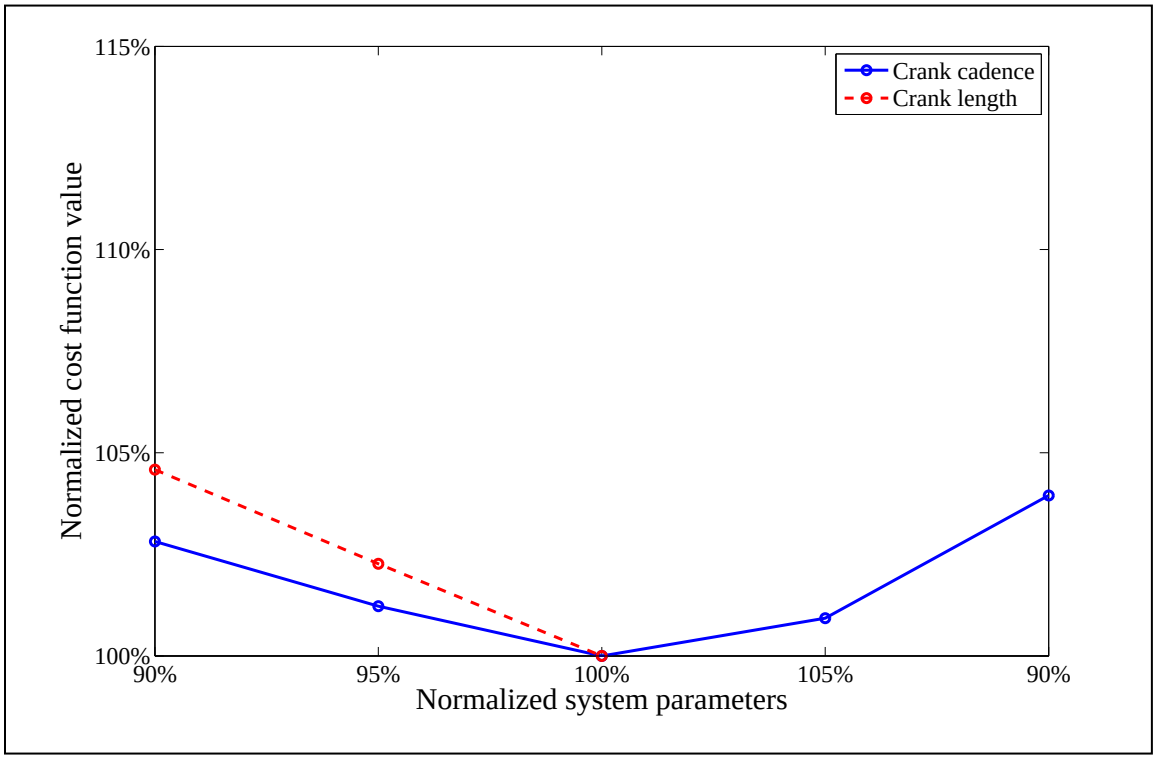

Figure 16. Normalized cost function value versus normalized system parameters for the circular system, indicating the relative sensitivity of the cost function to changes in circular system parameters. Results indicated the cost function was more sensitive to changes in crank length (dashed red line) than changes in cadence (solid blue line).

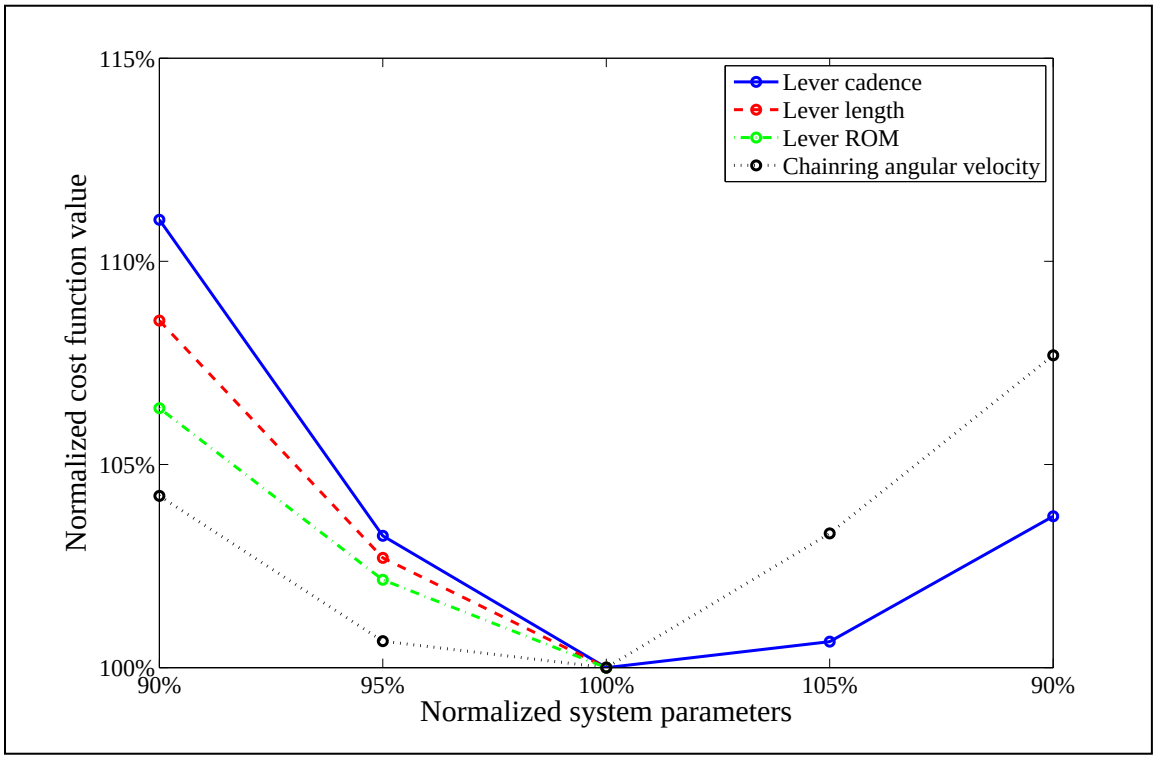

Figure 17. Normalized cost function value versus normalized system parameters for the lever system, indicating the relative sensitivity of the cost function to changes in lever system parameters. Results indicated that when decreasing the parameter values the cost function was most sensitive to changes in lever cadence (solid blue line), followed by lever length (dashed red line), range of motion (ROM) (dashed-dotted green line), and average chainring angular velocity (dotted black line).

parameter was applied. When reducing the system parameters, the cost function was most sensitive to changes in lever cadence, followed by lever length, lever ROM and average angular chainring velocity. For lever length and lever ROM, only the impact of reducing the parameter values were assessed. The impacts of increasing the lever length and lever ROM were not evaluated due to the fact that an increase in either of these parameter values caused the range of motion constraint at the hip to be exceeded. Cost function sensitivity to changes in lever cadence and average chainring angular velocity was not symmetrical around the optimal value.

DISCUSSION

Circular System

Cadence. Considerable research has examined preferred cycling cadence and cadences at which selected physiological and/or mechanical performance variables are either minimized (e.g., aerobic demand or oxygen consumption rate) or maximized (e.g., mechanical power). Most economical cadences (i.e., the cadence at which energy cost is lowest) fall roughly between 40 rpm and 80 rpm (e.g., Boning, Gonen & Maassen, 1984; Coast & Welch, 1985; Marsh and Martin, 1993; 1997; Seabury, Adams, & Ramey, 1977), whereas other performance indicators have typically reflected higher optimal cadences. For example, MacIntosh, Neptune, and Horton (2000) averaged the EMG amplitude of seven lower extremity muscles and found the cadence at which average EMG was the lowest was 86 rpm for cycling power output of 200 W and 99 rpm for 300 W. Marsh, Martin and Sanderson (2000) found the cadence at which the sum of the average absolute joint moments for the lower extremities were minimized was 96 rpm for 250 W cycling.

The optimal cadence predicted by the moment-based model used in the current study (96 rpm) was more similar to optimal cadences found in studies using indicators of muscle functioning (EMG or joint moments) than typically reported values for most economical cadence. The cadence preferred by cyclists is comparable to these muscle function-based values and have been reported between 90 rpm and 100 rpm (e.g., Hagberg, Mullin, Giese, & Spitznagel, 1981; Marsh & Martin, 1993; 1997). These preferred cadences, which were recorded during laboratory testing, are also similar to cadences used during actual race conditions. For example, Lucia, Hoyos, and Chicharro

(2001) reported preferred cadences of 89 rpm during level, steady state time trials and 92 rpm during long flat stages for professional cyclists during three major, multi-stage races (Giro d'Italia, Tour de France, Vuelta Espana).

Other modeling study results of cycling suggest similar or slightly higher optimal cadences than the 96 rpm optimal cadence predicted in this study. Using moment-based cost functions, Gonzalez and Hull (1989) and Redfield and Hull (1986a) reported optimal cadence values of 115 rpm and 105 rpm, respectively, for a 200 W power output. Using an optimization based on muscle stresses of 12 lower limb muscles for a 200 W cycling task, Hull, Gonzalez, and Redfield (1988) found optimal cadences ranging from 95-100 rpm. Neptune and Hull (1999) considered various neuromuscular quantities related to muscle activation, force, stress and endurance and found that all of these properties were minimized at a cadence of 90 rpm for a 265 W power level (when comparing simulations at 75, 90, 105 rpm).

From this overview, it is apparent that many modeling studies predict optimal cadences similar to or modestly higher than preferred cadences normally reported for experienced cyclists. Hull and Jorge (1985) and Redfield and Hull (1986a) discussed how the interaction of pedal force and cadence explains the optimal cadences estimated by moment-based models. They separated joint moment contributions based on moments due to pedal forces, which they referred to as static moments, and moments due to segment motion, referred to as kinematic moments. At low cadences (<70 rpm) static moments are high and contribute largely to the joint moments, whereas at high cadences (> 130 rpm) kinematic moments are the major contributor to net joint moments. Hull and Jorge (1985) suggested that at a cadence value somewhere in the middle of this range

(70-130 rpm) the combined contribution of static and kinematic moments would be at a minimum and therefore provide an optimum solution.

Crank length. Based on popular literature in cycling it seems that a 0.17 m crank length is the most commonly used, although researchers generally suggest that crank length is positively correlated with leg length and should therefore vary with leg length (e.g., Burke & Pritt, 2003; Carmichael et al., 1982; Martin & Spirduso, 2001). Burke and Pritt (2003) indicate that a 0.170 m crank length is suitable for cyclists of average proportions with a height between 1.65 and 1.83 m. They also report that shorter cyclists should consider crank lengths between 0.165 m and 0.168 m and taller cyclists should consider lengths between 0.180 m and 0.185 m.

Experimental studies evaluating the effect of crank length on steady state power output cycling have been limited and results have not been consistent. Carmichael, Loomis, and Hodgson (1982) studied cyclists using six crank lengths ranging from 0.15 m to 0.2 m and found optimal crank length to be positively correlated to leg length. Their prediction equation would suggest an optimal crank length of 0.157 m for the rider modeled in the current study. Carmichael and colleagues noted that crank length change also had a modest effect on energy expenditure. They found that a 0.01 m change from optimum crank length increased mean VO_2 by 4%. Conversely, Conrad and Thomas (1983) found no correlation between crank length and any leg segment length measure and no significant difference in VO_2 values with crank lengths ranging from 0.165 m and 0.18 m.

Other studies examining crank length influences have focused mainly on maximum power cycling. Inbar, Dotan, Trousil, and Dvir (1983) found that the optimal

crank length for maximum power output during a 30 s Wingate test was 0.166 m. With respect to the sensitivity of subjects' performance to changes in crank length, they found that changing the crank length by ± 0.05 m reduced power output by only 1%. More recently, Too and Landwer (2000) examined five crank lengths (0.11 m, 0.145 m, 0.18 m, 0.23 m and 0.265 m) and found power was maximized at crank lengths of 0.145 m and 0.18 m, with no significant power difference between the two lengths. Using a regression equation to fit the data, the optimal crank length for maximizing power output was predicted to be 0.2 m and changing the crank length by ± 0.05 m was predicted to reduce power output by 7%.

Based on minimizing the moment-based cost function in the current study, the optimal crank length for the modeled circular system was 0.2 m, which was the maximum allowable value in the range of 0.14 m to 0.2 m. Other investigators using a modeling approach have reported lower optimal crank lengths. Hull and Gonzalez (1988) and Gonzalez and Hull (1989) estimated optimal crank lengths of 0.145 m and 0.14 m, respectively, for 200 W cycling. A longer crank length for a given cadence implies faster linear velocity of the legs. This will increase the kinematic moments referred to earlier and decrease the static moments. Again, a trade-off exists such that the sum of these components is at a minimum at the optimized value. The length of the crank also has an effect on the ROM at the lower extremity joints. Model results indicated that increasing the length of the crank arm from the standard 0.17 m to 0.2 m increased the hip ROM from 50° to 58° , and the knee ROM from 74° to 83°. Increasing the crank length to higher values might affect the ability of the lower extremity muscles to produce power. Considering the fact that the optimization routine selected the longest

possible crank length in the range, it is conceivable that longer crank lengths might lower the minimum cost function value even more. However, as mentioned above, longer crank lengths have implications for joint ROM's and also reduce the ground clearance for the bicycle. These factors led to the decision not to increase the crank length beyond the 0.2 m maximum value set for the optimization analyses.

The optimal crank length predicted in the current study (0.2 m) differs from the shorter crank lengths predicted by Hull and colleagues (0.145 m and 0.14 m; Hull & Gonzalez, 1988; Gonzalez & Hull, 1989). Hull and Gonzalez (1988) noted their moment-based cost function approached a minimum for both long crank lengths combined with low cadences and short crank lengths combined with high cadences. Modest differences between the models, such as refinements made in the current model in terms of weighting of the knee moment, use of relative rather than absolute moment contributions and different ankle kinematics, may have been sufficient to shift the optimal solution towards a longer crank length in the present study. Furthermore, the sensitivity analysis conducted in the current study demonstrated crank length had only a modest effect on the cost function. The cost function increased by approximately 5% for a 10% change in crank length (figure 16, p. 39). In summary, experimental and modeling results suggest that modification of crank length appears to have a minimal effect on power output, energy expenditure, and moment-based cost function values, even though several researchers have recommended matching crank length with leg length for optimal performance.

Lever System

Cadence. Optimal cadence for the lever system was much slower than the optimal cadence for the circular system. At 48 cpm, the lever system takes 1.25 s to complete the motion cycle, which is twice the time it takes the circular system to complete a rotation at a cadence of 96 rpm. Although the lever system takes much longer to complete its motion compared to the circular system, only 41 % (0.51 s) of this time is spent transferring power from the lever to the chainring. The rest of the time the lever is either catching up to the chainring speed to engage or slowing down following disengagement of the lever from the chainring. The relatively low lever cadence allows more time for the levers to catch up with chainring speed, which reduces peak lever accelerations and the joint moments needed to produce these accelerations.

The optimal average chainring angular velocity was 113 rpm, which was not only much higher than the 48 cpm of the lever, but also higher than the 96 rpm optimal cadence for the circular system. Recall the angular velocities of the chainring and lever are identical when the two are engaged (i.e., approximately 113 rpm), which is the period when propulsive power is generated. For both the lever and circular systems, propulsive torque is generated predominantly by the leg that is pushing down on the crank/lever. Both systems produce peak power during the phase when the lever/crank of this leg is roughly between 90° and 180° past top dead center. During this period, the angular positions and displacements of the legs were similar for the two systems. The two systems also had equal crank/lever lengths (0.2 m). Peak instantaneous power generated during this period by the lever system, however, was 2.2 times higher than that for the circular system. Redfield and Hull (1986a) and MacIntosh et al. (2000) showed optimal

cadence in traditional cycling increases with increasing power output. That is, both studies indicated high power production is associated with high angular velocity of the crank and chainring. The higher optimal chainring angular velocity (113 rpm vs. 96 rpm for the circular system), and therefore the higher lever velocity during the period of high power production, that was predicted by the model in the current study is consistent with the substantially higher peak power generated by the lever system (1033 W vs. 480 W for the circular system).

In summary, optimal cadence results for the lever suggest that a low lever cadence is selected to reduce joint moments required to bring the lever up to the same speed as the chainring. The high optimal value for the average chainring angular velocity is based on the same principle of optimal power transfer as for the circular system. The higher peak power generated by the lever system, however, requires a higher chainring and lever angular velocity compared to the circular system.

Lever length and ROM. The use of a longer lever was initially anticipated to be beneficial for the lever system as a longer lever would increase the moment arm of the force applied through the pedal and reduce the amount of force necessary at the lever to produce the required power output. However, results of this study revealed that the optimum lever length was 0.2 m, which was at the lower end of the allowable range. The reason for this shorter than expected lever length is related to the effect that the lever length has on the ROM of the levers. A longer lever length reduces the ROM of the lever movement path because of constraints placed on minimum knee and hip angles and ground clearance limitations. A reduced ROM resulted in a smaller proportion of cycle time spent with the lever engaged with the chainring, thereby limiting the period of

power transmission from the legs to the chainring and increasing power needed during this briefer period. In contrast, a shorter lever length does not exceed joint and ground clearance constraints and can have a larger lever ROM, which leads to a larger angular displacement through which the lever and chainring can be engaged. From this perspective, one might suggest the system would select a shorter lever length which allows for the largest possible lever ROM, with the levers moving further around the 360° allowable range. A further increase in ROM would situate both levers more posteriorly with respect to the lever axis, which put the lower extremities in a position at which they cannot effectively contribute to power production. This has been shown for circular pedaling, where the power production capability of the legs are at a minimum when the crank is posterior with respect to the crank axis (e.g., Gregor et al., 1985; Kautz & Hull, 1995; Redfield & Hull, 1986a). Thus, increasing the lever ROM even further is not advantageous.

Considering the combination of lever length and ROM, the system optimization process favored a configuration with a relatively short lever length combined with a relatively large ROM.

Interdependence of system parameters. It is important to realize that the four system parameters for the lever system (i.e., lever length, lever cadence, lever ROM, and average chainring angular velocity) are interdependent. Changes in any of the parameters, therefore, affect the optimal values of the others and the associated cost function of the optimal system. It is interesting to take note of the relative effect of changing one of the parameters on the remaining parameters. For example, when the lever length was fixed at the maximum allowable value of 0.51 m instead of the optimum 0.2 m length, the

optimization routine selected the following values for the other three parameters: lever cadence = 132 cpm, average chainring angular velocity = 40 rpm (lower limit), and lever angular ROM = 36°. The minimized cost function value (1395 $N^2 \cdot m^2$) for this system was more than twice the value for the optimized system with a 0.2 m lever (531 $N^2 \cdot m^2$). The first important factor contributing to the increase in cost function was the substantially limited lever ROM that was a result of the ground clearance constraint. The system selected the largest allowable ROM (36° vs. 254° for the optimal system) within the new system constraints. In order to minimize the effort required to increase the lever cadence to the same angular velocity as the chainring during the limited ROM, the optimum chainring angular velocity selected was low. Even though the chainring angular velocity selected was the lowest possible value allowed, this still meant that the lever cadence was high (132 cpm). Choosing a high lever cadence was the only way the system was capable of moving through the small ROM, with the associated accelerations at the start and the end of movement, and still be able connect to the chainring and transfer the required power to the chainring. Although longer levers would theoretically have implied decreased joint moments due to the reduced force necessary at the levers, this factor did not reduce the overall cost function. The fast lever motion required in order to get the system engaged and disengaged over the small ROM, increased the joint moments substantially and overshadowed any possible benefits that longer levers might have afforded. The combined changes in these three parameters clearly demonstrate that the system functioned very differently when a long lever length was used as compared to the shorter optimal value. The shorter lever length allowed for a much larger ROM,

faster average chainring angular velocity, and lower lever cadence that in combination minimized the cost function.

Comparison of Circular and Lever Systems

The minimum cost function value for the optimized lever system was 29% higher than for the optimized circular system, which indicates greater human effort was needed to propel the system at the required 250 W average power output level. The joint moment profiles for the circular and lever propulsion systems provide insight into the higher cost for the lever system. Two differences between the moment profiles for the two systems are especially prominent. First, the peak moments at the hip, knee and ankle were considerably larger for the lever system than for the circular system. These peak moments occurred during the phase when the lever is engaged to the chainring. For steady state cycling the average power at the chainring must be maintained over the motion cycle. When the lever and chainring were not engaged, which was 59% of the total cycle time, the angular velocity of the chainring decreased which resulted in a drop in instantaneous power at the chainring. To increase the instantaneous power at the chainring the lower extremities must transfer power to the system at the lever interface. During the engaged phase, which lasted only 41% of the total motion cycle, high moments were needed to transfer power to the chainring and to the rest of the bicycle. Because of the small proportion of the lever cycle during which the lever and chainring were engaged and power was transferred to the bicycle, instantaneous propulsive power showed large fluctuations. For the lever system, the instantaneous power output at the chainring was very low when the lever and chainring were disengaged. However, when the lever and chainring were engaged and the cyclist was doing positive work on the

system, high power was produced by the necessarily high joint moments seen for the lever system. In circular pedaling, the crank and chainring were engaged throughout the motion cycle and power was continuously transferred to the chainring. The range of instantaneous power during the motion cycle was much lower as compared to the lever system (figure 13, p 36). As a consequence, the joint moments also show substantially less fluctuation and lower peak values during circular pedaling.

A second prominent difference between circular and lever system joint moment profiles is the higher number of flexor-extensor transitions that occurred during the lever cycle of motion compared to the circular system. These flexor-extensor transitions are associated with the movement path and angular velocity of the levers. The angular velocity of the chainring and crank for the circular system remain nearly constant. Model results showed only a 0.4% fluctuation about the average angular velocity (96 rpm) of the chainring and crank. In contrast, the lever system undergoes several periods of significant acceleration throughout its motion cycle. The lever angular velocity ranged from zero at the start and end of a half cycle of motion to a maximum of 114 rpm during the engaged state in the middle of each half cycle of motion. The lever accelerations directly relate to the moments at the joints and therefore the muscular effort needed to drive the system. Harrison (1970) commented on large kinetic energy losses in a lever propulsion mechanism as the system undergoes fluctuations in speed in every half cycle of motion and noted these kinetic energy losses are greatest when the frequency of the movement is highest. Whitt and Wilson (1982) also highlighted the same concern when discussing the disadvantages of a linear drive propulsion mechanism. The relatively low

lever cadence selected for the optimal lever system in the present study is consistent with a solution that would minimize kinetic energy losses in the system.

Study Limitations

While this study has provided insight into the feasibility of an alternative cycling propulsion system, there are several limitations of the study that should be noted. The system was reduced to a one degree of freedom model by constraining ankle motion, a decision made to simplify the simulation and optimization. Experimentally measured joint ankle ROM for circular pedaling is approximately 25° (Hull & Hawkins, 1990). The use of a fixed ankle joint in the model is therefore inconsistent with experimental results. This does not only alter ankle kinematics, but also hip and knee kinematics. However, the influence of these kinematic differences on the cost function was assumed to be minor since good comparison was found in the validation study between experimental and model ankle joint moments generated by the simulation. A second limitation of this study relates to the use of a moment-based model, rather than a muscle driven model. A moment-based model used does not incorporate mechanical and physiological properties of muscle-tendon units, most notably muscle-length and force-velocity properties; gives no consideration to uni- and multiarticular muscle structure and function in the lower extremities; and does not address load sharing across multiple muscles spanning a given joint. More specific to the mechanical characteristics of musculature, a moment-based model does not effectively represent the decline in moment producing capability of musculature as joint angular velocity increases, nor dependence of the ability to produce moments on the joint angle. This limitation is of particular importance because the maximum joint angular velocities for the lever system were

substantially higher than those for the circular system and because maximum joint moments coincided with these high joint velocities. Thus, a moment-based approach provides a highly simplified view of muscle contributions to a complex motion like cycling. Nevertheless, by including directional maximum isometric constraints on the joint moments, as well as reducing the contribution of negative joint work to the cost function value, an attempt was made to create a more physiologically sound model. In addition, a moment-based model can still be informative, especially if elucidating muscle function is not a required outcome. Hull et al. (1988), for example, showed that a moment-based cost function was as effective in estimating optimal cadence as a more complex muscle-stress based cost function. Finally, it should be noted that the lever system in this study is an idealized mechanical model in which the clutch engages instantaneously without any losses. This instantaneous engagement is evident in the discontinuities of the joint moment profiles of the lever system. Further, muscles are incapable of instantaneous generation of high forces and moments. A more realistic representation of fully operational physical system combined with a more realistic representation of muscle contributions would reflect higher losses and reduce the overall performance of the actual system.

Future Directions

This study was limited to the assessment of the human effort needed to maintain 250 W power output with a traditional circular crank system and a specific lever design. While results indicated the lever system was inferior to the circular system for 250 W cycling, there may be other locomotion applications and other performance criteria for which a lever system may offer advantages.

One obvious application would arise when selecting a lower power output as goal. The selected power output of 250 W in this study is typical for experienced, highly fit cyclists in endurance events (Vogt et al., 2007). Recreational cyclists do not necessarily maintain these high levels of power output when cycling for recreation and/or as a means of transport. Lower power output might cause substantial changes in the lever-chainring interaction of the lever system, and possibly make the lever system compare more favorably to the circular system. Consequently, further assessment of lever systems under a variety of power outputs is warranted.

Secondly, although minimizing human effort to maintain a given power output is a valid objective, this is not the only criterion that can be used to evaluate a design. Other criteria might result in different outcomes. Currently there exists a commercially available lever propelled system, the Step 'n Go tricycle (Treadle Power Inc., Burlington, VT), that is used in rehabilitation settings (Miller, Peach, & Keller, 2001). This device has a lever or treadle system situated below the handle bars at the level of the front wheel axle. Riders can push on the pedals while standing or with their weight supported while seated. Miller and colleagues claim that the Step 'n Go cycle device reduces joint ROM's and can be a viable means of transportation for individuals with cognitive, orthopedic, and neuromuscular conditions. Using different criteria for design evaluation, e.g., limiting joint ROM's, may provide the specific lever system with a distinct advantage over the traditional circular system.

To further increase the understanding of the effect of the proposed lever system and other similar systems on the human body, extending the current moment-based model to a muscle-driven model would provide further insights into the advantages and

disadvantages of a lever driven propulsion system. Not only would such an approach enable more accurate representation of moment producing capabilities at the joints with respect to joint angle and joint angular velocities, but it would also provide the ability to examine individual muscle contributions and joint loading. The increased complexity of a muscle-driven modeling approach might offer better insight into how the rider-bicycle system functions as a whole.

In summary, if minimizing muscular effort is not the major objective behind the design, lever pedaling systems might have advantages over the traditional circular system. Further investigations into the current system and other alternative cycling designs are warranted to more fully characterize potential advantages and disadvantages of such systems.

Conclusion

The primary purpose of this computer modeling and simulation study was to compare a traditional circular drive mechanism with a proposed lever pedaling design with respect to human effort required to achieve a power output of 250 W. Because power transfer from the cyclist to the bicycle does not occur continuously for the lever system which results in phases of high acceleration throughout the motion cycle, the lever system is less effective in transferring power from the cyclist to the bicycle. Consequently, it is concluded that the traditional circular propulsion system seen on bicycles requires less human effort to sustain a given power output than that needed for the lever system proposed in this study.

REFERENCES

Abbott, B. C., Bigland, B., & Ritchie, J. M. (1952). The physiological cost of negative work. *Journal of Physiology, 117*(3), 380-90.

Abbott, A. V., Wilson, D. G. (1995). Human power in history. In A. V. Abbott, & D. G. Wilson (Eds.), *Human-powered vehicles* (pp. 1-11). Champaign, IL: Human Kinetics.

Ahlquist, L. E., Bassett, D. R. Jr, Sufit, R., Nagle, F. J., & Thomas, D. P. (1992). The effect of pedaling frequency on glycogen depletion rates in type I and type II quadriceps muscle fibers during submaximal cycling exercise. *European Journal of Applied Physiology and Occupational Physiology, 65*, 360-364.

Anderson, F. C., & Pandy, M. G. (1999). A Dynamic Optimization Solution for Vertical Jumping in Three Dimensions. *Computer Methods in Biomechanics and Biomedical Engineering, 2*(3), 201-231.

Baum, B. S., & Li, L. (2003). Lower extremity muscle activities during cycling are influenced by load and frequency. *Journal of Electromyography and Kinesiology, 13*, 181-190.

Boning, D., Gonen, Y., & Maassen, N. (1984). Relationship between work load, pedal frequency, and physical fitness. *International Journal of Sports Medicine, 5*, 92-97.

Broker, J. P. (2003). Cycling biomechanics: Road and mountain. In E. R. Burke (Ed.), *High-tech cycling* (2nd ed., pp. 119-174). Champaign, IL: Human Kinetics.

Broker, J. P., & Gregor, R. J. (1996). Current issues in cycling biomechanics. In E. R. Burke (Ed.), *High-tech cycling* (pp. 145-166). Champaign, IL: Human Kinetics.

Burke, E. R., Pruitt, A. L. (2003). Body position for cycling. In E. R. Burke (Ed.), *High-tech cycling* (2nd ed., pp. 69-92). Champaign, IL: Human Kinetics.

Cannon, D. T., Kolkhorst, F. W., & Cipriani, D. J. (2007). Effect of pedaling technique on muscle activity and cycling efficiency. *European Journal of Applied Physiology, 99*, 659-664.

Carmichael, J. K. S., Loomis, J. L., Hodgson, J. L. (1982). The effect of crank length on oxygen consumption and heart rate when cycling at a constant output (Abstract). *Medicine and Science in Sports and Exercise, 14,* 162.

Cavanagh, P. R., & Williams, K. R. (1982). The effect of stride length variation on oxygen uptake during distance running. *Medicine and Science in Sports and Exercise, 14*, 30-35.

Coast, J. R., & Welch, H.G. (1985). Linear increase in optimal pedal rate with increased power output in cycle ergometry. *European Journal of Applied Physiology and Occupational Physiology, 53*, 339-342.

Conrad, D. P., & Thomas, T. R. (1983). Bicycle crank arm length and oxygen consumption in trained cyclists (Abstract). *Medicine and Science in Sports and Exercise, 15,* 111.

Cullen, L. K., Andrew, K., Lair, K. R., Widger, M. J., & Timson, B. F. (1992). Efficiency of trained cyclists using circular and noncircular chainrings. *International Journal of Sports Medicine, 13*, 264-269.

Davis, R. R., & Hull, M. L. (1981). Measurement of pedal loading in bicycling: II. Analysis and results. *Journal of Biomechanics, 14*, 857-872.

Davy, D. T., & Audu, M. L. (1987). A dynamic optimization technique for predicting muscle forces in the swing phase of gait. *Journal of Biomechanics. 20*, 187-201.

Dempster, W. T. (1955). Space requirements of the seated operator. *WADC Technical Report 55-159*. Wright Patterson Air Force Base, Dayton, OH.

Drillis, R., & Contini, R. (1966). Body segment parameters. New York, New York: Office of Vocational Rehabilitation. Report No.: 1166-03.

Dorel, S., Bourdin, M., Van Praagh, E., Lacour, J. R., & Hautier, C. A. (2003). Influence of two pedalling rate conditions on mechanical output and physiological responses during all-out intermittent exercise. *European Journal of Applied Physiology, 89*(2), 157-165.

Ericson, M. O., & Nisell, R. (1988). Efficiency of pedal forces during ergometer cycling. *International Journal of Sports Medicine, 9*, 118-122.

Faria, E. W., Parker, D. L., & Faria, I. E. (2005). The science of cycling: factors affecting performance - part 2. *Sports Medicine, 35*, 313-337.

Fregly, B. J., & Zajac, F. E. (1996). A state-space analysis of mechanical energy generation, absorption, and transfer during pedaling. *Journal of Biomechanics, 29*, 81-90.

Fregly, B. J., Zajac, F. E., & Dairaghi, C. A. (2000). Bicycle drive system dynamics: theory and experimental validation. *Journal of Biomechanical Engineering, 122*, 446-452.

Garside, I., & Doran, D. A. (2000). Effects of bicycle frame ergonomics on triathlon 10-km running performance. *Journal of Sports Sciences, 18*, 825-833.

Gonzalez, H., & Hull, M. L. (1989). Multivariable optimization of cycling biomechanics. *Journal of Biomechanics, 22*, 1151-1161.

Gregor, R. J., Cavanagh, P. R., & LaFortune, M. (1985). Knee flexor moments during propulsion in cycling--a creative solution to Lombard's Paradox. *Journal of Biomechanics, 18*, 307-316.

Hagberg, J. M., Mullin, J. P., Giese, M. D., & Spitznagel, E. (1981). Effect of pedaling rate on submaximal exercise responses of competitive cyclists. *Journal of Applied Physiology, 51*(2), 447-451.

Hamley, E. J., & Thomas, V. (1967). Physiological and postural factors in the calibration of the bicycle ergometer. *Journal of Physiology, 191*, 55P-56P.

Harrison, J. Y. (1970). Maximizing human power output by suitable selection of motion cycle and load. *Human factors, 12*(3), 315-329.

Haug, E. J. (1989). *Computer Aided Kinematics and Dynamics of Mechanical Systems: Volume I: Basis Methods*. Boston: Allyn and Bacon.

Heil, D. P., Wilcox, A. R., & Quinn, C. M. (1995). Cardiorespiratory responses to seat-tube angle variation during steady-state cycling. *Medicine and Science in Sports and Exercise, 27*, 730-735.

Henderson, S. C., Ellis, R. W., Klimovitch, G., & Brooks, G. A. (1977). The effects of circular and elliptical chainwheels on steady-rate cycle ergometer work efficiency. *Medicine and Science in Sports, 9*, 202-207.

Hill, A.V. (1938). The heat of shortening and the dynamic constants of muscles. *Proceedings of the Royal Society B: Biological Science, 126*, 136-195.

Holt, K. G., Hamill, J., & Andres, R. O. (1991). Predicting the minimal energy costs of human walking. *Medicine and Science in Sports and Exercise, 23*, 491-498.

Hue, O., Chamari, K., Damiani, M., Blonc, S., & Hertogh, C. (2007). The use of an eccentric chainring during an outdoor 1km all-outcycling test. *Journal of Science and Medicine in Sport, 10*(3), 180-186.

Hue, O., Galy, O., Hertogh, C., Casties, J. F., & Prefaut, C. (2001). Enhancing cycling performance using an eccentric chainring. *Medicine and Science in Sports and Exercise, 33*, 1006-1010.

Hull, M. L., & Gonzalez, H. (1988). Bivariate optimization of pedalling rate and crank arm length in cycling. *Journal of Biomechanics, 21*, 839-849.

Hull, M. L., Gonzalez, H. K., & Redfield R. (1988). Optimization of pedaling rate in cycling using a muscle stress-based objective function. *International Journal of Sport Biomechanics, 4*, 1-20.

Hull, M. L., Hawkins, D. A. (1990). Analysis of muscular work in multisegmental movements: applications to cycling. In J. M. Winters, & S. L-Y. Woo (Eds.), *Multiple Muscle Systems: Biomechanics and Movement Organization* (pp. 621-638). New York: Springer.

Hull, M. L., & Jorge, M. (1985). A method for biomechanical analysis of bicycle pedalling. *Journal of Biomechanics, 18*, 631-644.

Hull, M. L., Kautz, S., & Beard, A. (1991). An angular velocity profile in cycling derived from mechanical energy analysis. *Journal of Biomechanics, 24*, 577-586.

Hull, M. L., Williams, M., Williams, K., & Kautz, S. (1992). Physiological response to cycling with both circular and noncircular chainrings. *Medicine and Science in Sports and Exercise, 24*, 1114-1122.

Inbar, O., Dotan, R., Trousil, T., & Dvir, Z. (1983). The effect of bicycle crank-length variation upon power performance. *Ergonomics, 26*, 1139-1146.

Kautz, S. A. (1992). Biomechanics of pedaling with non-circular and circular chainrings in cycling. Ph.D. thesis, Biomedical Engineering Group, University of California, Davis.

Kautz, S. A., & Hull, M. L. (1993). A theoretical basis for interpreting the force applied to the pedal in cycling. *Journal of Biomechanics, 26*, 155-165.

Kautz, S. A., & Hull, M. L. (1995). Dynamic optimization analysis for equipment setup problems in endurance cycling. *Journal of Biomechanics, 28*, 1391-1401.

Kautz, S. A., & Neptune, R. R. (2002). Biomechanical determinants of pedaling energetics: internal and external work are not independent. *Exercise and Sport Sciences Reviews, 30*, 159-165.

Korff, T., Romer, L. M., Mayhew, I., & Martin, J. C. (2007). Effect of pedaling technique on mechanical effectiveness and efficiency in cyclists. *Medicine and Science in Sports and Exercise, 39*, 991-995.

Kyle, C. R. (1991). Alternative bicycle transmissions. *Cycling Science, 3*, 33-38.

Kyle, C. R. (2003). Selecting cycling equipment. In E. R. Burke (Ed.), *High-Tech Cycling* (2nd ed., pp. 1-48). Champaign, IL: Human Kinetics.

Lollgen, H., Graham, T., & Sjogaard, G. (1980). Muscle metabolites, force, and perceived exertion bicycling at varying pedal rates. *Medicine and Science in Sports and Exercise, 12*, 345-351.

Lucia, A., Balmer, J., Davison, R. C., Perez, M., Santalla, A., & Smith, P.M. (2004). Effects of the rotor pedalling system on the performance of trained cyclists during incremental and constant-load cycle-ergometer tests. *International Journal of Sports Medicine, 25*, 479-485.

Lucia, A., Hoyos, J., & Chicharro, J. L. (2001). Preferred pedalling cadence in professional cycling. *Medicine and Science in Sports and Exercise, 33*, 1361-1366.

MacIntosh, B. R., Neptune, R. R., & Horton, J. F. (2000). Cadence, power, and muscle activation in cycle ergometry. *Medicine and Science in Sports and Exercise, 32*, 1281-1287.

Markhede, G., & Grimby, G. (1980). Measurement of strength of hip joint muscles. *Scandinavian Journal of Rehabilitation Medicine, 12*, 169-174.

Marsh, A. P., & Martin, P. E. (1993). The association between cycling experience and preferred and most economical cadences. *Medicine and Science in Sports and Exercise, 25*, 1269-1274.

Marsh, A. P., & Martin, P. E. (1995). The relationship between cadence and lower extremity EMG in cyclists and noncyclists. *Medicine and Science in Sports and Exercise, 27*, 217-225.

Marsh, A. P., & Martin, P. E. (1997). Effect of cycling experience, aerobic power, and power output on preferred and most economical cycling cadences. *Medicine and Science in Sports and Exercise, 29*, 1225-1232.

Marsh, A. P., & Martin, P.E. (1998). Perceived exertion and the preferred cycling cadence. *Medicine and Science in Sports and Exercise, 30*, 942-948.

Marsh, A. P., Martin, P. E., & Sanderson, D. J. (2000). Is a joint moment-based cost function associated with preferred cycling cadence? *Journal of Biomechanics, 33*, 173-180.

Marsh, E., Sale, D., McComas, A. J., & Quinlan, J. (1981). Influence of joint position on ankle dorsiflexion in humans. *Journal of Applied Physiology, 51*, 160-167.

Martin, J. C., Lamb, S. M., & Brown, N. A. (2002). Pedal trajectory alters maximal single-leg cycling power. *Medicine and Science in Sports and Exercise, 34*, 1332-1336.

Martin, J. C., Milliken, D. L., Cobb, J. E., McFadden, K. L., & Coggan, A., R. (1998). Validation of a mathematical model for road cycling power. *Journal of Applied Biomechanics, 14*, 276-291.

Martin, J. C., & Spirduso, W. W. (2001). Determinants of maximal cycling power: crank length, pedaling rate and pedal speed. *European Journal of Applied Physiology, 84*, 413-418.

McCartney, N., Obminski, G., & Heigenhauser, G. J. (1985). Torque-velocity relationship in isokinetic cycling exercise. *Journal of Applied Physiology, 58*, 1459-1462.

McLean, B. D., & Lafortune, M. A. (1991). Influence of cadence on mechanical parameters of pedaling. *Proceedings of XIIIth International Congress of Biomechanics, Perth, Australia*, pp. 102-104.

Miller, M. S., Peach, J. P., & Keller, T. S. (2001). Electromyographic analysis of a human powered stepper cycle during seated and standing riding. *Journal of Electromyography and Kinesiology, 11,* 413-423.

Miller, N. R., & Ross, D. (1980). The Design of Variable-Ratio Chain Drives for Bicycles and Ergometers - Application to a Maximum Power Bicycle Drive. *Journal of Mechanical Design, 102*, 711-717.

Minetti, A. E., Pinkerton, J., & Zamparo, P. (2001). From bipedalism to bicyclism: evolution in energetics and biomechanics of historic bicycles. *Proceedings of the Royal Society B: Biological Sciences, 268*, 1351-60.

Mornieux, G., Guenette, J. A., Sheel, A. W., & Sanderson, D. J. (2007). Influence of cadence, power output and hypoxia on the joint moment distribution during cycling. *European Journal of Applied Physiology, 102*(1), 11-18.

Nemeth, G., Ekholm, J., Arborelius, U. P., Harms-Ringdahl, K., & Schuldt, K. (1983). Influence of knee flexion on isometric hip extensor strength. *Scandinavian Journal of Rehabilitation Medicine, 15*, 97-101.

Neptune, R. R. (1999). Optimization algorithm performance in determining optimal controls in human movement analyses. *Journal of Biomechanical Engineering, 121*, 249-252.

Neptune, R. R., & Hull, M. L. (1998). Evaluation of performance criteria for simulation of submaximal steady-state cycling using a forward dynamic model. *Journal of Biomechanical Engineering, 120*, 334-341.

Neptune, R. R., & Hull, M. L. (1999). A theoretical analysis of preferred pedaling rate selection in endurance cycling. *Journal of Biomechanics, 32*, 409-415.

Neptune, R. R., & Van Den Bogert, A.J. (1998). Standard mechanical energy analyses do not correlate with muscle work in cycling. *Journal of Biomechanics, 31*, 239-245.

Newmiller, J., Hull, M. L., & Zajac, F. E. (1988). A mechanically decoupled two force component bicycle pedal dynamometer. *Journal of Biomechanics, 21*, 375-386.

Nordeen-Snyder, K. S. (1977). The effect of bicycle seat height variation upon oxygen consumption and lower limb kinematics. *Medicine and Science in Sports, 9*, 113-117.

Okajima, S. (1983). Designing chainwheels to optimize the human engine. *Bike Tech, 2*, 1-7.

Pandy, M. G. (2001). Computer modeling and simulation of human movement. *Annual Review of Biomedical Engineering, 3*, 245-273.

Pandy, M. G., & Zajac, F. E. (1991). Optimal muscular coordination strategies for jumping. *Journal of Biomechanics, 24*, 1-10.

Patterson, R. P., & Moreno, M. I. (1990). Bicycle pedalling forces as a function of pedalling rate and power output. *Medicine and Science in Sports and Exercise, 22*, 512-516.

Perry, D. B. (1995). *Bike cult: The ultimate guide to human-powered vehicles*. New York, NY: Four Walls Eight Windows.

Price, R. (1995). Drive-train design. In A. V. Abbott, & D. G. Wilson (Eds.), *Human-Powered Vehicles* (pp. 173-196). Champaign, IL: Human Kinetics.

Price, D., & Donne, B. (1997). Effect of variation in seat tube angle at different seat heights on submaximal cycling performance in man. *Journal of Sports Sciences, 15*(4), 395-402.

Raasch, C. C., Zajac, F. E., Ma, B., & Levine, W. S. (1997). Muscle coordination of maximum-speed pedaling. *Journal of Biomechanics, 30*, 595-602.

Ratel, S., Duche, P., Hautier, C. A., Williams, C. A., & Bedu, M. (2004). Physiological responses during cycling with noncircular "Harmonic" and circular chainrings. *European Journal of Applied Physiology, 91*, 100-104.

Redfield, R., & Hull, M. L. (1986a). On the relation between joint moments and pedalling rates at constant power in bicycling. *Journal of Biomechanics, 19*, 317-329.

Redfield, R., & Hull, M. L. (1986b). Prediction of pedal forces in cycling using optimization methods. *Journal of Biomechanics, 19*, 523-540.

Ricard, M. D., Hills-Meyer, P., Miller, M. G., & Michael, T. J. (2006). The effects of bicycle frame geometry on muscle activation and power during a Wingate anaerobic test. *Journal of Sports Science and Medicine, 5*(1), 25-32.

Roosa, D. (1988). Shimano Biopace. *Bicycle Guide, 5*, 79-83.

Sanderson, D. J. (1991). The influence of cadence and power output on the biomechanics of force application during steady-rate cycling in competitive and recreational cyclists. *Journal of Sports Sciences, 9(*2), 191-203.

Sanderson, D. J., Martin, P. E., Honeyman, G., & Keefer, J. (2006). Gastrocnemius and soleus muscle length, velocity, and EMG responses to changes in pedalling cadence. *Journal of Electromyography and Kinesiology, 16*(6), 642-649.

Santalla, A., Manzano, J. M., Perez, M., & Lucia, A. (2002). A new pedaling design: the Rotor - effects on cycling performance. *Medicine and Science in Sports and Exercise, 34*, 1854-1858.

Scudder, G. N. (1980). Torque curves produced at the knee during isometric and isokinetic exercise. *Archives of Physical Medicine and Rehabilitation, 61*, 68-73.

Shennum, P. L., & DeVries, H. A. (1976). The effect of saddle height on oxygen consumption during bicycle ergometer work. *Medicine and Science in Sports, 8*, 119-121.

Takaishi, T., Yasuda, Y., Ono, T., & Moritani, T. (1996). Optimal pedaling rate estimated from neuromuscular fatigue for cyclists. *Medicine and Science in Sports and Exercise, 28*, 1492-1497.

Takaishi, T., Yasuda, Y., & Moritani, T. (1994). Neuromuscular fatigue during prolonged pedalling exercise at different pedalling rates. *European Journal of Applied Physiology and Occupational Physiology, 69*(2), 154-158.

Thelen, D. G., Anderson, F. C., & Delp, S. L. (2003). Generating dynamic simulations of movement using computed muscle control. *Journal of Biomechanics, 36*, 321-328.

Too, D., & Landwer, G. E. (2000). The effect of pedal crank arm length on joint angle and power production in upright cycle ergometry. *Journal of Sports Sciences, 18*, 153-161.

Umberger, B. R., Gerritsen, K. G., & Martin, P. E. (2006). Muscle fiber type effects on energetically optimal cadences in cycling. *Journal of Biomechanics, 39*, 1472-1479.

Van Soest, O., & Casius, L. J. (2000). Which factors determine the optimal pedaling rate in sprint cycling? *Medicine and Science in Sports and Exercise, 32*, 1927-1934.

Van Ingen Schenau, G. J., Boots, P. J., De Groot, G., Snackers, R. J., & Van Woensel, W. W. (1992). The constrained control of force and position in multi-joint movements. *Neuroscience, 46*, 197-207.

Vogt, S., Schumacher, Y. O., Roecker, K., Dickhuth, H. H., Schoberer, U., Schmid, A., & Heinrich, L. (2007). Power output during the Tour de France. *International Journal of Sports Medicine, 28*, 756-761.

Whitt, R. W., & Wilson, D. G. (1982). *Bicycling science* (2nd ed.). Cambridge, MA: MIT Press.

Yoshihuku, Y., & Herzog, W. (1990). Optimal design parameters of the bicycle-rider system for maximal muscle power output. *Journal of Biomechanics, 23*, 1069-1079.

Yoshihuku, Y. & Herzog, W. (1996). Maximal muscle power output in cycling: a modelling approach. *Journal of Sports Sciences, 14*(2), 139-157.

Zajac, F. E. (2002). Understanding muscle coordination of the human leg with dynamical simulations. *Journal of Biomechanics, 35*, 1011-1018.

Zajac, F. E., Neptune, R. R., & Kautz, S. A. (2002). Biomechanics and muscle coordination of human walking. Part I: introduction to concepts, power transfer, dynamics and simulations. *Gait and Posture, 16*, 215-232.

Zameziati, K., Mornieux, G., Rouffet, D., & Belli, A. (2006). Relationship between the increase of effectiveness indexes and the increase of muscular efficiency with cycling power. *European Journal of Applied Physiology, 96*, 274-281.

Zamparo, P., Minetti, A., Di Prampero, P. (2002). Mechanical efficiency of cycling with a new developed pedal-crank. *Journal of Biomechanics, 35*, 1387-1398.

Zarrugh, M. Y., Todd, F. N., & Ralston, H. J. (1974). Optimization of energy expenditure during level walking. *European Journal of Applied Physiology and Occupational Physiology, 33*(4), 293-306.

APPENDIX A

Human Model Characteristics

Cyclist Anthropometric and Inertial Properties (for 50th percentile U.S. rider with a body mass of 77.8 kg and height of 1.78 m).

Segment Length:

Thigh	0.436 m
Shank	0.438 m
Foot	0.139 m

Segment Center of Mass (distance measured from proximal joint):

Thigh	0.189 m
Shank	0.190 m
Foot	0.060 m

Segment Mass:

Thigh	7.780 kg
Shank	3.618 kg
Foot	1.128 kg

Segment Moment of inertia:

Thigh	0.154 $kg \cdot m^2$
Shank	0.063 $kg \cdot m^2$
Foot	0.005 $kg \cdot m^2$

(Segment lengths: Drillis & Contini, 1966; segment centers of mass, masses, moments of inertia: Dempster, 1955)

Maximum Isometric Joint Moment Values

Hip:

Hip extension	290 N·m
Hip flexion	180 N·m

Knee:

Knee extension	290 N·m
Knee flexion	170 N·m

Ankle:

Ankle plantar flexion	170 N·m
Ankle dorsiflexion	50 N·m

(Hip extension: Nemeth et al., 1983; hip flexion: Markhede & Grimby, 1980; knee extension and flexion: Scudder, 1980; ankle plantar flexion: Sale et al., 1982); ankle dorsiflexion: Marsh et al., 1981).

APPENDIX B

Preliminary Analyses - Refinements of Moment-Based Cost Functions Improve Prediction of Experimental Moment Profiles in Cycling•

Introduction

Many cycling simulations (e.g., Gonzalez & Hull, 1989; Kautz & Hull, 1995) have employed joint moment-based computer models. A common cost function in simulations is based on the sum of squares of ankle, knee, and hip moments (e.g., Kautz & Hull, 1995; Redfield & Hull, 1986). In its simplest form absolute joint moments are used with equal weighting of concentric and eccentric contributions and equal contributions of the three joints. Potential refinements include using net joint moments expressed relative to maximum flexion and extension moment capacities, representing eccentric effort as some fraction of concentric effort, and weighting contributions from the ankle, knee, and hip differently (e.g., Kautz (1992) doubled the relative cost of the knee in cycling simulations). Our purpose was to evaluate the effect of these three refinements on the accuracy of predicting experimentally-derived lower extremity moments for 250 W cycling at 90 rpm. We predicted each of these refinements would result in more accurate lower extremity moment profiles.

Methods

The leg-bicycle system was modeled as a planar five bar-linkage for each leg. The three degree of freedom (DOF) model was reduced to a one DOF system by constraining the ankle motion to follow experimentally collected data. The problem was formulated using a dynamic forward optimization framework that minimized a given cost function

---

• The content of this appendix was submitted as an abstract to the North American Conference on Biomechanics 2008 by H. van Werkhoven, H.J. Sommer, and P.E. Martin.

for the system task and constraints. Joint moments were parameterized using 12 discrete nodes; values between nodes were calculated through interpolation. The optimization problem was solved using a standard non-linear optimization routine. Four cost functions were used:

CF1: $\int_0^{t_f} \left(M_h^{\,2} + M_k^{\,2} + M_a^{\,2} \right) dt$

CF1 used absolute moment amplitudes, provided no distinction between concentric and eccentric contributions, and equally weighted effort at the hip, knee, and ankle. It served as the nominal condition to which other cost functions were compared.

CF2: $\int_0^{t_f} \left(\%M_h^{\,2} + \%M_k^{\,2} + \%M_a^{\,2} \right) dt$

CF2 expressed moments as a percentage of maximum isometric moment capacity.

CF3: $\int_0^{t_f} \left(M_h^{\,*2} + M_k^{\,*2} + M_a^{\,*2} \right) dt$

CF3 weighted eccentric contributions at 1/3 those of concentric contributions.

CF4: $\int_0^{t_f} \left(M_h^{\,2} + 2M_k^{\,2} + M_a^{\,2} \right) dt$

CF4 doubled the importance of knee contributions as suggested by Kautz (1992).

A final model (ALL) incorporated all three modifications to examine their collective effect. Optimized joint moment histories for all cost functions were compared to experimental cycling joint moments from Kautz and Hull (1995). Root mean square error (RMSE) between experimental and simulated results were calculated for each cost function at each joint and averaged across joints.

Results

ALL matched experimental hip joint moment most accurately, although each of the cost functions underestimated maximum hip extension moments (Figure B-1). CF2 predicted experimental knee joint moment most accurately (Figure B-1). Each of the other cost functions underestimated the knee extensor moment. The ankle moment was simulated effectively by all cost functions (Figure B-1), but was matched most closely by ALL. The mean RMSE between experimental results and simulation outputs using individual cost functions was the lowest for CF2, followed by CF4, CF3 and CF1 (Table B-1). The difference between CF3 and CF1, however, was negligible. ALL showed the biggest reduction in RMSE.

Discussion

A moment-based cost function expressing moments relative to maximum capabilities (CF2); which recognizes that moment generating capacity is not equal across the ankle, knee, and hip; improved prediction of experimental moment profiles substantially relative to the nominal case (CF1). Increasing the importance of the knee moment (CF4) made the second largest improvement in prediction of experimental profiles. This result suggests the relative importance of the knee musculature during the cycling task. Reducing the importance of eccentric contributions (CF3) had little effect on model predictive ability. This is presumably linked to the limited eccentric effort reflected in the cycling task. Overall, results indicate more physiologically sound cost functions improve the accuracy of prediction of experimental results.

Table B-1. Mean RMSE across all joints for the different cost functions and percent change relative to the original cost function (CF1).

	CF1	CF2	CF3	CF4	ALL
RMSE	**17.3**	**16.1**	**17.1**	**16.5**	**14.3**
% change	-	6.7%	1.1%	4.6%	17.3%

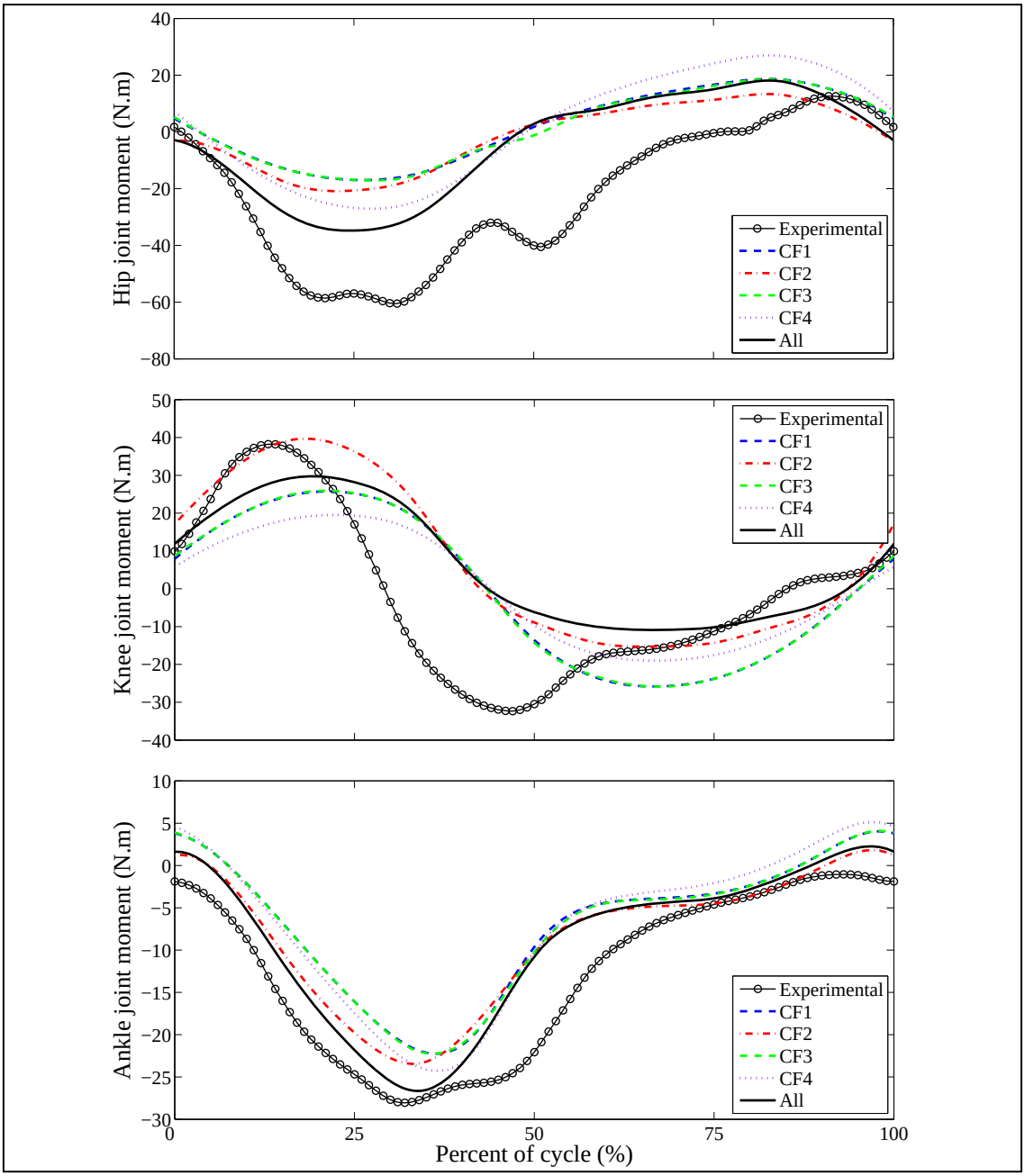

Figure B-1. Experimental and simulated joint moments at the hip (top), knee (middle), and ankle (bottom).

APPENDIX C

Literature Review

Introduction

The aim of this literature review is to gain insight into the design of the human-bicycle interface. The review will consider how power is transferred from the human to the bicycle and finally to the ground in order to propel the bicycle forward. The main focus is on modeling and simulation research studying the interface between the lower limbs of the cyclist and the drive system, and factors that might affect this interaction. Other effects, such as aerodynamics and material design of the bicycle, are not considered in this review.

The first section gives a brief history of the human-bicycle interface, highlighting some of the major design changes that have occurred over time. Characteristics of power transfer during conventional cycling are discussed next. Insight into power transfer during conventional cycling serves as a platform from which to discuss and compare alternative cycling drive mechanisms. Subsequently, different modeling and simulation strategies used to gain an understanding of cycling are reviewed. Various methods and advantages and disadvantages of each will be discussed. This is followed by a discussion of previous modeling and simulation studies related to the drive mechanism. The focus will be on various designs that have challenged the conventional circular pedal and crank system. Where applicable and where such studies exist, experimental work is included. Other design issues not necessarily related to the drive mechanism, as well as some physiological variables, namely cadence and muscle functioning, are also discussed, as these might have an effect on the optimal design of an alternative drive mechanism.

A Brief History of the Human-Bicycle Interface

The origin of the bicycle can probably be traced back to the invention of the Draisienne or the Hobby Horse (1817) by the German Karl von Drais (Abbot & Wilson, 1995). In this design, the cyclist had no mechanical system to transfer power to the bicycle, but instead generated propulsion by pushing directly against the ground with the feet (Figure C-1a). This design was soon followed by a system where the cyclist could use both leg and arm power. In Gompertz's velocipede of 1821, the cyclist still pushed with the feet on the ground, but could also provide power using the arms. A ratchet drive was connected to the front wheel, enabling users to pull on a bar with the hands, which then delivered power to the front wheel through a lever with sector gear (Figure C-1b). Around 1840 the MacMillan velocipede was built, which was the first design to transfer leg power directly to the wheels, instead of pushing on the ground (Abbot & Wilson, 1995). This design used a treadle system, where the feet moved levers that were connected to the back wheel (Figure C-1c). This of course ensured that the legs were elevated off the ground, making it the first truly self-balancing bicycle design (Whitt & Wilson, 1982). The feet were situated anterior and inferior to the body, and moved continuously forward and backward in an arc to generate power. The Boneshaker, introduced in the 1860s, was the first system to use a pedal crank mechanism. The pedal and crank was however directly connected to the front wheel axle (Figure C-1d). This design was followed by the High Wheeler, also called 'ordinary' or 'penny farthing' (Minetti, Pinkerton, & Zamparo, 2001) (Figure C-1e). For this system, drive mechanism was still connected to the front wheel, but the size of the front wheel was increased, the rational being that each pedal revolution would make the bicycle go further (Perry, 1995).

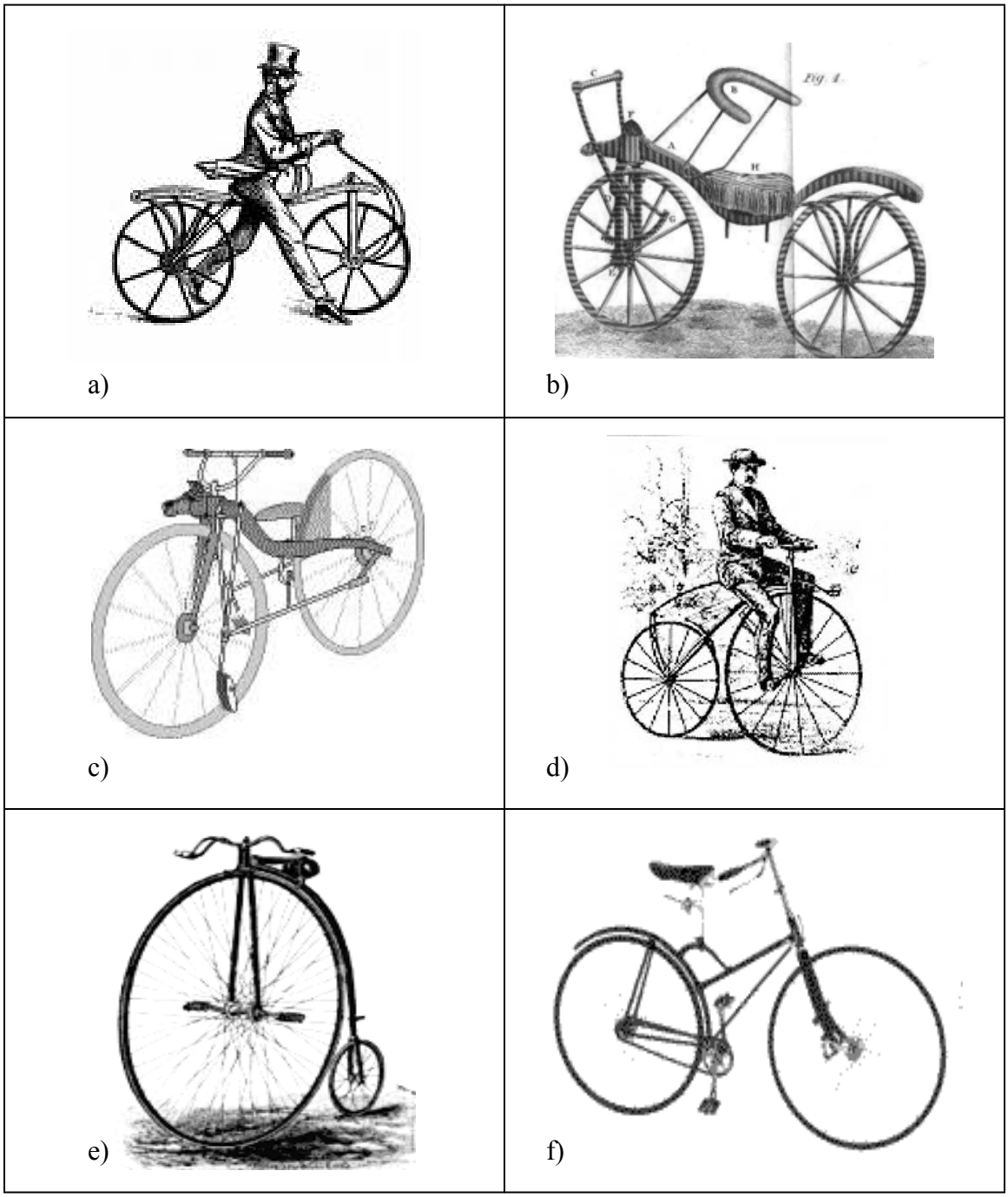

Figure C-1. Different bicycle designs. (a) Draisienne or Hobby Horse; (b) Gompertz's velocipede; (c) MacMillan velocipede; (d) Boneshaker; (e) High Wheeler; (f) Safety *

* Sources: a) http://www.phys.uri.edu/~tony/bicycle/bikehist.html
b) http://www.ingenious.org.uk/See/Transport/Railwaysheraldry
c) http://www.harvestfields.ca/eshop/bicycles.htm
d) http://asrlab.org/archive/bike_wheel/whyShake.htm
e) & f) http://www.pedalinghistory.com/PHhistory.html

The last significant change in design of the bicycle propulsion system came with the introduction of a bicycle with a chain-driven rear wheel, the so-called Safety or Rover (1880's) (Minetti et al., 2001). This design employed equally sized wheels, smaller than the High Wheeler, making it easier to mount and dismount (Figure C-1f). Furthermore, the chain-driven rear wheel design separated the steering wheel (front) from the drive wheel (back), allowing for easier handling (Minetti et al., 2001). Since the introduction of the Safety, the way humans propel the bicycle has remained relatively unchanged.

In a study to investigate whether these advances in bicycle design have actually improved performance, Minetti and colleagues (2001) compared different bicycles that were used throughout history, starting with the original Hobby Horse and ending with a modern bicycle. Five subjects rode the different bicycles on a track at submaximal speeds and a comparison of metabolic cost (J/m) between bicycles showed that apart from the original Safety bicycle (non-pneumatic tires), all other designs showed decreased metabolic cost compared to their predecessors. It seems that the bicycle has come a long way since the original Hobby Horse in 1820. The way in which the cyclist generates and transmits power to propel the bicycle forward has undergone some dramatic changes over this time span. In the last 40 years, some new designs that alter the conventional circular pedal and crank method of propulsion have also been proposed, although they have not had a major impact on today's general bicycle design. These designs are discussed more thoroughly in a subsequent section of this review.

Characteristics of power transfer during conventional cycling

During conventional cycling the power generated by the legs are transferred to the drive system at the pedals. The pedals follow a circular path and are connected to the

crank arms. Power transferred to the crank axle depends greatly on the forces produced at the pedals. Considering the force produced by a cyclist throughout the complete crank revolution, it is evident this force generated is not constant throughout the 360° cycle (Figure 2). Most researchers (e.g., Ericson & Nisell, 1988; Sanderson, 1991; Korff, Romer, Mayhew, & Martin, 2007) study the pedal forces from a two dimensional perspective in the sagittal plane, neglecting the medio-lateral forces, although some studies do include three dimensional component analyses (e.g., Davis & Hull, 1981; Zameziati, Monieux, Rouffet, & Belli, 2006). Three dimensional force analyses are important in research related to issues such overuse knee injuries and bicycle component design (Newmiller, Hull, & Zajac, 1988), but because medio-lateral forces cannot

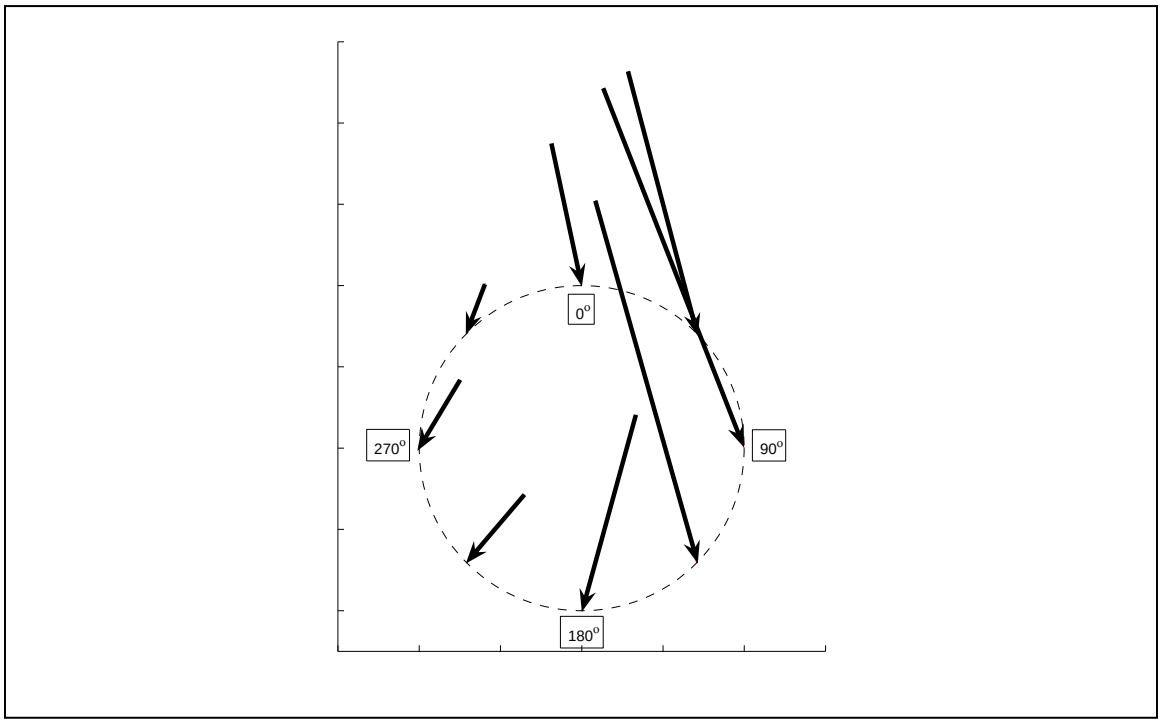

Figure C-2. Force profile of a recreational cyclist showing direction and relative magnitude of the resultant force on the left pedal. Values are shown at eight different positions of a full revolution during the laboratory task (300 W, 84 rpm) on a Velodyne cycling ergometer.

contribute to the driving torque it is often ignored by researchers when considering cycling performance. Focusing only on the sagittal plane, pedal force can be partitioned into horizontal and vertical components (Figure C-3), or normal (perpendicular to crank) and tangential (parallel to crank) components (Figure C-4). Using both these methods Ericson and Nisell (1988) described some basic characteristics of force production during submaximal testing (0, 120 and 240 W) of six recreational cyclists. They showed that vertical forces were much higher than horizontal forces (Figure C-3), which they concluded was mainly due to muscular action, the weight of the limb, as well as inertial forces. Furthermore, their results showed that normal force was maximum around the region of 90° and minimum around the region of 270° (Figure C-4). These results are

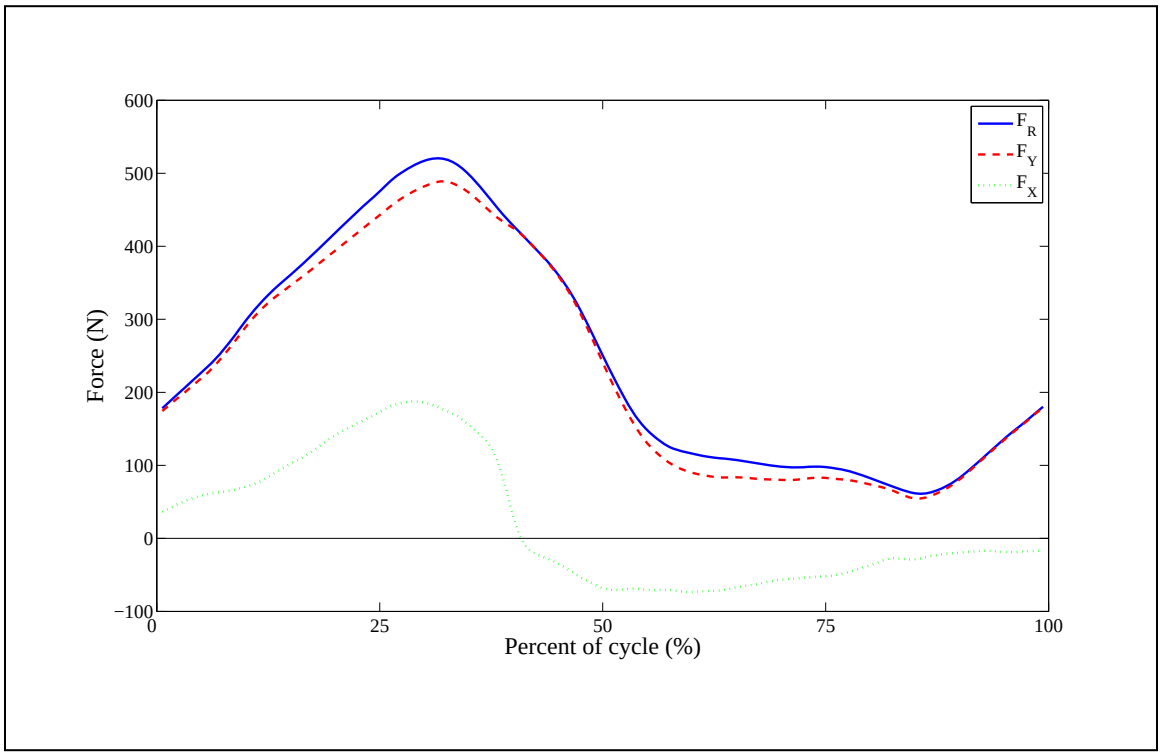

Figure C-3. The resultant force (F_R – blue solid line) and vertical (F_y – red dashed line) and horizontal (F_Y – green dotted line) force components at the left pedal of a recreational cyclist during a laboratory task (300 W, 84 rpm) on a Velodyne cycling ergometer.

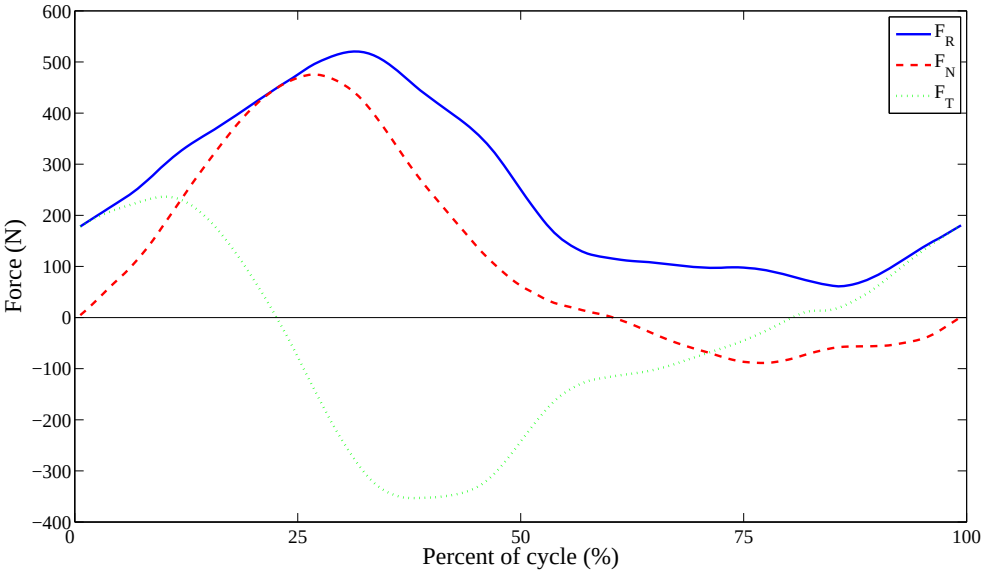

Figure C-4. The resultant force (F_R – blue solid line) and normal (F_N – red dashed line) and tangential (F_T – green dotted line) force components at the left pedal of a recreational cyclist during a laboratory task (300 W, 84 rpm) on a Velodyne cycling ergometer.

consistent with results of other researchers (e.g., Davis & Hull, 1981; Gregor, Cavanagh, & LaFortune, 1985; Zameziati, Monieux, Rouffet, & Belli, 2006). The product of the normal force and crank length equals the crank torque and the total crank torque generated is the combination of crank torque generated by the two legs (Figure C-5). During one cycle there are two torque peaks which occur at roughly 90° and 270° degrees, and two low points, which corresponds roughly to top and bottom dead center. Due to the fact that crank angular velocity stays relatively constant during a crank cycle (Broker, 2003; Hull & Jorge, 1985), the shape of the power transfer function at the crank axle has a similar form as the torque function, with peaks at 90° and 270° degrees and low points at top and bottom dead center.

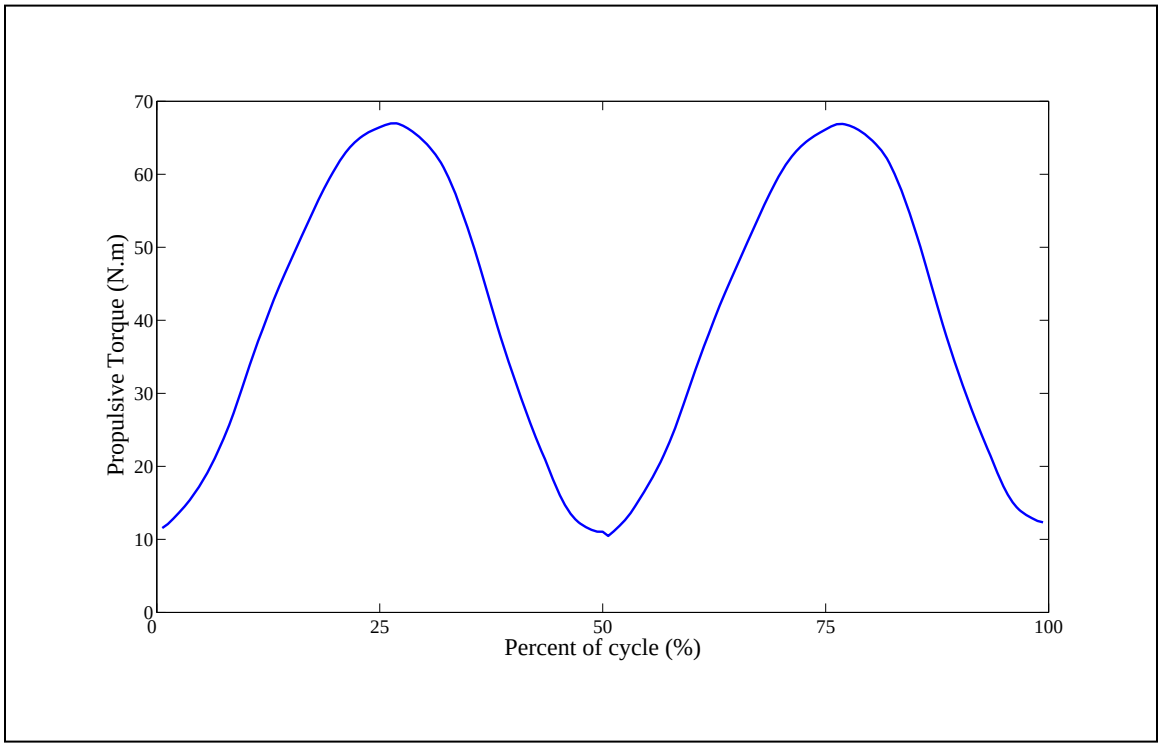

Figure C-5. The propulsive torque around the crank axle due to forces produced by both legs from a recreational cyclist during a laboratory task (300 W, 84 rpm) on a Velodyne cycling ergometer.

Many researchers (e.g., Korff, Romer, Mayhew, & Martin, 2007; LaFortune & Cavanagh, 1983; Sanderson, 1991; Zameziati, Monieux, Rouffet, & Belli, 2006) have used this difference between effective or normal force and ineffective or tangential forces to gain insight into aspects of the cycling task. The terms effective and ineffective relates to the fact that the driving crank torque is produced by the normal or effective force, whereas the ineffective or perpendicular force does not directly contribute to the generated crank torque. Sanderson (1991) investigated the effect of cadence and power on index of effectiveness (IE), which is the ratio of effective force to resultant force throughout a crank cycle. He found that as cadence increases (60, 80, 100 rpm), IE declined, and as power output increased from 100 W to 235 W, IE increased. These

results were similar for both competitive and recreational cyclists. More recently Zameziati et al. (2006) studies the relationship between IE and muscular efficiency in ten subjects during a sub-maximal test starting at 100 W with 30 W increments every 5 min at a constant 80 rpm cadence. They found that IE during the full revolution, as well as IE during the upstroke, was correlated with gross efficiency (GE) and net efficiency (NE). The fact that IE during the upstroke was correlated with efficiency, showed the importance of the so-called recovery phase. Korff et al. (2007) however found that the relationship between IE and efficiency does not hold true at constant power output, when IE is manipulated. During their experiment, eight subjects used different pedaling techniques: pulling during the upstroke, pushing during the downstroke, constant circular pedaling, and preferred pedaling technique, during a 6 min submaximal test at 200 W and 90 rpm. No significant correlation was found between the IE of the specific technique and GE. Although the preferred pedaling technique showed the highest GE, it had the second lowest IE.

Subdividing the pedal forces in to effective and ineffective forces, has however been criticized (e.g., Broker, 2003). Broker (2003), as well as Kautz and Hull (1993), have shown that measured pedal forces consist of a muscular component, which are forces produced by the human, as well as a fundamental component, which is due to the inertial and gravitational effects of the cycling task. A big constituent of the ineffective force is due to this fundamental component, which Broker argues is vital to maintain the position of the lower limbs on the pedals. The use of concepts of effective and ineffective forces and the related IE therefore seems to be a contentious issue when used as a measure of cycling efficiency.

It is important to take the force producing capabilities of the human rider into consideration when analyzing the human bicycle interface. When designing any human system interface the characteristics of power production and transfer needs to be optimized if the goal is to ensure that human performance is enhanced.

Overview of Computer Modeling and Simulation of Cycling

Modeling and simulation studies focusing on human movement have become more prevalent in recent years (e.g., Anderson & Pandy, 1999; Neptune & Hull, 1999; Raasch, Zajac, Ma, & Levine, 1997; Zajac, 2002). Researchers believe that modeling and simulation can help us understand how the neuromuscular and musculoskeletal system interacts to produce movement (Pandy, 2001). Many quantities that cannot be quantified in vivo can be elucidated by using a modeling and simulation approach. Furthermore, the increasing capabilities of computers have made it possible to perform very complex simulations in a fraction of the time compared to the early attempts. New optimization algorithms used during simulations are frequently being explored (e.g., Neptune, 1999; Thelen, Anderson & Delp, 2003) and parallel computing is reducing computational time significantly (Pandy, 2001).

The primary movements during cycling is mostly performed in one plane, the hip joint center movement is relatively small (Nordeen & Cavanagh, 1975) and the footpath is constrained by the pedal motion. This constrained lower extremity movements in cycling makes it a relatively simple dynamic task to study, compared to a task like walking for example (Zajac, Neptune, & Kautz, 2002). This relative simplicity also means that cycling can readily be studied using a modeling and simulation framework.

Various approaches are available to do modeling and simulation of human movement, and therefore cycling. Models can be simple, considering for example only joint torques and joint forces (e.g., Gonzalez & Hull, 1989; Kautz & Hull, 1995; Redfield & Hull, 1986b), or more complex, where individual muscle models are generated and used to generate simulations (e.g., Neptune & Hull, 1999; Raasch et al., 1997; Umberger, Gerritsen, & Martin, 2006). Complex models are more costly from a computational viewpoint, but the fact that the main actuators in the system (i.e., the muscles) are included, makes this a more physiologically sound method. If the purpose of the simulations is to gain information on muscle control and functioning complex models are essential.

Another key distinction in modeling studies, apart from model complexity, is whether an inverse or forward dynamics approach is being applied. In an inverse dynamics approach noninvasive measurements of body motion and external forces serve as input into motion equations in order to calculate the joint moments and/or muscle forces (Pandy, 2001). Hull and colleagues (e.g., Gonzalez & Hull, 1989; Hull & Gonzalez, 1988; Redfield & Hull, 1986b) used such an approach to do several studies on optimal bicycle setup. Pedal forces were measured for one case of pedaling and then scaled according to changes in power output, crank length, and pedaling rate, in order to predict values for other pedaling cases. To obtain valid results, accurate measurements of body segmental kinematics are however vital (Anderson & Pandy, 2001), and if this is not possible, the use of an inverse dynamic approach is limited. In a forward dynamics approach, muscle activation or joint moments are the inputs (the causes) to the system and the corresponding body motions (the effects) are then calculated (Pandy, 2001). A

major advantage of this method is that the external forces (e.g., pedal forces in cycling) are included when the equations of motion are being satisfied (e.g., Kautz & Hull, 1995), and are therefore part of the variable set being solved for.

When there is more than one result for the combination of joint moments and/or muscle forces to satisfy a given system of dynamic equations for a motor task, some form of optimization routine is often used to find the best solution (e.g., Kautz & Hull, 1995; Raasch et al., 1997). For inverse dynamics, or static optimization, a different optimization problem is solved for each time step of the task, which makes this approach computationally efficient compared to the forward dynamic optimization approach (Anderson & Pandy, 2001). Using a forward dynamics, or dynamic optimization, the optimization problem is solved throughout the complete movement (Pandy, 2001), which is computationally more expensive. This 'best solution' generated by the optimization routine is usually defined as a solution that satisfies the movement constraints as well as minimizing or maximizing (depending on the task) some objective function. The objective function is a reflection of the actual objective of the human while performing the given motor task. As an example, if the task is maximal speed cycling, then the objective function would be to minimize the time it takes to finish the task. During submaximal tasks, the objective function is often related to some physiological indicator of human effort. In cycling, objective functions based on joint moments (e.g., Gonzalez & Hull, 1989; Redfield & Hull, 1986b), muscle stresses, (e.g., Hull, Gonzalez, & Redfield, 1988) and muscle energetics (Umberger et al., 2006) have been used. A joint moment based objective function is one of the more simplistic functions used. This type of function calculates optimal values (i.e., joint moments) to perform a given task that

would minimize, for example, the sum of squared joint moments, or sum of average absolute joint moments, which is believed to directly relate to muscular effort (Redfield & Hull, 1986b). Hull and colleagues (Gonzalez & Hull, 1989; Hull & Gonzalez, 1988; Redfield & Hull, 1986b) used this approach in a series of modeling studies on cycling to find optimal values for bicycle setup parameters. In a more recent study, Hull and colleagues (Hull et al., 1988) used a more complex muscle-stress based cost function to examine optimal cycling cadence. Their results were comparable to those from previous simulation efforts using a moment-based cost function. Hull et al. (1988) concluded that a joint moment-based cost function might therefore be more "attractive because of its computational simplicity" (p.18). Objective functions based on some indicator of muscle function (e.g., muscle stresses or muscle energetics) are valuable in understanding human functioning at the muscle level, but come at an extra computational cost.

Apart from the optimization methods mentioned, another approach used in forward dynamic simulation studies is a tracking method, where the solution is constrained to follow some measurable variable (e.g., movement kinematics, external kinetics, EMG). This method, however, puts constraints on the possible optimal outcomes and limits its usefulness. Tracking can not be employed if a novel task, such as pedaling with a new bicycle drive design, is studied due to the fact that the variables usually tracked are unknown.

Deciding on the modeling and simulation approach to use is therefore influenced by many aspects. The purpose of the specific study, available computational power, available input data and many other factors will guide the researcher in choosing the most appropriate framework. Results of modeling and simulation studies should however be

interpreted with caution. A model is only a representation of an actual system and various assumptions are generally needed to create the model and to generate the appropriate simulations. Where possible, experimental protocols should be used to strengthen results obtained from modeling and simulation studies.

Alternative drive designs

Hull, Kautz, and Beard (1991) commented on the fact that an infinite variety of foot paths can possibly exist in a cycling task and that this path as well as velocity have the potential to affect human performance. However, modeling and simulation studies focusing on alternatives to the standard circular bicycle propulsion system have been limited. These studies have mainly focused on variations in angular velocity and effective moment arm of the crank using non-circular chainrings, while the circular trajectory of the foot contact point with the pedal remains unchanged. Experimental work has been done on non-circular chainrings, variable length crank arms, as well as variable phase rotating cranks. These modeling studies and experimental work are discussed below.

In one of the first modeling studies to look at an alternative design, Miller and Ross (1980) used a non-linear programming method to design an optimized non-circular chainring for maximum power output. They experimentally determined the maximum static moments a cyclist could produce at discrete crank angles throughout the crank cycle and then assumed a hyperbolic decrease in moments at increased speeds, in agreement with force-velocity relationship of muscles (Hill, 1938). Having the joint moment-speed relationships, the second step was to calculate the moment versus crank angle as a function of angular velocity for the dynamic effects (i.e. inertial and

gravitational effects) of the moving legs. Subsequently the angular velocity profile that would produce maximum average cycle power was determined and the chainring that would generate this profile was designed (Figure C-6). The design generated was an elliptical chainring with major axis lagging the crank arm by roughly 60°. This design reduced crank angular velocity and increased chainring moment arm when the crank was close to 90° and 270° and it increased crank angular velocity and reduced chainring moment arm when the crank was close to top and bottom dead center. The design would theoretically increase power output by 12.6% compared to a circular chainring. To date no experimental results have been collected to verify the predicted power output increase of this design. The design of the commercially available Biopace was also based on a modeling paradigm. Okajima (1983) used the principle of impedance matching, which is

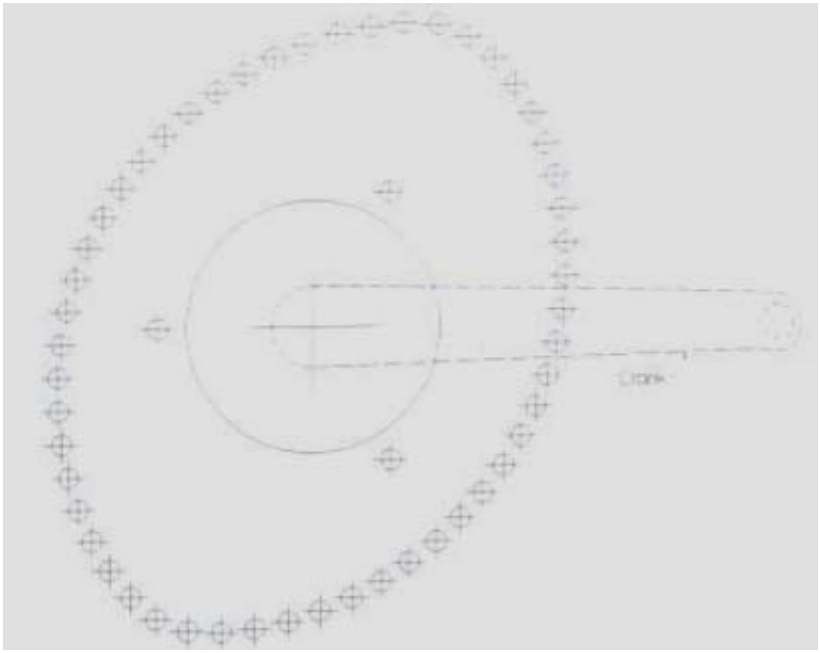

Figure C-6. Shape of theoretical chainring designed by Miller and Ross. Source: Miller and Ross (1980).

commonly used in electrical circuitry, as part of the design approach. The purpose of impedance matching in cycling would be to match the speed and torque at which the muscles work with the speed and torque needed to produce a given power output at the wheel. Okajima refers to the 'weakest link' in the system as being the knee joint and it could be assumed from the discussion that the impedance matching method was applied to match final power output to the knee joint muscle capabilities. Okajima also predicted that the final design would reduce kinetic energy losses of the legs, as well as reduce the coordination skills required by the cyclist. Using computer simulations, of which the exact details were not specified, a crank-velocity pattern for optimum power transfer was deduced. Because of some sharp motion fluctuations (i.e., large variations in chainring radius over small angle changes) in the theoretical design that could not be realized using an actual chainring, the final Biopace chainring was slightly modified (Figure C-7). It is

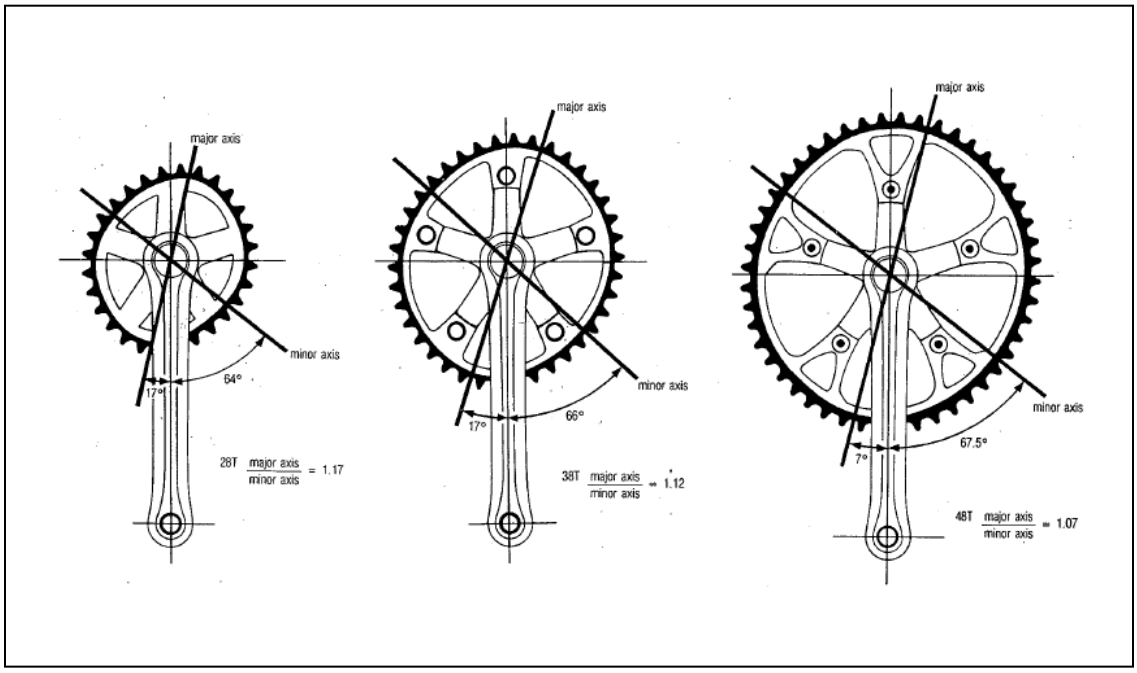

Figure C-7. Biopace chainrings designed by Okajima. Source: Okajima (1983).

noted that an important difference between their design and previous elliptical chainring designs (e.g., Miller & Ross, 1980) was that major axis of the elliptical chainring was very close to being parallel with the crank arms. This caused maximum crank angular velocity to be close to the horizontal (90° and 270°) and not at top and bottom dead center. Chainring moment arm was increased when the crank moved through top and bottom dead center and decreased when the crank was at 90° and 270°. Experimental results (Cullen, Andrew, Lair, Widger, & Timson, 1992; Hull, Williams, Williams, & Kautz, 1992), however, have shown no significant improvement using the Biopace non-circular chainring. Cullen and colleagues compared $\dot{V}O_2$, heart rate (HR), and Rating of Perceived Exertion (RPE) of seven trained cyclists while riding with circular and noncircular (Biopace) chainrings and found no differences in any of the measured parameters during submaximal testing. Hull and colleagues compared $\dot{V}O_2$, HR and lactate levels of 11 trained cyclists tested while riding with three different non-circular chainrings, one being the Shimano Biopace, as well as a conventional circular chainring. Results showed no significant difference in any of the physiological parameters while riding at an individual work rates which elucidated 60% $\dot{V}O_{2\max}$ (mean of 189 W) or 80% $\dot{V}O_{2\max}$ (mean of 266 W). In 1991, Hull, Kautz, and Beard also proposed a non-circular chainring design that would vary crank angular velocity to increase efficiency of the cycling task. The bicycle-rider system was modeled as a five-bar linkage (thigh, shank, foot, crank arm, and seat tube). Because this model allows for two degrees of freedom (crank and pedal angle), experimental data from five subjects were used to establish ankle

position as a function of pedal angle. The experimental data also served as input to a rigid link model to calculate kinetic, potential and total mechanical energy of the system over a complete cycle. Hull and colleagues showed that normal angular velocity variations during steady state cycling with circular cranks cause fluctuations in the total mechanical energy of the system, which is directly related to internal work. They then derived a crank angular velocity profile which would keep the total mechanical work constant, thereby reducing the internal work in the system. Their proposed chainring design produced a crank angular velocity and chainring moment arm profile very similar to the design of Miller and Ross (1980), in contrast to the design of Okajima (1983). In other words, the major axis of the chainring was roughly perpendicular with the crank arms. In an experimental follow-up study in 1992, Hull and colleagues (Hull et al., 1992) compared a chainring that reduced internal work to one that increased internal work. The chainring that reduced internal work had the crank in line with the minor axis of the ellipse and caused maximum angular velocity to occur at 0° and 180°. The chainring that increased internal work had the crank 10° in front of the major axis and maximum angular velocity occurred at 100° and 280°. They found no significant differences between the two chainring designs in $\dot{V}O_2$, HR and lactate levels at a low (60% $\dot{V}O_{2\max}$) and high (80% $\dot{V}O_{2\max}$) work rate. These physiological parameters were also found to be no different than values obtained from conventional circular chainring or the Biopace design. Recently, however, Kautz & Neptune (2002) refuted the idea that reduction in internal work could lead to increased efficiency, which was originally proposed by Hull and colleagues. They found that internal and external work were not independent, and

that a reduction in internal work might also cause changes in external work done. Kautz and Neptune argued that changes in mechanical energy of the legs (internal work) play an important role in production of external work. To base the design of the human-bicycle interface on the principle of reduction of internal work therefore seems to be invalid given these findings.

A more recent study on an alternative drive design (Kautz & Hull, 1995) used the principal of dynamic optimization and specifically optimal control theory to generate an alternative chainring design. This approach has become common place in modeling and simulation studies of locomotion (e.g. Davy & Audu, 1987; Neptune & van den Bogert, 1998, Neptune & Hull, 1999; Pandy & Zajac, 1991). This study specifically analyzed endurance cycling at 90 rpm and a 250 W power output. A similar model of the bicycle-rider as the one used by Hull, Kautz, and Beard (1991) was employed, but with both legs being modeled. Intersegmental moments at the hip and knee were used as inputs, and crank accelerations as well as net joint moments at the hip, knee and ankle were outputs of the optimization routine. The chosen cost function was one which minimized the time integral of squared moments over a pedal cycle. The resulting design was a non-circular chainring that reduced the cost function value by 1.4% (Figure C-8). Although the results show that an improvement in performance might be possible, Kautz and Hull cautioned that the elliptical design was not optimized from a human muscle energetic transfer perspective due to the fact that large joint torques were needed during times when limbs were experiencing high velocities. From a human perspective, the force-velocity relationship of the muscles might therefore make this design infeasible. The actual design was also not physically realizable due to cusps in the circumference, which

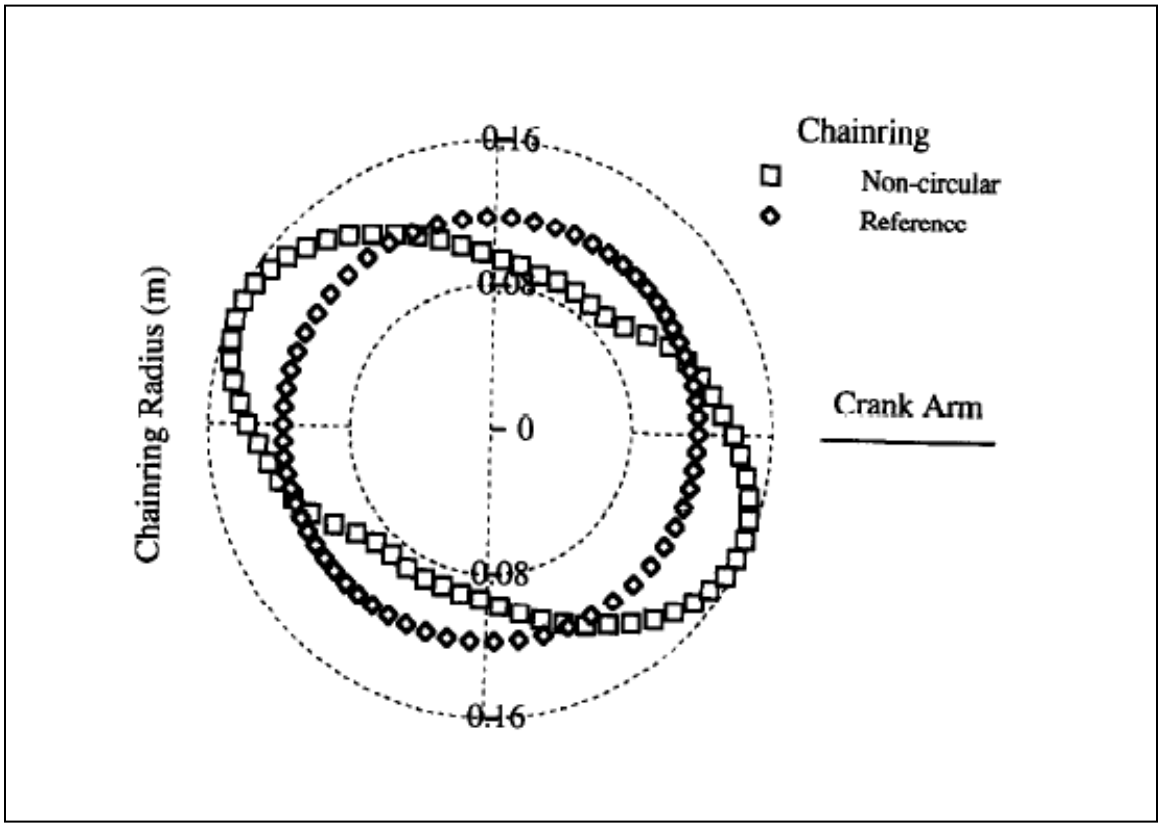

Figure C-8. Shape of theoretical non-circular chainring designed by Kautz and Hull compared to conventional circular design. Source: Kautz and Hull (1995).

indicates that the circumference wasn't a smooth surface. Changing this design to make it practically realizable would cause a reduction in the maximum potential benefit that the system could provide. Miller and Ross (1980) and Okajima (1983) also both mentioned changes in their original designs were needed to make it feasible to construct and use. Modeling and simulation studies based on optimization should be seen as a first attempt to design a system. Inevitably practical issues might force a need for modifications. This study by Kautz and Hull (1995) showed the use of a dynamic optimization framework is promising method for design evaluation, although no experimental testing results have been published.

Other experimental work on non-circular chainring systems (Harrison, 1970; Henderson, Ellis, Klimovitch, & Brooks, 1977; Ratel, Duche, Hautier, Williams, & Bedu, 2004) has not shown any convincing evidence to suggest that this alternative drive mechanism might be superior. In fact, only Henderson et al. (1977) found performance improvements, but for a limited case. They compared three different elliptical chainrings with the conventional circular chainring during steady state cycling tests on a Monark bicycle ergometer with subjects cycling at 50 rpm and four different workloads (50 W, 100 W, 150 W, 200 W). Their results showed a significant reduction in oxygen consumption of 2.4% at only one of the four submaximal workloads (150 W) using the E° configuration (Figure C-9).

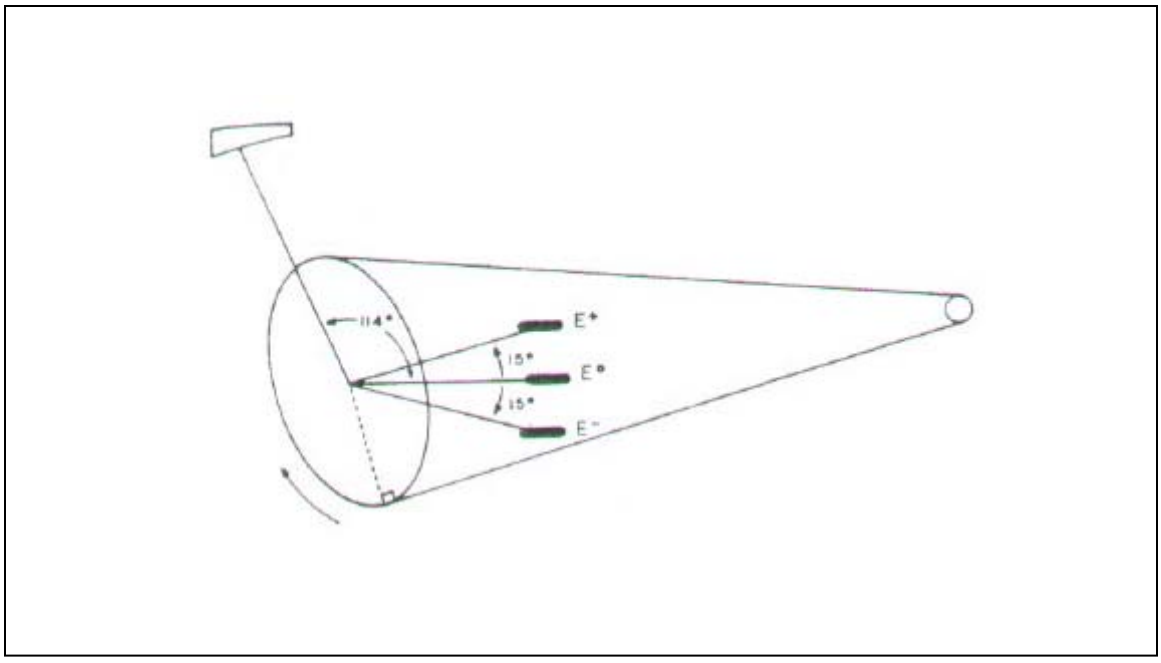

Figure C-9. Basic diagram showing three elliptical chainring configurations studied by Henderson et al. The different configurations changed the angle between the major axis of the elliptical chainring and the crank. A chainring with minor-major axis ratio of 0.714 was used. Source: Henderson et al. (1977).

Although most studies, both modeling and experimental, have focused on non-circular chainrings, other bicycle drive designs have also received some attention. Hue and colleagues (Hue, Chamari, Damiani, Blonc, & Hertogh, 2007; Hue, Galy, Hertogh, Casties, & Prefaut, 2001) as well as Zamparo and colleagues (Zamparo, Minetti, & Di Prampero, 2002) tested systems that functionally shifted the center of rotation of the pedal path in front of the chainring center of rotation (Figure C-10 and Figure C-11). Although the pedal still followed a circular path, the specific designs caused the functional crank arm length to be similar to the centric or standard drive crank at top and bottom dead center, but longer at 90° (forward horizontal) and shorter at 270° (back horizontal). The theoretical advantage of such a system is stated as being able to increase

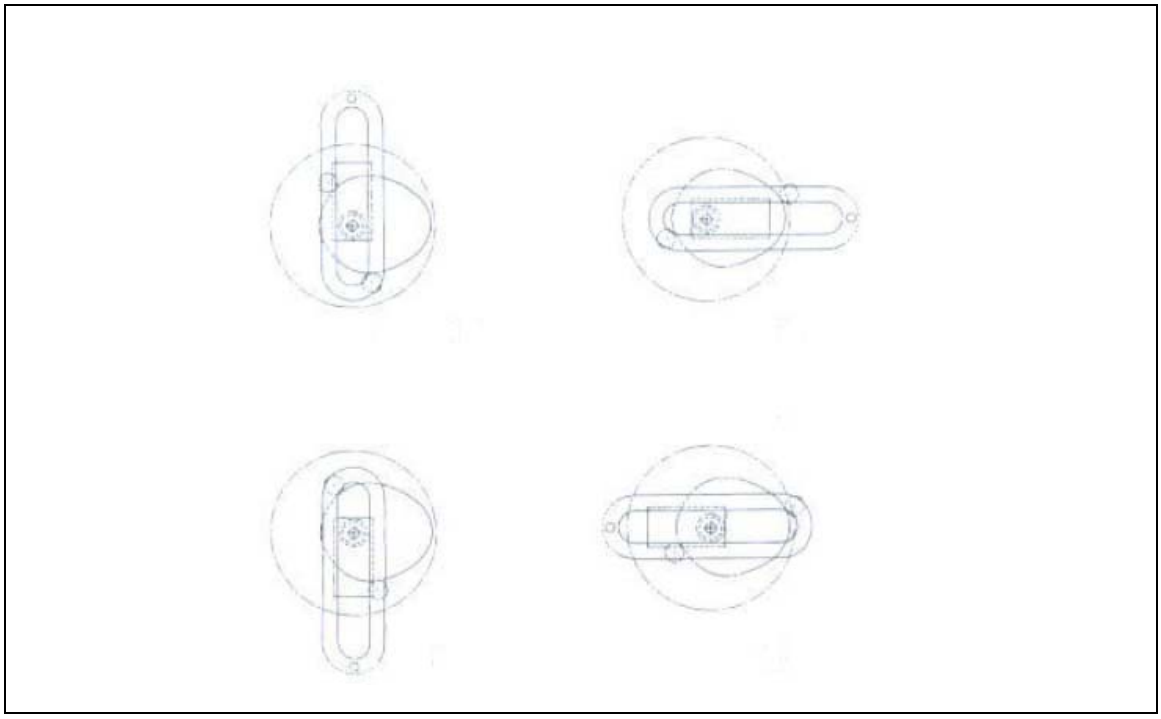

Figure C-10. Schematic showing the eccentric chainring studied by Hue et al. Two sliding crank arms and an elliptical cam changes the crank lengths throughout the pedaling cycle. At 0° and 180° the crank lengths are 0.175 m, but this length is increased at 90° (0.2 m) and decreased at 270° (0.15 m). Source: Hue et al. (2001).

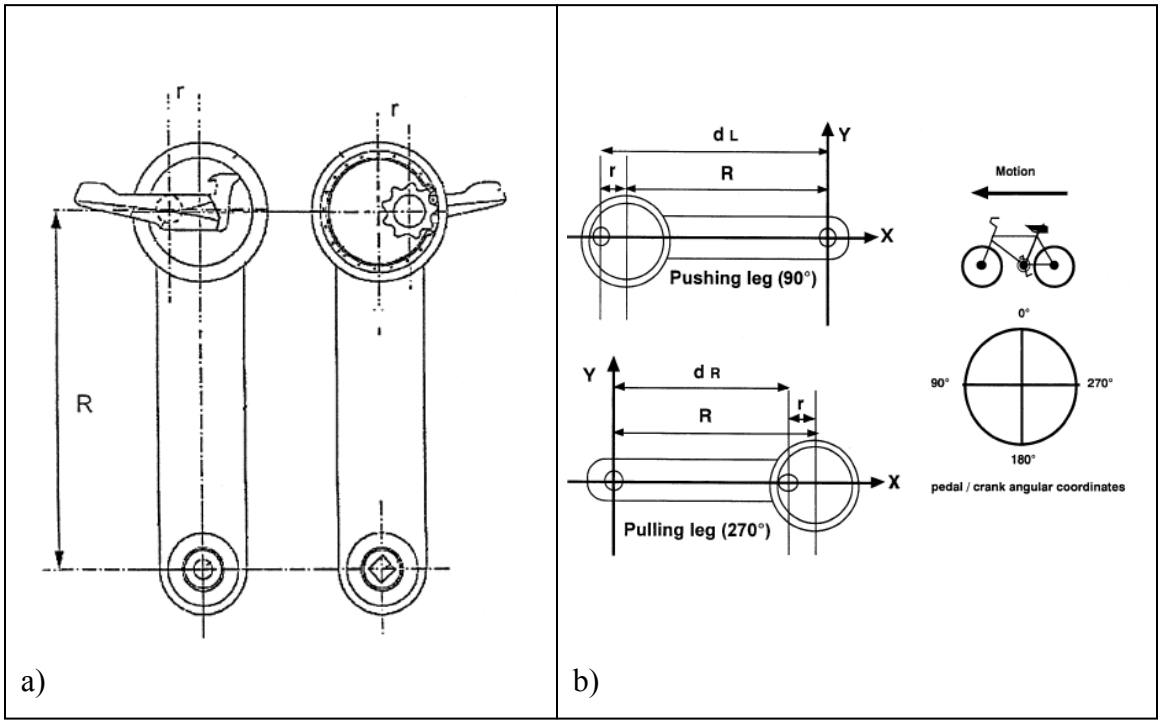

Figure C-11. (a) Schematic of pedal-crank system studied by Zamparo and colleagues. (b) Diagram showing maximum pedal-crank distance at 90° and minimum distance occurring at 270°. Source: Zamparo et al. (2002).

the torque generated during the pushing phase by increasing the moment arm, and decrease the counter-torque during the recovery phase by shortening the moment arm. In contrasting 1 km laboratory trial performance of competitive cyclists and triathletes for the centric and eccentric drive systems, Hue et al. (2001) observed a significant reduction in 1 km trial time of 4.83 seconds for the eccentric condition. Interestingly, there were no significant changes in any cardiorespiratory variables. However, in a follow-up study, Hue et al. (2007) tested the same design in an actual track cycling event: a 1000 m time trial. Twelve cyclists performed an outdoor 1000 m time trial with either a conventional round or the eccentric chainring. No differences in total ride time, lactate levels, HR or individual lap times were observed between the two drive systems. Zamparo et al. (2002)

tested their proposed design on seven road cyclists who cycled on a stationary ergometer on two separate days, one day for traditional cycling and one for the alternative pedal crank system. Cycling cadence was fixed at 60 rpm and the power value started at 50W and was increased by 50 W every 5 minutes. There were no significant differences between the two drive systems at lower intensities of 50-200 W with respect to HR, expired ventilation, oxygen consumption, respiratory exchange ratio, and GE. At 250-300W the alternative pedal crank system showed reduced oxygen consumption values (3.72 $l.min^{-1}$ vs. 3.84 $l.min^{-1}$) and higher gross efficiency (23.4% vs. 22.1%).

Martin, Lamb, and Brown (2002) hypothesized that average power output would be increased if a greater proportion of the cycle time is spent on leg-extension, implying more time spent during the power stroke. To test their hypothesis they used a one-leg ergometer setup with an offset drive sprocket to get the required leg trajectories (Figure C-12). By offsetting the drive sprocket by 20 mm, 58% of the sprocket's circumference crossed the centerline of the crank axle during the leg-extension phase, causing a change in total time spent in leg-extension. Seven trained cyclists were tested on the modified system which either caused equal leg extension-flexion, 58% extension and 42% flexion, or 42% extension and 58% flexion. The protocol used was in the form of maximal power tests lasting 3-4 seconds each. The results showed that maximum power averaged over a complete crank cycle was highest (636 W) during the condition for which the leg was in extension for a longer period, and lowest (520 W) when leg-extension was less than 50% of the cycle time. During the equal leg extension-flexion protocol, the maximum power averaged over a cycle was 613 W. These findings suggest that lower extension velocity caused by the longer leg-extension time was beneficial for maximal power production.

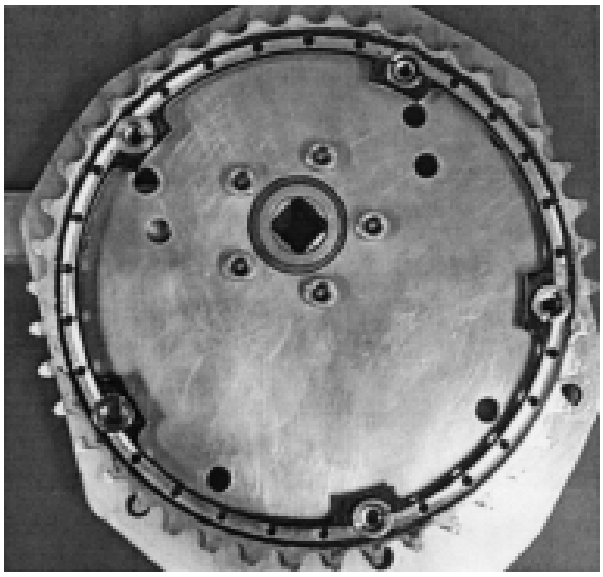

Figure C-12. The offset drive sprocket used in the study by Martin and colleagues. This sprocket was repositioned 20 mm from the crank axle. Source: Martin et al. (2002).

Martin et al. suggested this could be due to increased muscle excitation and the fact that the leg is in the optimal mechanical advantage phase for a longer time.

A system which changes the phase between the two legs during cycling without changing the path of the feet has also been proposed. Santalla et al. (2002) studied a design in which the two cranks do not maintain a 180° relationship with one another throughout the crank cycle. When the cranks are in the horizontal position, they are 180° out of phase, but otherwise the angle between the cranks varies (Figure C-13). The reasoning behind the design is that this system would eliminate the so called dead spots during cycling which occurs when the pedals are at top and bottom dead center at the same time. During these dead spots, occurring twice during a crank cycle, the power produced falls to a minimum. With this new design, called the Rotor system, an elliptical

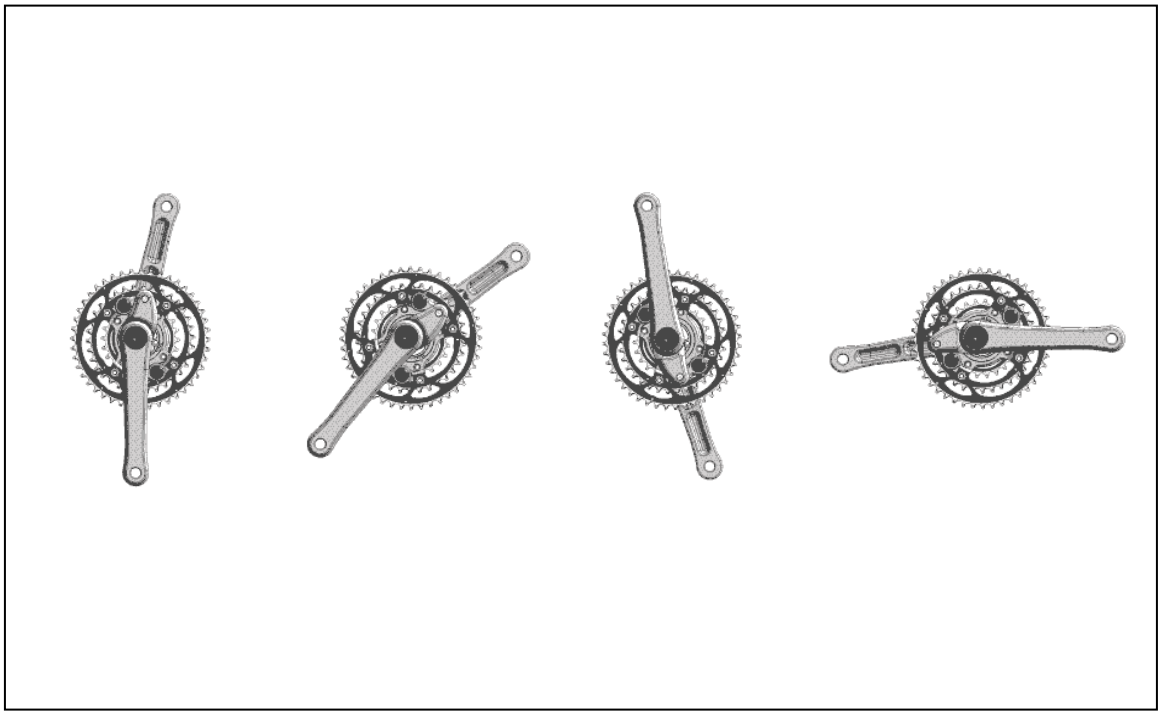

Figure C-13. The Rotor design showing the independent movement of the cranks. Source: http://www.rotorcranksusa.com/i1-rs4x.shtml.

gear system within the chainring mechanism ensures that the cranks are never at top and bottom dead center at the same time. Santalla and colleagues suggested this would allow cyclists to produce higher torque output for a greater proportion of the crank cycle. The study tested eight healthy young men, who were not experienced cyclists. The performance measurements were $\dot{V}O_{2\,max}$, lactate threshold (LT), gross (GE) and delta efficiency (DE). Starting at 75 W, power output was increased by 25 W every three minutes until subjects reached volitional exhaustion. The results showed no significant benefit with respect to $\dot{V}O_{2\,max}$, HR, blood lactate concentration (BLa) or GE for the new design. However, DE was higher when using the Rotor crank system at moderate to high intensities (60 – 90% $\dot{V}O_{2\,max}$). In a follow up study by the same research group (Lucia et

al., 2004), the Rotor system was also tested on 10 trained cyclists performing an incremental test until exhaustion as well as a submaximal test at a constant power output which was equivalent to 80% of the highest power output that was maintained during the incremental test. The Rotor system did not show any significant advantage over the conventional system. The authors suggested, however, that the system also needs to be tested during short-term supramaximal efforts, like a Wingate test, to see whether the proposed theoretical advantages could be situation specific.

Studies that do not look at the conventional bicycle system are limited. In one such study, Harrison (1970) investigated various movement types and the ability to produce maximum power using a multipurpose ergometer. The various motions were a basic leg cycling motion; a rowing movement with feet fixed and seat fixed; a rowing movement with feet fixed and seat moving; a rowing movement with the feet moving and seat fixed; and a rowing movement with both feet and seat moving. Except for the cycling motion, the other motions were setup to be both free and forced during separate trials. During free motion trials, the subjects had to decelerate and change direction of the movement at the end of a stroke while during forces motion trials an external mechanism stopped the movement at the end of the stroke. Free motion caused considerable kinetic energy to be lost at the end of strokes when the limbs experienced phases of acceleration (Harrison, 1970). Harrison showed that the forced rowing motion where the feet were allowed to move and the seat was fixed allowed for maximum power generation, more than cyclic motion of the legs alone. For this rowing motion a mean power output for the 5 subjects for a 10 s period was approximately 1030 W compared to 630 W for cycling alone. One has to keep in mind though, that during the rowing task the

arms and legs could generate power, whereas in cycling only the legs can contribute. However, the investigation by Harrison does show that humans are capably of producing a substantial amount of power without necessarily using circular leg motion, as is used in conventional cycling.

It is evident that no alternative drive mechanism has had a major impact on cycling performance to date. The use of modeling and simulation studies to look at alternative drive designs for cycling has been limited, and all the modeling studies mentioned have focused on non-circular chainrings. In most cases in which experimental research has shown some form of improvement, it is only evident in limited situations or on limited measured parameters. Except for the mechanism studied by Harrison (1970), none of the other mechanisms discussed caused changes in the foot contact path of the lower limbs. All designs were based on affecting the angular velocity and/or moment arm during the crank cycle and how these changes would benefit the human-bicycle interface. The fact that an infinite variety of foot paths can possibly be used in a cycling task (Hull et al., 1991) is not reflected in the discussed designs. Harrison (1970) suggested that elliptical motion of the foot itself, rather than the chainring, might lead to a better design. To our knowledge, no modeling and simulation work to date has studied the effect of changes in the foot contact trajectory itself on cycling performance.

Other bicycle design issues

The geometric variables of seat height, seat tube angle, longitudinal foot position on the pedal and crank arm length all affect joint loads (Gonzalez & Hull, 1989) and play an important role in ultimate power delivery to the drive train of the bicycle (Faria, Parker, & Faria, 2005). Putting aside novel drive designs, equipment configuration issues

like these are important in cycling and have been the subject of many experimental studies (e.g., Hamley & Thomas, 1967; Heil, Wilcox, Quinn, 1995; Inbar, Dotan, Trousil, & Dvir, 1983; Martin & Spirduso, 2001; Ricard, Hills-Meyer, Miller, & Michael, 2006). However, only a few modeling studies have attempted to elucidate optimum bicycle configuration aspects.

In a series of modeling studies, Hull and colleagues (Gonzalez & Hull, 1989; Hull & Gonzalez, 1988; Redfield & Hull, 1986b) sought to optimize the bicycle geometry and pedaling cadence by finding values that would minimize the sum of absolute hip and knee moments. Using an inverse dynamics approach, experimental pedal forces were initially measured during steady state submaximal cycling (Hull & Jorge, 1985) and used to solve for the net joint moments at the ankle, knee and hip. To optimize the effect of crank length and cadence, pedal forces were scaled to keep the power output constant. A bivariate optimization approach (Hull & Gonzalez, 1988), which looked at the effect of pedaling rate and crank arm length, yielded optimum values of 110 rpm and 0.145 m, respectively. Gonzalez and Hull (1989) found similar results in the final study of the series. Using a more complex multivariate approach, they solved for a combination of parameters that minimized the hip and knee moment cost function for a person of average size. Specifically, the moment cost function was minimized at a pedaling rate of 115 rpm with crank arm length of 0.14 m and seat tube angle (STA) of 76°. The optimal seat height, defined as the distance from the top of the saddle along the seat tube to the pedal spindle when the pedal is at its most distal position, was equal to 97% trochanteric leg length and longitudinal foot position on the pedal equal to 54% of foot length. Importantly, with respect to the optimized results, they found that these results depend

heavily on rider size, and suggested bicycle equipment should be tailored to the individual rider (Gonzalez & Hull, 1989). These optimum values do differ from the results of a number of experimental studies (e.g., Martin & Spirduso, 2001; Hamley & Thomas, 1967; Nordeen-Snyder, 1977; Heil et al., 1995; Garside & Doran, 2000). However, Hull and Gonzalez (1988) suggest that results closer to actual experimental results could be obtained if the cost function used took into account the force-length and force-velocity characteristics of muscles (Hull & Gonzalez, 1988). They suggested that further studies should include these model complexities.

The use of a more complex muscle model was later exploited by Yoshihuku and Herzog (1990) in a maximal power output modeling study. Using a lumped muscle model, for which functional muscle groups were defined, they found a maximal power output of 1100 W was generated at a pedal length of 170 mm, a slightly reclined position of the cyclist's trunk, a distance of 0.51 m from the hip axis to the crank axle, and a cadence of 155 rpm. The distance of 0.51 m from the hip axis to the crank shaft translates to a trochanteric leg length of only 78%. These results are very different from those of Gonzalez & Hull (1989) and experimental results, but the model employed by Yoshihuku and Herzog used only a two segment model of the leg (thigh and shank), with the ankle not considered. The assumption that the ankle joint coincides with the pedal shaft also means that the all the muscles crossing the ankle joint were not included. These muscles do however play an important role in cycling (Zajac, Ma, & Levine, 1997).

Experimental results on the effect of crank length on performance, whether for steady state submaximal or maximum power output cycling, generally suggest that the

crank length is positively correlated with leg length (e.g. Burke & Pruitt, 2003; Carmichael, Loomis, & Hodgson, 1982; Martin & Spirduso, 2001). Most experimental studies have focused on maximum power cycling tasks (e.g., Inbar et al., 1983; Martin & Spirduso, 2001; Too & Landwer, 2000) and have shown crank lengths resulting in maximum average power vary between 0.145 m and 0.2 m. Burke et al. (2003) suggest that a 0.17 m crank arm length is suitable for cyclists of average proportions (height between 1.65 m and 1.83 m), and that shorter cyclists can consider crank arm lengths of between 0.165 m and 0.168 m and taller cyclists crank arm lengths between 0.18 m and 0.185 m. However, according to Inbar et al. (1983), as well as Martin and Spirduso (2001), using a standard crank length of 0.17 m only minimally effects maximum power output.

Experimental results on seat height (Hamley & Thomas, 1967; Nordeen-Snyder, 1977; Shennum & de Vries, 1976) show that a value between 98% and 102% trochanteric height to be optimum. Seat height being defined as the distance from the top of the saddle along the seat tube to the pedal spindle when the pedal is at its most distal position. These values seem to be similar for maximum power output (Hamley & Thomas, 1967) and steady state submaximal cycling (Nordeen-Snyder, 1977; Shennum & de Vries, 1976).

Preferred seat tube angles (STA) used by cyclists have been shown to be dependant on the type of event – cyclists in road races normally prefer an STA of between 72° and 76°, while triathletes use higher STA's (between 76° and 78°), (Heil et al., 1995; Garside & Doran, 2000). Experimental studies on STA generally show larger

STA's to be more effective. Heil et al. (1995) showed that mean $\dot{V}O_2$, HR, and RPE values at 83° and 90° were significantly lower than values at 69° during submaximal testing of 25 trained competitive triathletes and cyclists. Comparing STA's of 68°, 74°, and 80°, Price and Donne (1997) found that at an STA of 80° the mean $\dot{V}O_2$ was significantly lower for fourteen competitive cyclists performing submaximal exercise at 200 W. Ricard, Hills-Meyer, Miller, & Michael (2006) found that although power output was similar for STA's of 72° and 82° during a 30s-Wingate test, at 82° there was a significant reduction in muscular activation quantified by EMG of the biceps femoris muscle for 12 experienced cyclists.

Many experimental studies have been done to elucidate the optimal bicycle setup to maximize performance. The use of modeling and simulation principles to gain insight into optimal bicycle setup has been limited. A modeling and simulation framework do however offer some advantages over an experimental approach, such as the ability to use multivariate approaches and test over large ranges of possible values of the optimized variables. These options are not always available to researchers when working with human subjects.

Cadence and muscle function

The body of cycling research literature has a much stronger focus on muscle function and other physiological factors that influence cycling performance than bicycle design issues. Many complex models have been employed in this area (e.g., Fregly & Zajac, 1996; Raasch et al., 1997; Umberger, Gerritsen & Martin, 2006; Van Soest & Casius, 2000) and have improved our understanding of muscle control and functioning

during the cycling task. Experimental studies have looked at a variety of factors that can influence human functioning during the cycling task, for example neuromuscular fatigue (e.g., Takaishi, Yasuda, Ono, & Moritani, 1996; Takaishi, Yasuda, & Moritani, 1994), muscle fiber type (e.g., Ahlquist, Bassett, Sufit, Nagle, & Thomas, 1992; Umberger et al., 2006), force application (e.g., Patterson & Moreno, 1990; Sanderson, 1991), muscle activation (e.g., Sanderson, Martin, Honeyman, & Keefer, 2006), perceived exertion (e.g., Marsh, & Martin, 1998; Lollgen, Graham & Sjogaard, 1980), and many more.

The preferred or most optimum cadence during cycling has been an issue that has received considerable attention over many decades. In certain locomotion tasks, it seems that preferred cadence and most optimum cadence from an energy expenditure perspective (lowest oxygen consumption) are similar. Examples of this phenomena can be seen in walking (e.g., Holt, Hamill, & Andres, 1991; Zarrugh, Todd, & Ralston, 1974) and running (e.g., Cavanagh & Williams, 1982). This does not seem to be the case for cycling. Preferred cadence has been found to be consistently higher than the most economical cadence, i.e. the cadence that results in the lowest aerobic demand or energy cost, during submaximal steady state cycling. Typical preferred cadence between 90 rpm and 100 rpm (e.g., Hagberg, Mullin, Giese, & Spitznagel, 1981; Marsh & Martin, 1993; 1997), whereas most economical cadence values reported fall roughly between 40 rpm and 80 rpm (e.g., Boning, Gonen, & Maassen, 1984; Coast & Welch, 1985; Marsh & Martin, 1993; 1997; Seabury, Adams, & Ramey, 1977).

Looking at the role that muscle fiber type might play in determining optimal cadence, Umberger et al. (2006) employed a Hill type muscle model (12 muscles modeled per leg) to study a submaximal cycling task. Umberger and colleagues varied

muscle parameters to incorporate the varying characteristics of the different fiber types. The cadence at which energy expenditure rates where minimized differed by 9 rpm between the fast twitch model (64 rpm) and the slow twitch model (55 rpm). Both these values fall well within the range of most economical cadences reported from experimental studies discussed previously. This small variation is surprising considering that the fast and slow twitch muscle models used were relatively extreme with respect to the fiber type distributions. The fast twitch model, as well as the slow twitch model represented an approximate two standard deviation difference from mean muscle fiber type distribution values used. Furthermore, their results showed that muscle mechanical efficiency was higher for the slow twitch model than the fast twitch model in general, and that maximal muscle mechanical efficiency occurred at a higher cadence (maximum at 84 rpm) for the fast twitch model compared to the slow twitch model (maximum at 72 rpm). This study suggests that muscle fiber type affects the energetics of the pedaling task, and that this might be a key determinant of preferred cadence.

Other modeling studies looking at optimal cadences for submaximal cycling have found similar but varying results. Neptune and Hull (1999) found that neuromuscular quantities related to muscle activation, force, stress, and endurance were all minimized at a cadence of 90 rpm. Gonzalez and Hull (1989), using a joint torque actuated model, reported an optimal cadence of 115 rpm. Redfield and Hull (1986a), who looked only at the effect of cadence as a single parameter, reported an optimal value of 105 rpm. Hull, Gonzalez, & Redfield (1988) also used an optimization based on muscle stresses for 12 lower limb muscles and found optimal cadence values in the range of 95-100 rpm. Experimental results (Lucia, Hoyos, & Chicharro, 2001) for seven professional cyclists

during actual race conditions (Giro d'Italia, Tour de France, and Vuelta a Espana) have shown that the preferred cadence depends on type of stage encountered, but that the average preferred cadence during level ground individual time trials (89.3 rpm) and during flat long group stages (92.4 rpm) was similar to values reported as preferred during laboratory testing (90-100 rpm) (e.g., Hagberg, Mullin, Giese, & Spitznagel, 1981; Marsh & Martin, 1997).

Modeling studies focusing on sprint cycling have in general shown higher optimal cadences than those for submaximal cycling. Van Soest and Casius (2000) showed that for a sprint cycling task the optimal cadence was 120 rpm, with a 1067 W power output. Their study highlighted the importance of muscle activation dynamics – if activation dynamics was not included in their model, the optimal pedaling rate increased substantially. Two maximal power modeling studies (Yoshihuku & Herzog, 1990; 1996) found optimal pedaling rates varying from 139 to 176 rpm, with power outputs between 1000 W and 1300 W. These big variations came about as different force-length relations and muscle length definitions were used in order to see the effect of these parameters on optimum results. Clearly the effects were significant. Experimental laboratory results for optimal cadence when producing maximal power output show typical values between 110 rpm and 136 rpm (e.g., Dorel, Bourdin, Van Praagh, Lacour, & Hautier, 2003; Martin & Spirduso, 2001; McCartney, Obminski, & Heigenhauser, 1985).

In addition to optimal cadence issues, the functioning of individual lower limb muscles during the cyclic task has received much attention (e.g., Fregly & Zajac, 1996; Raasch et al., 1997; Zajac, Neptune, & Kautz, 2002). These studies have attempted to elucidate the individual muscle contributions to the final power output at the crank.

Raasch et al. (1997) was the first to use a forward dynamic simulation framework with an optimal control algorithm to show how muscle energy transfer occurs during a maximal-speed cycling task. Finding the muscle excitation trajectories that would create kinematic and kinetic output results similar to actual experimental values, they were able to compute individual muscle contributions to the crank power. It was found for instance that the uniarticulate hip and knee extensors produced most of the propulsive power, but that not all of this power is transferred directly to the crank. More than 50% of this power is first delivered to the limb segments and then transferred to the crank by the ankle plantar flexors. Experimentally, the functioning of human muscles have been quantified using EMG measurements. Researchers have looked at the effects of various factors and how it influences the muscle function, for example load and cadence (Baum & Li, 2003; MacIntosh, Neptune, & Horton, 2000), pedaling technique (Cannon, Kolkhorst, & Cipriani, 2007), and cycling experience (Marsh & Martin, 1995). Comparisons of experimental muscle function results with modeling study outcomes is important to evaluate the appropriateness of current modeling approaches being used.

In summary, a variety of modeling studies have been used to evaluate the cycling task. Comparison of various results is however difficult, as many task specifics differ (i.e., maximum power, submaximal steady state, sprint cycling), as well as methods used to model these tasks. In many instances modeling studies are confirmed by experimental results, but this is not always the case. Nevertheless, modeling and simulation studies have increased our knowledge of how the human body operates during cycling and future research should further facilitate our understanding.